REGULATION OF METABOLIC REPROGRAMMING

BY MONDOA AND THIOREDOXIN

INTERACTING PROTEIN

by

Marc Geoffrey Elgort

A dissertation submitted to the faculty of
The University of Utah
in partial fulfillment of the requirements for the degree of

Doctor of Philosophy

Department of Oncological Sciences

The University of Utah

December 2010

The University of Utah Graduate School

STATEMENT OF DISSERTATION APPROVAL

The dissertation of **Marc Geoffrey Elgort**

has been approved by the following supervisory committee members:

Donald E. Ayer	, Chair	**August 12, 2010** Date Approved
Stephen L. Lessnick	, Member	**August 12, 2010** Date Approved
Edward Levine	, Member	**August 12, 2010** Date Approved
Jared Rutter	, Member	**August 12, 2010** Date Approved
Alana Welm	, Member	**August 12, 2010** Date Approved

and by **Barbara Graves**, Chair of the Department of **Oncological Sciences**

and by Charles A. Wight, Dean of The Graduate School.

ABSTRACT

Cell proliferation requires increased nutrient uptake and metabolic activities that drive macromolecular synthesis to support cell growth. While unicellular organisms proliferate when nutrients like glucose are available, this is not the case in metazoans. As glucose and other essential nutrients are readily available to cells in the context of a multicellular organism, these cells actively regulate the uptake and utilization of nutrients through elaborate signaling networks. In addition to increased nutrient uptake, proliferating cells must also reorganize their metabolic activities from primarily ATP producing to biosynthetic and ATP producing to support the doubling of cellular genomic and macromolecular content to produce two viable daughter cells. To accomplish this, metabolic reprogramming from oxidative metabolism in the mitochondria to aerobic glycolysis - the Warburg effect – occurs within the cell. Aerobic glycolysis, typically observed in rapidly proliferating tumor cells, drives synthesis of macromolecules such as lipids, protein and nucleic acids, by diverting metabolites from both glycolysis and the TCA cycle into biosynthetic pathways while maintaining ATP production. Growth factor signaling pathways orchestrate this metabolic reprogramming by directly influencing glucose uptake and activating transcriptional networks, such as Myc and HIF, to upregulate glycolytic flux. Thioredoxin interacting protein (TXNIP), a tumor suppressor and a direct and glucose-induced transcriptional target of MondoA, is a potent negative regulator of glucose uptake and glycolysis. Thus, TXNIP may inhibit cell growth and proliferation by restricting substrate availability for macromolecular synthesis. When quiescent cells are stimulated to proliferate TXNIP translation and MondoA-dependent

TXNIP transcription are acutely downregulated in response to growth factor signaling. Ectopic MondoA and TXNIP expression restricts glucose uptake and utilization resulting in restricted cell growth and proliferation. Thus downregulation of these activities might act in cooperation with activities such as Myc upregulation to drive metabolic reprogramming in response to proliferative signals.

TABLE OF CONTENTS

ABSTRACT iii

LIST OF FIGURES vii

ACKNOWLEDGEMENTS viii

CHAPTER

1. INTRODUCTION 1

    1.1 Overview 1
    1.2 The Warburg Paradox and Anabolic Metabolism 2
    1.3 Metabolic Reprogramming in Lymphocytes 7
    1.4 Receptor Tyrosine Kinase Signaling 11
    1.5 Myc, HIF and Glycolysis 17
    1.6 Thioredoxin Interacting Protein 20
    1.7 MondoA 23
    1.8 Summary 30
    1.9 References 32

2. TRANSCRIPTIONAL AND TRANSLATIONAL DOWNREGULATION OF THIOREDOXIN INTERACTING PROTEIN DRIVES METABOLIC REPROGRAMMING IN G_1 39

    2.1 Abstract 40
    2.2 Introduction 40
    2.3 Results 44
    2.4 Discussion 64
    2.5 Materials and Methods 69
    2.6 Acknowledgements 75
    2.7 References 76

3. SUMMARY 84

    3.1 References 94

APPENDICES

A. AN ACTIVATING MUTATION IN *SOS-1* IDENTIFIES ITS DBL DOMAIN AS A CRITICAL INHIBITOR OF THE EPIDERMAL GROWTH FACTOR RECEPTOR PATHWAY DURING *CAENORHABDITIS ELEGANS* VULVAL DEVELOPMENT 98

B. COORDINATION OF GLUCOSE AND GLUTAMINE UTILIZATION BY AN EXPANDED MYC NETWORK 112

LIST OF FIGURES

Figure Page

1.1 Schematic of glycolysis (cytoplasm) and TCA cycle (mitochondria) 4

1.2 Metabolic reprogramming in T cells 9

1.3 Simple schematic of receptor tyrosine kinase (RTK) signaling 13

1.4 MondoA and ChREBP comprise a parallel Myc-like transcription network 24

1.5 Structural similarities between MondoA, Mlx, Myc and Max 26

2.1 TXNIP downregulation correlates with metabolic reprogramming 46

2.2 Ectopic TXNIP expression restricts glucose uptake, glycolysis and blocks G_1 progression 49

2.3 Dominant-active MondoA blocks G_1 progression 51

2.4 MondoA-dependent TXNIP transcription is acutely inhibited by serum 55

2.5 TXNIP expression is refractory to upregulation in early G_1 56

2.6 TXNIP translation is acutely inhibited by serum in early G_1 58

2.7 Acute growth factor signaling downregulates TXNIP expression 61

2.8 Acute Ras-MAPK activation downregulates TXNIP translation 63

3.1 MondoA and TXNIP regulation during the G_0/G_1 transition 87

3.2 Lysophosphatidic acid (LPA) and phorbol-12-myristate-13-acetate (PMA) downregulate TXNIP mRNA 89

ACKNOWLEDGEMENTS

I would first like to thank my advisor, Don Ayer, for giving me a lab to work in and a thesis to pursue after my previous advisor, Nadeem Moghal, left the University of Utah to work in Toronto. Don's guidance, knowledge and enthusiasm have created an environment conducive to learning, performing and generally made me feel like the Ayer lab was home. I truly look forward to interacting with Don in the future on both a professional and personal level. I'd also like to thank Nadeem who, while he was here, helped me to expand my knowledge of RTK signaling and further inspired my desire to learn. I was in a lab before Nadeem's, albeit briefly, and I'd like to thank Jared Rutter for my time in his lab at the beginning of my graduate school experience. Jared inspired my renewed excitement toward science and for that I am grateful.

My committee has also been instrumental in my getting through this program. Steve Lessnick, who has been on all three of my committees, has provided scientific insight and personal advice and reassurance. Ed Levine has been a sounding board for both my work and personal frustrations as has Alana Welm. I've already thanked Don and Jared. I'd also like to thank Matt Topham at this point for discussions and his review of our manuscript presented in Chapter 2.

The people at HCI in the department of Oncological Sciences have also been instrumental in my getting to this point. Friends in the Ayer, Cairns, Lessnick, Trede, Ullman, Beckerly, Graves, Welm (both) and Rosenblatt labs have helped keep me sane, or at least as sane as I was before I started. The administrative folks, specifically Dee Dalponte, Jessica Hampton, Norma Haas, Sarah Weiland and Tonya Avery, have made my life easier, put up with my nonsense and have generally been friends. Thanks.

I've saved the most important person until the end, as it would be impossible for me to thank her in even the same context as the wonderful people above. Suzanne, my wife, my roommate and my BFF, thank you so much for being there then and now and forever; I don't know what I'd do without you.

CHAPTER 1

INTRODUCTION

1.1 Overview

In metazoans, cell proliferation is required for normal organismal function. Its roles include, but are not limited to, embryogenesis, development, growth and maintenance of function of many adult tissues. Aberrant proliferation is a defining feature of tumorigenesis. Much of the work done over the past several decades to understand the mechanisms leading to and controlling cell proliferation has led to the identification and dissection of exquisitely regulated growth-factor signaling pathways and transcriptional networks that enable cells to enter and successfully traverse the cell cycle. Clearly, these are also the pathways that are corrupted and exploited during tumorigenesis.

Proliferating cells are faced with major challenges. The onset of proliferation requires that a cell must ultimately divide into two identical daughter cells, indicating that it is not only necessary to completely duplicate its genome but it is also required to double its biomass prior to mitosis. This presents unique metabolic challenges to the cell as it must increase the synthesis of proteins, lipids and nucleic acids in response to proliferative signals. Resting or quiescent cells have significantly different metabolic needs than those of proliferating cells. Therefore, once stimulated to proliferate, these cells must reorganize their metabolic pathways such that both energy producing and biosynthetic pathways are enabled to allow sufficient cell growth. In addition to metabolic reprogramming, proliferating cells must also increase uptake of extracellular nutrients to

maintain flux through the metabolic pathways that drive cell growth. Rapidly proliferating cancer cells demonstrate increased uptake and utilization of glucose and glutamine and generate adenosine 5'-triphosphate (ATP) primarily by aerobic glycolysis. Work involving proliferating lymphocytes and hematopoietic stem cells suggests that this is not a feature unique to cancer cells but rather required by all proliferating cells. While the signals that stimulate cell proliferation are also involved in orchestrating metabolic reprogramming, little is known about the downstream effectors involved in this process. Elucidating the regulatory processes involved in metabolic reprogramming and ultimately cell growth is therefore important for a more comprehensive understanding of not only normal cell processes but for the pathogenesis of diseases such as cancer.

1.2 The Warburg Paradox and Anabolic Metabolism

In the 1920s, Otto Warburg observed that cancer cells metabolize glucose in a manner different from cells in normal tissues (1). In the presence of sufficient oxygen to support mitochondrial oxidative phosphorylation, tumor cells tended to catabolize glucose to lactate at high rates rather than oxidizing it as in normal cells (2). Warburg's initial explanation for this was that tumors had defects in mitochondrial function or oxidative phosphorylation which resulted in a compensatory increase in glycolytic flux (2), but it is now clear that many tumors not only have normal mitochondria but their tricarboxylic acid (TCA) cycles and electron transport chains (ETC) are intact (3). Nonetheless, Warburg's observations presented a paradox: Why would rapidly proliferating cells with such a great need for energy (ATP) utilize a wasteful and seemingly inefficient form of metabolism? While this paradox is still not completely resolved, studies in normal proliferating lymphocytes suggest that aerobic glycolysis, the Warburg effect, is not unique to tumors (section 1.3).

Cells require a constant supply of energy to maintain the biological processes that allow them to function and survive. The most fundamental source of cellular nutrition is glucose. In most metazoans, glucose metabolism dominates energy production. In mammalian cells, glucose enters the cell through one or many transmembrane hexose transporters belonging to the GLUT family (4). Once in the cytoplasm, glucose is phosphorylated by a hexokinase to glucose-6-phosphate (G6P) in the first step of glycolysis to prevent its diffusion out of the cell and allow further glycolytic catabolism (5). Once committed to glycolysis after conversion by phosphofructokinase (PFK), the six-carbon sugar is further metabolized to two three-carbon pyruvate molecules which yield two ATP and NADH (nicotinamide adenine dinucleotide (NAD^+), reduced) molecules per pyruvate in the process (5). If oxygen is not limiting (aerobic metabolism) pyruvate enters the mitochondria and is converted to acetyl coenzyme A (CoA) where it enters the citric acid or TCA cycle (Figure 1.1) (5). Flux through the TCA cycle produces NADH and $FADH_2$ (flavin adenine dinucleotide (FAD), reduced) which fuel maximal ATP production by oxidative phosphorylation (6). Up to 36 molecules of ATP can be generated from one molecule of glucose in this manner (6). If oxygen is limiting (anaerobic metabolism), pyruvate is further metabolized to lactate which is excreted from the cell, yielding a net two ATP molecules per glucose molecule (6). Tumors tend to have anaerobic microenvironments, and thus utilize anaerobic metabolism to derive energy for cellular function (6), so it is important to distinguish this from proliferative metabolism which is aerobic. It is clear that glucose metabolism by the TCA cycle seems to produce more energy and less waste in the form of lactate than glycolysis alone, so why would a proliferating cell under aerobic conditions utilize a seemingly wasteful and low-energy yielding process as its main form of metabolism? An answer to this question comes from an understanding of both the metabolic needs of a proliferating cell and the

Figure 1.1 Schematic of glycolysis (cytoplasm) and the TCA cycle (mitochondria). Generally depicted are: ATP production by the electron transport chain (ETC) in the mitochondrial matix, NAD^+ generation by LDHA and site of glutaminolysis. Lactate is excreted from the cell by an MCT (monocarboxylate transporter). Also depicts branch points where pathway intermediates can participate in macromolecular synthesis.

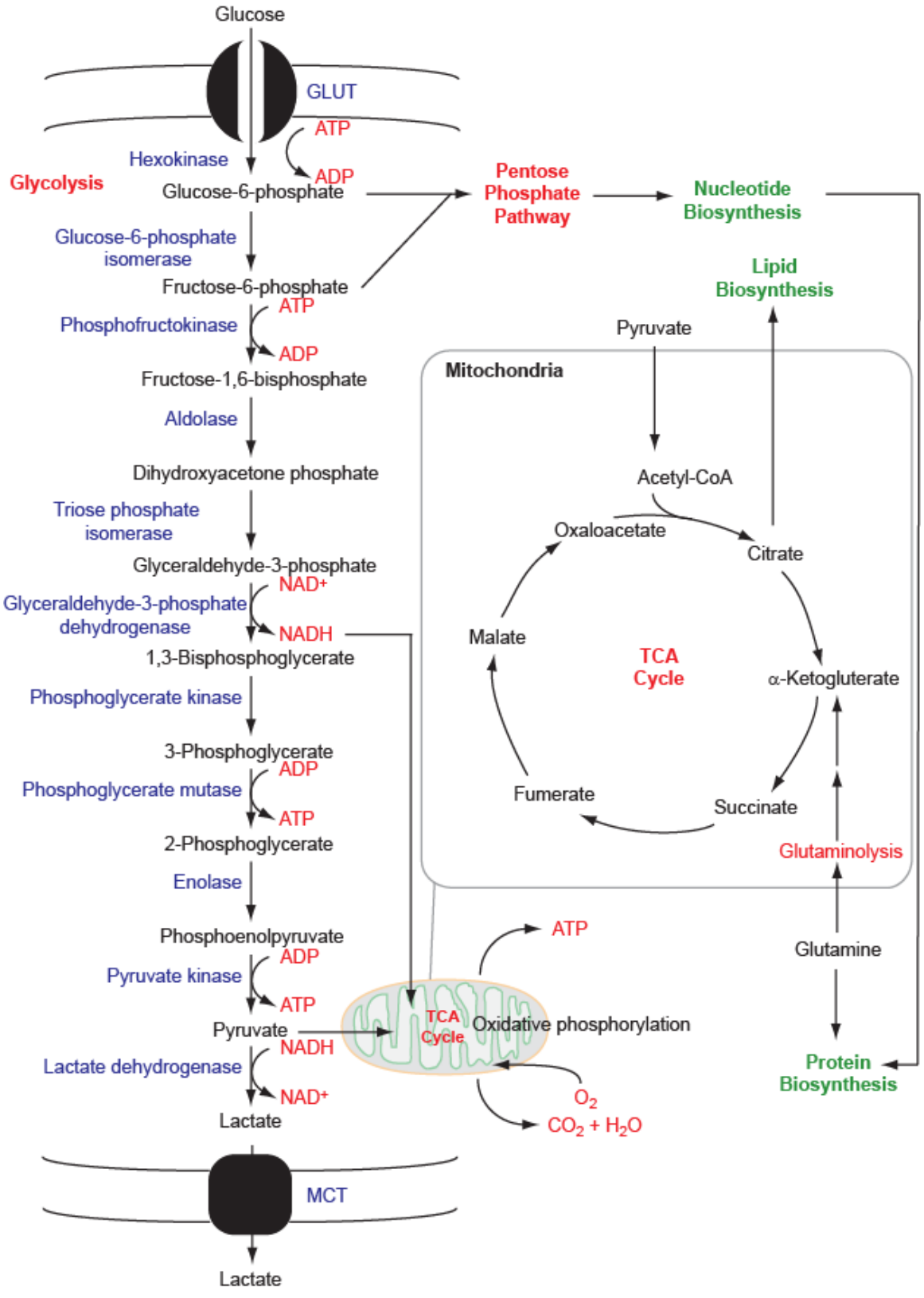
Glucose
GLUT
ATP
Hexokinase
ADP
Glycolysis
Glucose-6-phosphate
Pentose Phosphate Pathway
Nucleotide Biosynthesis
Glucose-6-phosphate isomerase
Fructose-6-phosphate
Lipid Biosynthesis
ATP
Phosphofructokinase
ADP
Pyruvate
Mitochondria
Fructose-1,6-bisphosphate
Aldolase
Dihydroxyacetone phosphate
Acetyl-CoA
Triose phosphate isomerase
Oxaloacetate
Citrate
Glyceraldehyde-3-phosphate
NAD+
Glyceraldehyde-3-phosphate dehydrogenase
NADH
Malate
TCA Cycle
α-Ketogluterate
1,3-Bisphosphoglycerate
Phosphoglycerate kinase
3-Phosphoglycerate
ADP
Phosphoglycerate mutase
ATP
Fumerate
Succinate
2-Phosphoglycerate
Glutaminolysis
Enolase
Phosphoenolpyruvate
ATP
Glutamine
ADP
Pyruvate kinase
ATP
TCA Cycle
Oxidative phosphorylation
Pyruvate
NADH
Protein Biosynthesis
Lactate dehydrogenase
NAD+
O2
Lactate
CO2 + H2O
MCT
Lactate

metabolic demands of macromolecular biosynthesis. In short, aerobic glycolysis is a necessary component of anabolic metabolism.

In addition to generating ATP by oxidative phosphorylation, glucose metabolism also provides cells with intermediates required for biosynthetic pathways (6-10). G6P is shunted into the pentose phosphate pathway (PPP) to generate ribose sugars necessary for nucleotide biosynthesis as well as NADPH (7), citrate is exported from the mitochondria to generate fatty acids for lipids (9) and amino acids are derived from glycolytic and TCA cycle intermediates (9) (Figure 1.1). Additionally, pyruvate conversion to lactate by lactate dehydrogenase A (LDHA) produces NAD^+ which is necessary for reductive biosynthesis as well as ATP production from glycolysis (9). While the ATP yield from glycolysis compared to the TCA cycle is low, the flux through glycolysis to generate lactate is considerably higher than through the TCA cycle (11). This can help to resolve the Warburg paradox, at least partially, in two ways. First, the energy needs of the proliferating cell can be met by ATP production from glycolysis provided both glycolytic flux and glucose uptake are increased. Second, if a high flux pathway, like glycolysis, is upstream of and feeds into a lower flux pathway, like one that utilizes pathway intermediates as biosynthetic precursors, flux through the downstream pathway can be maintained while lactate production prevails through glycolysis (11). Since the TCA cycle is a lower flux pathway, with pyruvate to acetyl CoA conversion being limiting (12), TCA cycle intermediates can be used as biosynthetic precursors rather than being metabolized completely by this cycle to drive oxidative phosphorylation, while ATP production is supported by the high glycolytic flux (9). Given that utilization of TCA cycle metabolites in biosynthetic pathways potentially “empties” (catapleurosis) the TCA cycle quickly, the cycle can ultimately be “refilled” (anapleurosis) by conversion of the amino acids glutamine and aspartate to TCA cycle intermediates (13). Conversion of the highly abundant glutamine to α-ketoglutarate (α-KG) provides citrate which fuels fatty acid

biosynthesis is also further catabolized by the the TCA cycle intermediates downstream (Figure 1.1) (13). This model suggests that proliferating cells are able to engage in the necessary biosynthetic reactions required for cell growth while at the same time excreting lactate and thus, provides at least some resolution to the Warburg paradox.

1.3 Metabolic Reprogramming in Lymphocytes

As outlined in the previous section, aerobic glycolysis drives anabolic synthesis of the macromolecules required to support the high rates of proliferation seen in cancer. The process of tumorigenesis appears to require metabolic reprogramming from oxidative metabolism to aerobic glyolysis (14), and it is becoming clearer that activation of many oncogenes, e.g., Myc and Ras, and loss of tumor suppressors, e.g. PTEN, p53 and TXNIP, directly drive metabolic reprogramming (15-19). This suggests that the Warburg effect may contribute functionally to tumor cell growth rather than merely correlating with it. This would also indicate that aerobic glycolysis is a feature of normal proliferating cells, and in fact, this is the case.

Much of the work leading to an understanding of the switch from oxidative metabolism to aerobic glycolysis during proliferation in normal diploid cells has been done in lymphocytes (20). T lymphocytes (T cells) are an ideal model for studying metabolic and signaling in cells transitioning into a proliferative state. *In vivo*, they leave the thymus and enter the peripheral circulation as small quiescent cells. In the absence of trophic signals, they remain quiescent but upon stimulation by cytokine and antigen signals, they become activated and initiate a program of rapid growth and proliferation (20). As peripheral T cells can be isolated and used *in vitro*, it is possible to study regulation of both quiescence and proliferation.

In mammals, nutrients like glucose and glutamine are rarely limiting, and work from the Thompson laboratory and others has established that quiescent T cells actively

maintain quiescence by low-level signaling through cytokine and T cell receptors (TCR) (21). Essentially, glucose and other nutrients are taken up into the cells at a low rate (22). Glucose metabolism is divided evenly between lactate production through glycolysis and oxidative phoshorylation in the presence of low-level signals, primarily to maintain the quiescent state (23). In the complete absence of signals, glucose uptake is further decreased and the cells derive energy primarily from β-oxidation of fatty acids and lower level flux through the TCA cycle for survival (24). These data support a model whereby quiescent cells engage in oxidative metabolism for homeostasis and survival, suggesting that the flux of glucose through glycolysis is primarily utilized for pyruvate production to supply the TCA cycle with acetyl CoA (Figure 1.2).

Upon stimulation by antigens, T cells initiate a program of rapid growth and proliferation (23). In contrast to quiescent cells, the metabolism of an activated T cell is characterized by increased excretion of lactate and dramatically increased uptake of glucose (25) (Figure 1.2). GLUT1 transcriptional upregulation and subsequent translocation of GLUT1 to the plasma membrane in response to Akt activation (discussed in section 1.4) directly drives the dramatic increase in glucose uptake following CD28 costimulation *in vitro* (25). Further, ligation of the TCR (CD3) with CD28 results in increased glycolytic flux that is phosphatidylinositide 3-kinase (PI3K) dependent (discussed in section 1.4) (26). This increase in glucose uptake and utilization directly correlates with increases in lipid synthesis and more significantly cell growth. Essentially, activated T cells undergo metabolic reprogramming from oxidative metabolism to aerobic glycolysis upon activation in order to support the rapid growth required for a proliferative burst. In the absence of additional proliferative signals *in vitro*, e.g., the cytokine interleukin-3 (IL-3), T cells will not proliferate, making this an ideal system to study the signaling events regulating cell growth (25, 27). However, as T cells divide rapidly, as quickly as 6 hours, understanding the immediate and subsequently

Figure 1.2 Metabolic reprogramming in T cells. Quiescent cells take up glucose at a low rate which drives glycolysis at rates sufficient to generate ATP in the mitochondria via the TCA cycle for maintenance and survival. Fatty acids are oxidized in the mitochondria to provide additional substrates for TCA cycle function and energy production through oxidative phosphorylation. Upon cytokine and T cell receptor stimulation, T cells begin a program of rapid growth and proliferation. Akt-dependent GLUT1 mRNA upregulation and transporter translocation to the plasma membrane increases glucose uptake, and PI3K-dependent increase in glycolytic flux increases lactate excretion from the cell. The TCA cycle becomes “truncated” with metabolites being utilized for lipid synthesis. Amino acids, aspartate and glutamine “refill” the cycle via anapleurosis. ATP production is shifted from the mitochondrial matrix to the cytoplasm via glycolysis. Figure adapted from Fox, et al., (2005) Fuel feeds function: energy metabolism and the T-cell response. *Nat Rev Immunol* 5(11):844-52

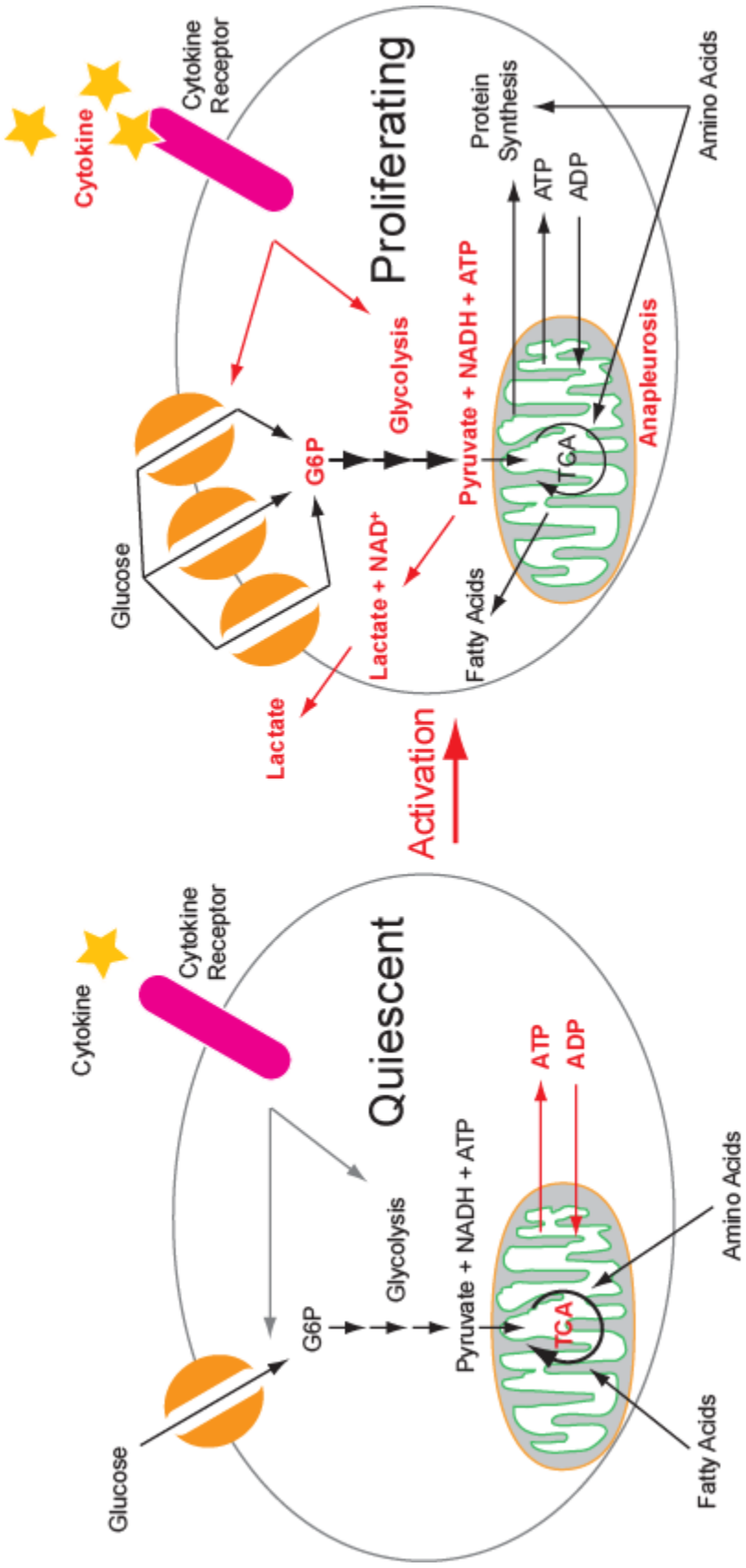
Cytokine
Cytokine Receptor
Proliferating
Protein Synthesis
ATP
ADP
Amino Acids
Glycolysis
Pyruvate + NADH + ATP
Anapleurosis
TCA
G6P
Glucose
Lactate + NAD+
Fatty Acids
Lactate
Activation
Cytokine
Cytokine Receptor
Quiescent
ATP
ADP
Glycolysis
Pyruvate + NADH + ATP
Amino Acids
TCA
G6P
Glucose
Fatty Acids

temporal regulation of metabolic reprogramming in the growth phase (G_1) of the cell cycle in response to proliferative signal becomes less tractable and as such, another system is explored in Chapter 2.

The work briefly outlined in this section indicates that metabolic reprogramming is required in cells transitioning from a quiescent state to one of proliferation. As PI3K and Akt signaling are required for both the increase in glucose uptake and glycolytic flux, this suggests a broader role for metabolic reprogramming in other cell types that undergo proliferation. PI3K and Akt can act as transducers of extracellular signaling propagated through growth factor receptors. As such, signal transduction by growth factor receptors and the broader implications of this signaling on metabolism will be discussed in section 1.4.

1.4 Receptor Tyrosine Kinase Signaling

As described in section 1.3, CD28 costimulation activates PI3K and Akt. While CD28 regulates growth in T cells by supporting metabolic reprogramming, another class of transmembrane signaling receptors, the receptor tyrosine kinases (RTKs) active in cell growth and proliferation, through their activation of PI3K and Ras, will be discussed in this section. The ErbB family member, epidermal growth factor receptor (EGFR) is one of the most studied members of the RTK superfamily, and as such, it serves as a model for discussing downstream signal transduction in this section. It is also important to note that the EGFR effector cascades that will be presented here are utilized by myriad signaling receptors (e.g., cytokine receptors and G protein coupled receptors [GPCRs]) and as such, signaling through the RTKs merely represents a model for the signaling paradigms outlined.

EGFR, and other members of the RTK superfamily, are composed of an extracellular ligand-binding domain, a single transmembrane domain and intracellular

tyrosine kinase domain followed by a non-catalytic carboxy-terminal tail (28, 29). The receptor is activated upon ligand binding (EGF) leading to receptor dimerization and subsequent auto-phosphorylation by the catalytic tyrosine kinase domain (29). Once phosphorylated, the intracellular domain acts a docking site for Src homology 2 (SH2) domain containing proteins which brings them to the intracellular surface of the plasma membrane and potentiates binding, activation and catalysis of downstream effectors (29). Two major effector pathways that will be discussed below are the PI3K/Akt pathway and the Ras/MAPK (mitogen-activated protein kinase or Erk [extra-cellular signal regulated kinase]) pathway (Figure 1.3).

Signaling specificity and heterogeneity is achieved, in part, through EGFR heterodimerization with other ErbB family members (29, 30). The signals tranduced though EGFR ultimately lead to cell proliferation, differentiation or survival. Given its role cell fate determination, it is not surprising that activating mutations in EGFR, primarily in the regulation of its kinase activity, have been observed in many cancers (31). A unique feature of EGFR is, unlike other receptors, its kinase domain is not regulated by additional phosphorylations within an activation loop of the domain; instead, it is controlled by receptor conformational changes induced by ligand binding and possibly the carboxy-terminal tail (31). Thus mutations in the activation loop leading to constitutive activation of the kinase domain in the absence of ligand binding require less specificity than those in other receptors and. As such, activating mutations in EGFR appear to be more prevalent in cancers and much work has been done in developing small molecule inhibitors of its kinase activity (31).

Once phosphorylated, EGFR can recruit many signal effectors depending on cellular context. PI3K, a member of the class I family of phosphoinositide kinases, is a heterodimeric kinase made up of a regulatory subunit (p85) and a catalytic subunit

Figure 1.3 Simple schematic of receptor tyrosine kinase (RTK) signaling highlighting general signal transduction through P13K and Ras networks. Ligand (e.g., EGF) binding to extracellular ligand-binding domain induces receptor dimerization and phosphorylation. With regard to signals transduced through PI3K, the regulatory domain of PI3K, p85, is recruited to the plasma membrane via RTK-p85 interactions. The catalytic domain, p110, phosphorylates $PI(4,5)P_2$ (PIP_2) residues in the plasma membrane to $PI(3,4,5)P_3$ (PIP_3), permitting Akt recruitment to the plasma where it is activated. PTEN dephosphorylates PIP_3 in the plasma membrane, thus attenuating PI3K signal propagation. Ras activation can also activate PI3K as depicted. With regard to signal transduction through Ras, an adapter like Grb2 is recruited to the active RTK which binds the Ras-GEF Sos, thus catalyzing GDP to GTP exchange on Ras and activating it. Activated Ras binds to Raf, permitting its phosphorylation and activation. Raf phosphorylates MEK which subsequently phosphorylates MAPK, which then translocates to the nucleus, where it can phosphorylate and activate transcription factors such as the c-Myc proto-oncogene. Downstream signals from both PI3K and Ras lead to proliferation, differentiation, growth and survival as discussed in the text.

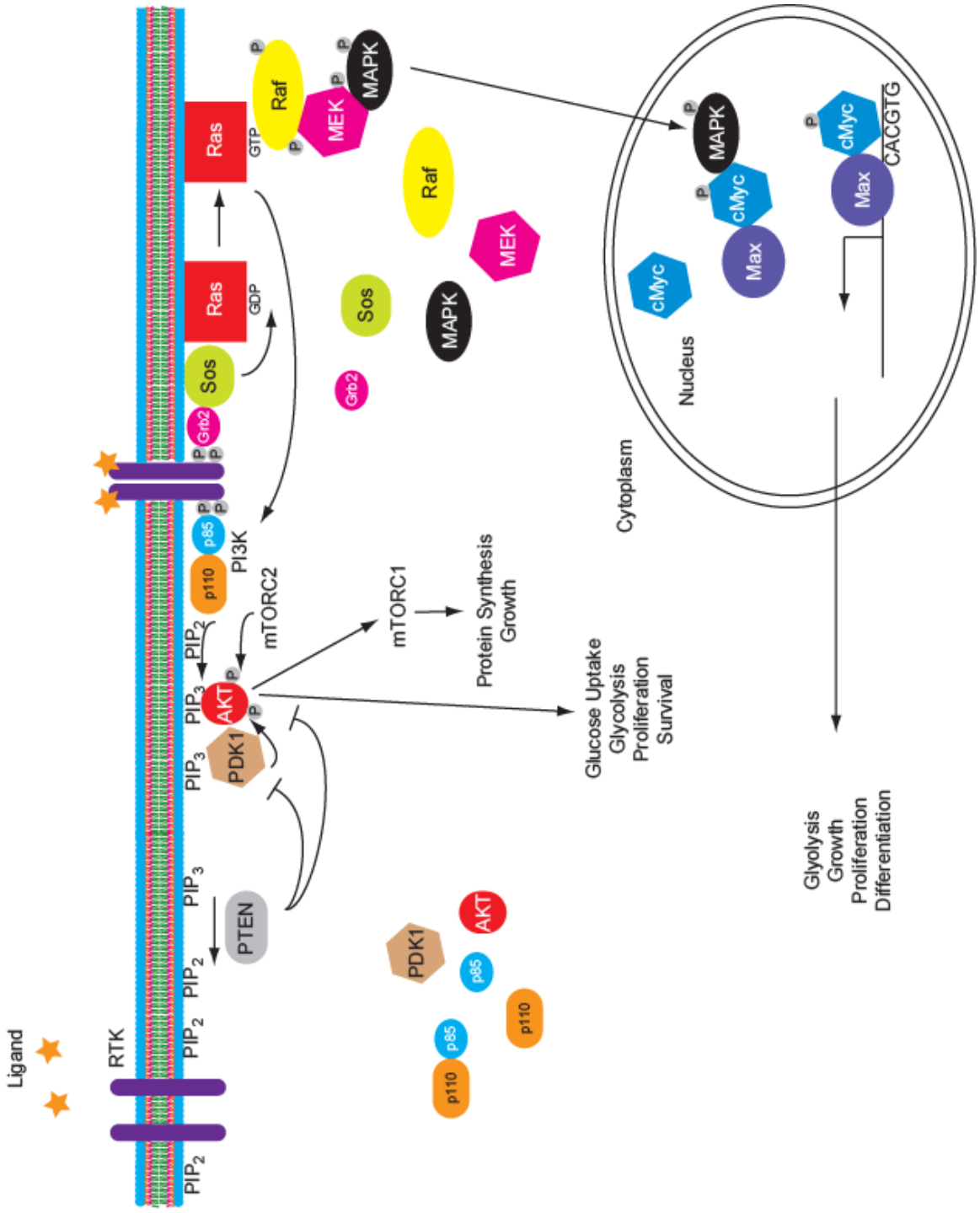
Ligand
RTK
PIP2
PIP2
PIP2
PIP3
PIP3
PTEN
PIP3
PDK1
AKT
P
PIP2
PIP3
mTORC2
PI3K
p85
p110
Grb2
Sos
Ras
GDP
Ras
GTP
Raf
MEK
MAPK
Raf
MEK
MAPK
Sos
Grb2
PDK1
AKT
p85
p110
p85
p110
mTORC1
Protein Synthesis
Growth
Glucose Uptake
Glycolysis
Proliferation
Survival
Cytoplasm
Nucleus
MAPK
cMyc
Max
cMyc
Max
CACGTG
Glycolysis
Growth
Proliferation
Differentiation

(p110) (32, 33). PI3K can be recruited directly to the receptor through p85 SH2 domain interactions or indirectly through other docking proteins like Grb2 or IRS-1 (33). Once recruited to the receptor and proximal to the plasma membrane, PI3K catalyzes the phosphorylation of phosphatidylinositide (4,5)-diphosphate ($PI(4,5)P_2$) residues in the plasma membrane to $PI(3,4,5)P_3$, which are potent signaling molecules (33). $PI(3,4,5)P_3$ can recruit cytosolic proteins containing pleckstrin homology (PH) domains, e.g. Akt, to the plasma membrane where they can be activated by other plasma membrane associated proteins and further transduce signals from the RTK (34). More specifically, once Akt is positioned at the plasma membrane, it is phosphorylated by its activating kinases, phosphoinositide dependent kinase 1 (PDK1) and mammalian target of rapamycin complex 2 (mTORC2) at threonine 308 and serine 473, respectively (34). Upon activation, Akt phosphorylates serines and threonines of other downstream effectors including, but far from limited to, mTORC1 and BAD, leading to cell growth, proliferation and survival (35, 36). Additionally, Akt1 activity is required for translocation of the insulin responsive glucose transporter, GLUT4 in response to activation of the insulin receptor (IR) (37). Finally, as discussed in section 1.3, Akt and PI3K activity are required for metabolic reprogramming in T cells.

PI3K signaling is attenuated by a number of mechanisms, but one of the best characterized is by the tumor suppressor phosphatase and tensin homolog (PTEN). Briefly, activated PTEN catalyzes the dephosphorylation of $PI(3,4,5)P_3$ to $PI(4,5)P_2$, thus inhibiting signaling downstream of PI3K (38). Just as activating mutations in PI3K lead to growth and survival of many cancers, mutations rendering PTEN catalytically inactive are also observed (38). Interestingly, deletion of the tumor suppressor thioredoxin interacting protein (TXNIP) leads to inactivation of PTEN (19). It is thought that the reactive oxygen species (ROS) generating activities of TXNIP activate PTEN, resulting

potentially in growth arrest and reduced glycolysis (19). TXNIP will be discussed in greater detail in section 1.6.

A second signaling cascade activated by RTKs is the Ras-MAPK pathway. Ras is a small membrane associated GTPase and its activity is regulated by the guanine exchange factor (GEF) son of sevenless (Sos) (39). Sos can be recruited to the plasma membrane and to Ras in number of ways upon RTK activation, however, a well characterized method involves docking to receptor bound Grb2 (39). Once activated, Ras can recruit a Raf protein (e.g., cRaf, Raf-1) leading to activation of its catalytic activity. Activated Raf phosphorylates the dual specificity kinase MEK (MAPK kinase) which subsequently phosphorylates MAPK (40). Phosphorylated MAPK translocates to the nucleus where it phosphorylates transcription factors containing MAPK phosphorylation sites such as Elk-1, cMyc and PPARγ (41-44). For certain transcription factors MAPK phosphorylation serves as an activating event, thus integrating extracellular signals with transcriptional programs. Ras-MAPK signaling ultimately leads to cell fate decisions such as proliferation and differentiation (30).

As many pathways lead to MAPK activation, it is confounding how this common endpoint produces different cell fates. It is clearer now that both the intensity and duration of MAPK activation plays a role (30, 45). Within the context of EGFR, attenuation of the signal transduced by EGF to MAPK is accomplished by receptor downregulation through ubiquitination by cCbl, Ras-GAP inhibition of Raf activation, as well as direct inhibition of phosphorylated MAPK by MAPK phosphatase (46-48). Work from Appendix A done in the laboratory of Nadeem Moghal addresses a novel mechanism of EGFR downregulation by an inhibitory domain of Sos (49). Mutations in the Cdc25 domain of Sos lead to a multivulva phenotype in *Caenorhabditis elegans* similar to EGFR and Ras mediated hyperactivation of MAPK. Recapitulation of this Cdc25 mutation in human Sos results in sustained MAPK activation in the presence of

EGF and further, similar mutations in Cdc25 have been observed in developmental disorders attributable to increased, but not constitutive, Ras activation. While the Cdc25 does not directly activate Ras, failure to inhibit EGFR kinase activity results in sustained Ras and MAPK activation downstream of EGF. While many mechanisms can lead to aberrant Ras activation, activating mutations of Ras are observed in many cancers and the high rates of glycolysis observed can be directly attributed to Ras activation of cMyc and Hif1α, which will be discussed in section 1.5 (50-54).

It is evident that both PI3K/Akt and Ras-MAPK signaling have critical roles in regulating cell growth and proliferation in response to extracellular signals. As discussed above, PI3K/Akt signaling also regulates glucose uptake and metabolism and is required for metabolic reprogramming in T cells. While Ras-MAPK signaling controls proliferation, it also directly regulates glycolysis through Myc and HIF-1α, suggesting that metabolic reprogramming is part of the proliferative program. Importantly, the effects on nutrient uptake and metabolism by both PI3K and Ras are rapid, occurring within a few hours of pathway activation, further underscoring that metabolic reprogramming is a necessary component of cell growth required for proliferation. We demonstrate in Chapter 2 that RTK signaling through Ras may also impact glucose uptake and glycolysis by regulating TXNIP, suggesting a new for role for Ras in metabolic reprogramming.

1.5 Myc, HIF and Glycolysis

A hallmark of most cancers is their enhanced proliferative capacity. As previously discussed, a metabolic component characterized by and contributing to this increased proliferation is the Warburg effect or aerobic glcyolysis, which drives and supports the macromolecular synthesis required for the cell growth necessary for proliferation. While growth factor signaling leads to increases in aerobic glycolysis discussed in section 1.4, a mechanism by which this is accomplished is through the direct activation of

transcriptional networks that directly upregulate the expression of genes involved in glycolysis. The cMyc oncogene, a transcription factor belonging to basic helix-loop-helix leucine zipper (bHLHZip) family of transcription factors, is mutated in many cancers and drives high aerobic glycolysis and cell cycle progression through activation of its many transcriptional targets (55). During oxygen deprivation and other environmental stresses another transcription factor, the hypoxia-inducible factor, HIF, is stabilized and metabolism is redirected to glycolysis, principally for survival (56). Myc and HIF share multiple transcriptional targets and compete for control of metabolism in the anaerobic tumor microenvironment, however, there is evidence that these activities cooperate during proliferation in the presence of oxygen. As discussed in section 1.4, Ras activation regulates metabolism required for cell growth through Myc and HIF (53, 54). This section will therefore discuss the transcriptional regulation of metabolic reprogramming by Myc and HIF.

Myc activates thousands of transcriptional targets through a complex network of protein-protein and protein-DNA interactions with other members of bHLHZIP family, Mad and Max (57). Myc:Max heterodimers bind to CACGTG or related E-box elements in the promoter regions of genes involved in metabolism, growth and proliferation and potently activate their transcription (57). In normal cells, Myc is induced by growth factor signaling, and it is constitutively expressed at high levels in many cancers. Myc drives cell cycle progression through its regulation of cyclins and cyclin-dependent kinases and is necessary for RNA polymerase I and III transcription of tRNA and rRNA, thus regulating protein synthesis (58-60). It also activates the transcription of most the genes that regulate carbon utilization (61). Consistent with a role in aerobic glycolysis, Myc upregulates GLUT1, hexokinase and LDHA, thus supporting increased glucose uptake, glycolytic flux and lactate production (62). Interestingly, two paralogs of the Myc

superfamily, MondoA and ChREBP also transcriptionally regulate glucose uptake and glycolysis (63-65). These will be discussed further in section 1.7.

In order to undergo macromolecular synthesis driven by aerobic glycolytic flux, the cell needs normal or enhanced mitochondrial function. Myc increases both mitochondrial biogenesis and function which consistent with its role in upregulating aerobic glycolysis. As outlined in section 1.2, anapleurosis, or the refilling of the TCA cycle, is an integral component of utilizing TCA cycle intermediates for macromolecular synthesis. One mechanism by which anapleurosis occurs is glutaminolysis or the metabolism of glutamine to α-KG (13). Myc has been shown to increase glutaminolysis by several mechanisms. Myc directly upregulates the transcription of the glutamine transporters SCL38A5 and SCL1A5 (66). Additionally, Myc has been shown to increase glutaminase expression by increasing glutaminase mRNA directly (66) and transcriptionally repressing miR-23a/b transcription which de-represses glutaminase transcription (67). Thus, in addition to its contribution to increasing aerobic glycolysis, Myc contributes to metabolic reprogramming through its regulation of mitochondrial biogenesis and function and might increase anapleurosis by regulating glutaminolysis. Notably, MondoA transcriptional activity has been shown to be negatively regulated by glutaminolysis, and this will be addressed in section 1.7. Additionally, Myc also drives anabolic synthesis of fatty acids and nucleotides directly through transcription of genes utilized in these pathways, however; as they also require TCA cycle intermediates, this indicates that the role Myc plays in metabolic reprogramming is quite comprehensive.

HIF belongs to the PER-ARNT-SIM (PAS) subfamily of the bHLHZIP family of transcription factors, and is active as heterodimer of HIF-α and HIF-β (also known as aryl hydrocarbon receptor nuclear translocator [ARNT]) subunits (62). HIF-β subunits are stably transcribed and translated, and while HIF-α subunits are as well, they are also

modified by prolyl hydroxylases in the presence of oxygen, permitting HIF-α association with and ubiquitination by the von Hippel-Lindau (VHL) tumor suppressor and subsequently degraded in a proteasome-dependent manner (56). Under anaerobic conditions, HIF-α subunits are stabilized following inactivation of the TCA cycle-dependent prolyl hydroxylases and HIF heterodimers translocate to the nucleus to activate the transcription of many glycolytic targets. HIF also regulates genes involved in cell survival as well as those that inhibit macromolecular synthesis, consistent with decreased TCA cycle and oxidative function (68).

While HIF is primarily considered to increase anaerobic glycolysis, there is also data suggesting that HIF functions to increase aerobic glycolysis in response to growth factor signaling during normoxia (69). PI3K and MAPK activation has been shown to increase HIF-1α translation (70-72). Knockdown of HIF-1α in hematopoietic stem cells (HSCs) cultured under normoxic conditions demonstrated decreased lactate production but converted pyruvate to lipids at a higher rate, correlating with increased growth and proliferation rates (69). These data suggest that HIF-1 is a key component of growth factor induced aerobic glycolysis in normoxia; however, HIF-1 also appears to repress lipid biosynthesis, which is likely compensated by Myc transcriptional targets (62). These data do however ascribe a function in metabolic regulation in normoxia by HIF-1 that is consistent with RTK signaling regulation of metabolic reprogramming. Clearly, transcriptional regulation of metabolic reprogramming is complex and a new aspect of this regulation by MondoA is described in Chapter 2.

1.6 Thioredoxin Interacting Protein

Thioredoxin interacting protein (TXNIP), also known as vitamin D up-regulated protein 1 (VDUP1) and thioredoxin binding-protein 2 (TBP2), was originally identified as a transcript induced by vitamin D_3. Initially, TXNIP was thought to exert its function

exclusively by negatively regulating thioredoxin (Trx) through direct binding and inhibition of Trx reducing activity and by preventing Trx interaction with other binding partners (73-75). It is evident now however that TXNIP interacts with multiple protein partners to exert its many functions (76, 77). TXNIP has subsequently been implicated in myriad cellular processes including proliferation, differentiation and diseases including metabolic syndrome (diabetes) and cancer (78, 79). Considered a tumor suppressor, TXNIP levels are reduced in tumors and its over-expression causes cell cycle arrest (80). TXNIP is required for quiescence and negatively regulates glucose uptake and glycolysis (81, 82). As such, TXNIP is an excellent and emerging candidate in the regulation of metabolic reprogramming. Notably, vitamin D_3, which upregulates TXNIP expression, has also been shown to downregulate cMyc expression, suggesting that the two proteins might coordinately regulate growth and metabolic reprogramming (83). Germane to our lab, TXNIP is a direct and glucose dependent target of MondoA (section 1.7) (64, 84, 85). This section will therefore discuss the impact of TXNIP on cell metabolism and proliferation.

TXNIP is a member of the α-arrestin family of proteins (86). Its expression is regulated by a variety of environmental stresses including serum starvation, heat shock, H_2O_2, irradiation, lactic acidosis and transforming growth factor-β (TGF-β), all of which negatively affect cell proliferation (75, 80, 87). Consistent with these stimuli, anti-proliferative agents, e.g., histone deactylase (HDAC) inhibitors, 5-fluorouricil, dexamethasone, were shown to increase TXNIP expression in tumor cells suggesting that loss of TXNIP is essential for the proliferation of some cancers (84, 88, 89). Consistent with these findings, high TXNIP expression portends a positive outcome in breast and gastric cancers (77, 87, 90).

Some clues to how TXNIP might function to arrest cell growth and proliferation come from studies in HSCs wherein TXNIP expression was shown to be essential for maintaining quiescence (81). Similar to T cells (section 1.3), HSCs are maintained in a quiescent state in bone marrow until they are stimulated to proliferate and subsequently differentiate (81). In this study, TXNIP was downregulated during HSC activation and $TXNIP^{-/-}$ mice demonstrated decreased long-term HSC populations and the capacity to repopulate HSCs was lost. These effects were due to hyperactive cell cycling, Wnt signaling and failure to induce expression of the cyclin inhibitor p21 under stress conditions. These data suggest that while TXNIP is required for HSC quiescence, it also might drive cell cycle arrest by a p53 dependent mechanism (91). TXNIP has also been shown to increase $p27^{Kip1}$ stability by binding to JAB1, which targets $p27^{Kip1}$ for degradation (76). As $p27^{Kip1}$ is necessary for quiescence, its stabilization by TXNIP might drive growth arrest. Thus TXNIP's role as tumor suppressor may be linked to its role in maintaining quiescence.

Another mechanism by which TXNIP negatively regulates proliferation is directly correlated with growth factor signal transduction. Data from TXNIP null MEFs implies that TXNIP activates PTEN by a REDOX-mediated mechanism and thus blocks signals transduced through PI3K (section 1.4) (19). As TXNIP inhibits Trx, it also inhibits Trx mediated NADPH-dependent disulfide reduction which oxidizes PTEN thus inactivating it (19). Since PTEN phosphatase activity dephosphorylates $PI(3,4,5)P_3$ residues in the plasma membrane required for Akt activation, signals downstream of PI3K are thus blocked by active PTEN (section 1.4). $TXNIP^{-/-}$ mice were unable to switch from glucose utilization (aerobic glycolysis) to β-oxidation upon food deprivation. The mice become hypoglycemic and hypertriglyceridemic consistent with increased aerobic glycolysis and macromolecular synthesis. These data are consistent with a model whereby TXNIP is regulated by nutrient conditions to optimize fuel selection based on growth or survival

and suggests that TXNIP upregulation might also regulate inhibit cell growth by blocking aerobic glycolysis.

TXNIP has also been shown to inhibit glucose uptake (64, 85). As TXNIP inhibits both glucose uptake and glycolysis, one way TXNIP might regulate cell growth is by restricting nutrient availability and utilization (82). TXNIP may affect cell nutrient utilization in several ways. Murine embryonic fibroblasts from $TXNIP^{-/-}$ mice have increased glucose uptake and lactate production compared to their wild type counterparts (19, 92). As discussed above, TXNIP deletion alone is sufficient to drive metabolic reprogramming toward aerobic glycolysis (19). Additionally, TXNIP destabilizes HIF1-α in normoxia (77). As HIF-1α activates the transcription of glycolytic genes (section 1.5), TXNIP may downregulate a transcriptional program that drives glycolysis (62). In combination with TXNIP regulation of PTEN, TXNIP may negatively regulate cell proliferation by controlling several of the core metabolic pathways required for cell growth. These observations provide the basis for examining TXNIP regulation in G_0/G_1 transition discussed in Chapter 2, where we demonstrate that TXNIP translational and transcriptional downregulation is required for metabolic reprogramming in fibroblasts re-entering the cell cycle from a quiescent state.

1.7 MondoA

MondoA is a bHLHZip transcription factor related to the Myc superfamily which bears superficial similarity to Myc, Max and Mxd (Mad) (Figure 1.4) (93, 94). MondoA dimerizes with another bHLHZip protein, Max-like protein (Mlx) and MondoA:Mlx dimers bind to and affect transcription from E-box related elements in the promoter regions of their target genes suggesting they might also regulate Myc:Max targets including those required for growth and metabolism (57). While MondoA:Mlx complexes appear to function in a manner similar to Myc:Max complexes, a distinguishing feature of

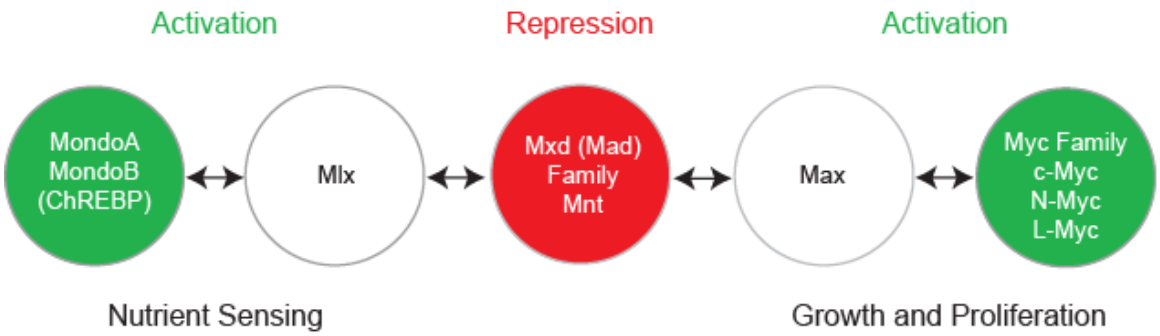

Figure 1.4 MondoA and ChREBP comprise a parallel Myc-like transcription network. MondoA activates transcription by dimerizing with Mlx. Generally, Myc activates transcription through dimerization with Max. Transcriptional repression occurs by Mlx and Max dimerization with Mxd (Mad) family members. Additionally, Mnt binds Max to repress Myc transcriptional targets. Transcriptional activation from both Myc and Mondo networks results in regulation of cell growth and metabolism discussed in the text.

MondoA:Mlx dimers is that they reside on the outer mitochondrial membrane and translocate to the nucleus to enable transcription in response to nutritional cues (63, 64, 84, 85). Much of the work characterizing MondoA function has been done by our lab and this section reviews the role we have identified for MondoA in glucose sensing and the ensuing adaptive transcriptional programs the MondoA:Mlx complexes enable. Specifically, MondoA:Mlx complexes exert their transcriptional control on the processes of metabolism and nutrient availability directly through regulation of transcriptional targets like TXNIP (section 1.6).

Structurally, MondoA bears superficial similarity to Myc (Figure 1.5). Its carboxy-terminal region contains a bHLHZip domain, a dimerization domain and a transcriptional activation domain similar are to Myc (93). Where MondoA structure deviates significantly from Myc is in its amino-terminal Mondo Conserved Regions (MCRs) (93). MondoA possesses five MCRs which regulate nuclear accumulation of MondoA:Mlx heterodimers in response to glucose-6-phoshate (discussed below) (85). Additionally, the dimerization and cytoplasmic localization domain (DCD) in the carboxy-terminus, common to MondoA and the Mlx isoforms α, β and γ, is uniquely required for MondoA:Mlx cytoplasmic retention (93). Another member of the Mondo family, the carbohydrate response element binding protein, ChREBP (MondoB), shares structural and regulatory similarities and will be further addressed later in this section.

Work form our lab has established that MondoA:Mlx complexes reside on the surface of the outer mitochondrial matrix (OMM) and shuttle between the mitochondria and nucleus (63, 64). Additional work established that extracellular glucose concentrations and more specifically, the intracellular glucose metabolite G6P concentrations promote MondoA:Mlx nuclear translocation (64, 85). ChREBP:Mlx complexes function similarly, and while the PPP intermediate xylulose-5-phosphate (X5P) drives nuclear translocation, G6P has also been recently implicated (95, 96).

Figure 1.5 Structural similarities between MondoA, Mlx, Myc and Max. The unifying feature within all is the basic helix-loop-helix leucine zipper (bHLHZip) domain which is similar in all Myc superfamily members allowing DNA binding to CACGTG or related E-box elements in the promoters of target genes. MondoA (and ChREBP) are approximately twice the size of Myc. MondoA and Mlx have dimerization and cytoplasmic localization domains (DCD) and Mondo family members have the regulatory Mondo Conserved Regions (MCRs) which are required for glucose regulated Mondo transcriptional activity.

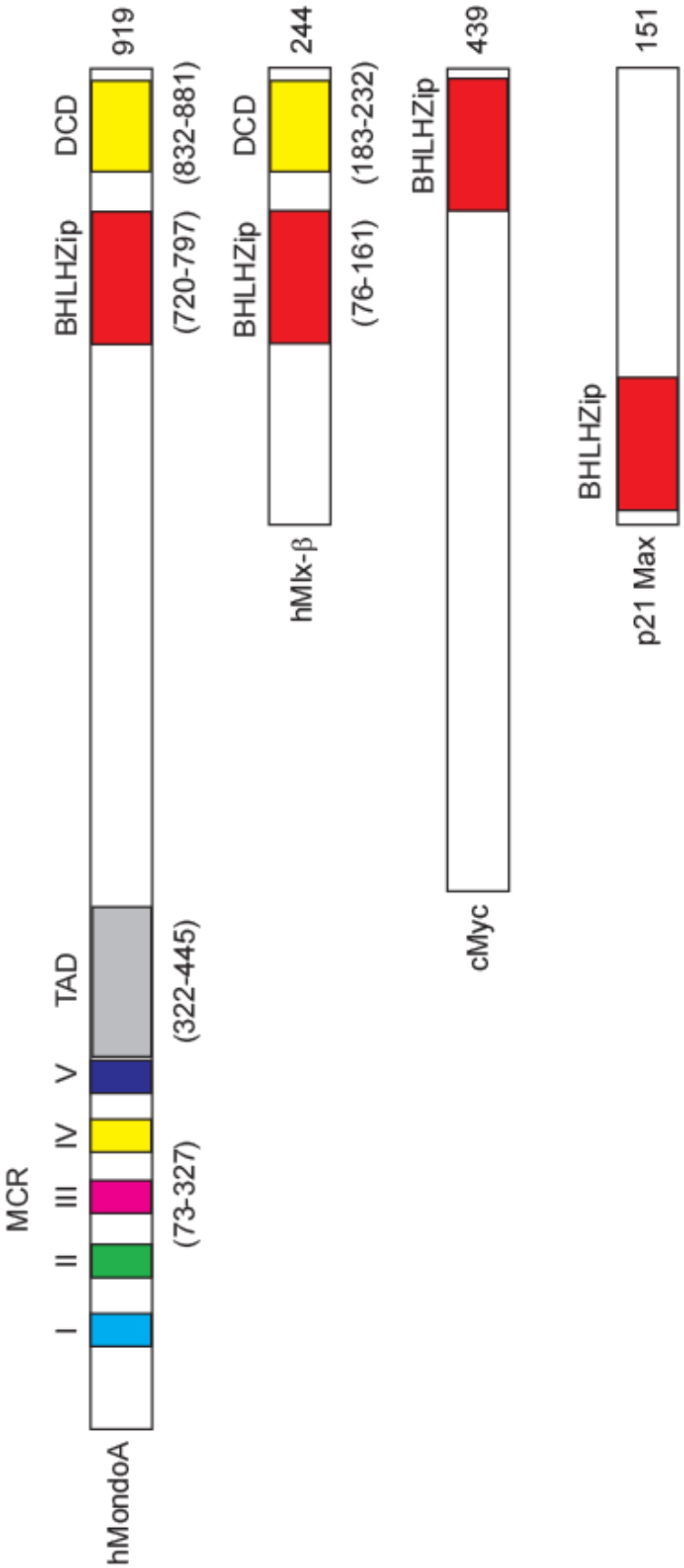
hMondoA
MCR
I
II
III
IV
V
TAD
(73-327)
(322-445)
BHLHZip
DCD
(720-797)
(832-881)
919
hMlx-β
BHLHZip
DCD
(76-161)
(183-232)
244
cMyc
BHLHZip
439
p21 Max
BHLHZip
151

Once in the nucleus, MondoA has been shown to activate genes involved in glycolysis including, hexokinase II (HKII), 6-phosphofructo-2-kinase/fructose-2,6-biphosphatase 3 (PFKFB3) and LDHA, however, it does not appear that these targets are glucose regulated MondoA targets (63). MondoA has been shown to be necessary for >75% of the transcriptional targets upregulated by glucose, suggesting that MondoA mitochondrial localization allows it to sense nutrient or bioenenergetic status and mount an adaptive transcriptional response (64). As such, we consider MondoA a glucose sensor and its nuclear accumulation, promoter binding and transcriptional activity at glucose regulated targets reflects cellular nutrient status (85).

As discussed in section 1.6, TXNIP is a direct and glucose regulated target of MondoA (64). MondoA binds directly to carbohydrate response elements (ChoRE) in the TXNIP promoter following elevations in G6P and MondoA knockout MEFs have no detectable TXNIP mRNA or protein expression (85). MondoA and TXNIP expression restrict glucose uptake; MondoA and TXNIP null MEFs exhibit high rates of glucose uptake compared to their wild type counterparts, and expression of a constitutively active MondoA allele missing the MCRs and containing a nuclear localization signal (ΔN237NLSMondoA) severely restricts glucose uptake while dramatically increasing TXNIP expression (64). This suggests that MondoA might transcriptionally link glucose availability to glycolytic rate; high G6P concentrations would signal that glucose uptake and phosphorylation by HKII is in excess for the downstream enzymes in glycolysis and as such MondoA upregulation of targets like TXNIP decrease the uptake of glucose into cell until the G6P accumulation is resolved. This model proposes that MondoA and TXNIP are part of a negative feedback regulatory circuit for glucose metabolism, ultimately controlling glycolytic rate by restricting substrate availability. TXNIP triggers apoptosis in pancreatic β-cells in response to hyperglycemia, suggesting that this

circuitry may simply allow the cell to respond to nutrient stress conditions (97). However, knockdown of MondoA in certain cell contexts increases cell growth and proliferation (84) and as seen in Chapter 2, ΔN237NLSMondoA restricts cells growth. While TXNIP has been shown to negatively regulate glycolysis, there is no direct evidence that MondoA, other than its transcriptional regulation of TXNIP, regulates glycolysis in this way. In fact, knockdown of MondoA in K562 cells was shown to reduce glycolytic flux (63). As discussed in Chapter 2, regulation of TXNIP translation, independent of its mRNA synthesis, plays an important role in its regulatory activities, and thus this paradox remains largely unresolved.

We have established that MondoA transcriptional activity restricts glucose uptake in several cell lines through its transcriptional upregulation of TXNIP. Our current understanding of MondoA function suggests a key role in integrating and coordinating signals from another major circulating nutrient, glutamine. While cells grown on plastic in the presence of glucose alone demonstrate high levels of TXNIP expression and do not grow, the addition of glutamine, which is absolutely required for growth, reduces TXNIP expression and permits cell proliferation (84). Essentially, glutamine converts MondoA from a transcriptional activator of TXNIP into a potent HDAC-dependent transcriptional repressor. As the glutamine repression of TXNIP by MondoA can be blocked by inhibitors of glutaminolysis (e.g., aminoxyacetate (AOA)) or mimicked by α-KG analogs, this suggests that MondoA-dependent transcriptional activity might be downregulated in response to anapleurosis. This would indicate that MondoA activity is in opposition to aerobic glycolysis and cell growth. This suggests a model whereby MondoA monitors glucose and glutamine-dependent signals that converge at the mitrochondria, essentially making MondoA a TCA cycle sensor. These data support a model where MondoA

negatively regulates cell growth by restricting substrate availability for aerobic glycolysis and as explored in Chapter 2, MondoA negatively regulates cell growth in this manner.

While MondoA loss has been shown to increase glucose uptake and cell proliferation on plastic and soft agar, its paralog ChREBP has been shown to do quite the opposite. ChREBP loss slows cell proliferation and reduces glucose uptake and lactate production, suggesting that it can stimulate aerobic glycolysis and thus anabolic growth (65). As MondoA and ChREBP are most highly expressed in the postmitotic tissues skeletal muscle and liver, respectively (94, 98), this suggests that they regulate energy homeostasis in somatic tissues by opposing mechanisms. Further complicating the involvement of MondoA and ChREBP in aerobic glycolysis, the liver-type pyruvate kinase (pklr) promoter was shown to require co-occupancy by both Myc and ChREBP for appropriate transcriptional activation (99). This suggests that ChREBP and MondoA may cooperate with Myc to regulate the expression of other targets active in glycolysis. While the mechanistic details of the Mondo family involvement in the partitioning of carbon flux necessary for cell growth and proliferation are only just emerging, it is clear they play an important role. In Chapter 2 we show that MondoA transcriptional activity negatively regulates entry into the cell cycle by restricting glucose availability and glycolytic flux, suggesting that downregulation of this activity is necessary for cell growth.

1.8 Summary

The sections outlined in this introduction provide for a framework for understanding the importance and complexity of metabolic reprogramming. While the phenomenon of metabolic reprogramming has become more broadly accepted, the underlying mechanisms regulating it are poorly understood. It is clearer that extra- and intracellular signaling pathways and transcriptional networks are integrally involved in cell growth and proliferation, but how they actually coordinate metabolism is only now

emerging. Aerobic glycolysis, the Warburg effect, once predominantly considered to be the metabolism of cancer, is now considered the metabolism of proliferation (2, 9, 27). Data from T cells suggest that signaling effectors down-stream of RTKs likely regulate metabolic reprogramming in other cell types. In cancers with activating mutations in RTKs or their down-stream effectors, increased glucose uptake and utilization by aerobic glycolysis is attributed to the affected pathways. PI3K signaling increases glucose uptake by mobilizing the translocation of GLUTs and Ras-MAPK signaling directly upregulates cMyc and Hif1α, both of which directly upregulate the transcription of most of the gene products acting in glycolysis. It is evident that the factors known to regulate cell proliferation also regulate the associated metabolic changes necessary to drive and support cell growth.

A further level of regulation of metabolic reprogramming has become apparent with the greater understanding of MondoA and TXNIP. The tumor suppressor TXNIP negatively regulates PI3K signaling, glucose uptake, glycolysis and proliferation and is therefore a likely candidate to participate in the regulation of metabolic reprogramming in proliferating cells. While the impact of TXNIP on glucose uptake and metabolism has not been shown to negatively affect proliferation directly, the necessity of macromolecular synthesis during cell growth suggests that this is likely. The transcription factor MondoA is required for TXNIP mRNA expression and negatively regulates glucose uptake, in part, through activating transcription of *TXNIP*. As such, MondoA is potentially involved the metabolic regulation of cell growth. The work presented in Chapter 2 provides evidence of roles for both MondoA and TXNIP in the regulation of metabolic reprogramming in cells transitioning from quiescence into the cell cycle and provides an initial mechanistic understanding of the regulation of MondoA and TXNIP during this transition.

1.9 References

1. Warburg O, Wind F, & Negelein E (1927) The metabolism of tumors in the body. *J Gen Physiol* 8(6):519-530.

2. Warburg O (1956) On the origin of cancer cells. *Science* 123(3191):309-314.

3. Garber K (2006) Energy deregulation: licensing tumors to grow. *Science* 312(5777):1158-1159.

4. Uldry M & Thorens B (2004) The SLC2 family of facilitated hexose and polyol transporters. *Pflugers Arch* 447(5):480-489.

5. Pelicano H, Martin DS, Xu RH, & Huang P (2006) Glycolysis inhibition for anticancer treatment. *Oncogene* 25(34):4633-4646.

6. Vander Heiden MG, Cantley LC, & Thompson CB (2009) Understanding the Warburg effect: the metabolic requirements of cell proliferation. *Science* 324(5930):1029-1033.

7. Gatenby RA & Gillies RJ (2004) Why do cancers have high aerobic glycolysis? *Nat Rev Cancer* 4(11):891-899.

8. DeBerardinis RJ (2008) Is cancer a disease of abnormal cellular metabolism? New angles on an old idea. *Genet Med* 10(11):767-777.

9. DeBerardinis RJ, Lum JJ, Hatzivassiliou G, & Thompson CB (2008) The biology of cancer: metabolic reprogramming fuels cell growth and proliferation. *Cell Metab* 7(1):11-20.

10. Kroemer G & Pouyssegur J (2008) Tumor cell metabolism: cancer's Achilles' heel. *Cancer Cell* 13(6):472-482.

11. Newsholme EA, Crabtree B, & Ardawi MS (1985) The role of high rates of glycolysis and glutamine utilization in rapidly dividing cells. *Biosci Rep* 5(5):393-400.

12. Curi R, Newsholme P, & Newsholme EA (1988) Metabolism of pyruvate by isolated rat mesenteric lymphocytes, lymphocyte mitochondria and isolated mouse macrophages. *Biochem J* 250(2):383-388.

13. DeBerardinis RJ & Cheng T (2010) Q's next: the diverse functions of glutamine in metabolism, cell biology and cancer. *Oncogene* 29(3):313-324.

14. Christofk HR*, et al.* (2008) The M2 splice isoform of pyruvate kinase is important for cancer metabolism and tumour growth. *Nature* 452(7184):230-233.

15. Morrish F, Isern N, Sadilek M, Jeffrey M, & Hockenbery DM (2009) c-Myc activates multiple metabolic networks to generate substrates for cell-cycle entry. *Oncogene* 28(27):2485-2491.

16. Liu X*, et al.* (2010) Warburg effect revisited: an epigenetic link between glycolysis and gastric carcinogenesis. *Oncogene* 29(3):442-450.

17. Blouin MJ*, et al.* (2010) Loss of function of PTEN alters the relationship between glucose concentration and cell proliferation, increases glycolysis, and sensitizes cells to 2-deoxyglucose. *Cancer Lett* 289(2):246-253.

18. Feng Z & Levine AJ (2010) The regulation of energy metabolism and the IGF-1/mTOR pathways by the p53 protein. *Trends Cell Biol* 20(7):427-434.

19. Hui ST*, et al.* (2008) Txnip balances metabolic and growth signaling via PTEN disulfide reduction. *Proc Natl Acad Sci U S A* 105(10):3921-3926.

20. Frauwirth KA & Thompson CB (2004) Regulation of T lymphocyte metabolism. *J Immunol* 172(8):4661-4665.

21. Hua X & Thompson CB (2001) Quiescent T cells: actively maintaining inactivity. *Nat Immunol* 2(12):1097-1098.

22. Tollefsbol TO & Cohen HJ (1985) Culture kinetics of glycolytic enzyme induction, glucose utilization, and thymidine incorporation of extended-exposure phytohemagglutinin-stimulated human lymphocytes. *J Cell Physiol* 122(1):98-104.

23. Hume DA, Radik JL, Ferber E, & Weidemann MJ (1978) Aerobic glycolysis and lymphocyte transformation. *Biochem J* 174(3):703-709.

24. Vander Heiden MG*, et al.* (2001) Growth factors can influence cell growth and survival through effects on glucose metabolism. *Mol Cell Biol* 21(17):5899-5912.

25. Frauwirth KA*, et al.* (2002) The CD28 signaling pathway regulates glucose metabolism. *Immunity* 16(6):769-777.

26. Wieman HL, Wofford JA, & Rathmell JC (2007) Cytokine stimulation promotes glucose uptake via phosphatidylinositol-3 kinase/Akt regulation of Glut1 activity and trafficking. *Mol Biol Cell* 18(4):1437-1446.

27. Fox CJ, Hammerman PS, & Thompson CB (2005) Fuel feeds function: energy metabolism and the T-cell response. *Nat Rev Immunol* 5(11):844-852.

28. Lemmon MA & Schlessinger J (2010) Cell signaling by receptor tyrosine kinases. *Cell* 141(7):1117-1134.

29. Linggi B & Carpenter G (2006) ErbB receptors: new insights on mechanisms and biology. *Trends Cell Biol* 16(12):649-656.

30. Tan PB & Kim SK (1999) Signaling specificity: the RTK/RAS/MAP kinase pathway in metazoans. *Trends Genet* 15(4):145-149.

31. Pines G, Kostler WJ, & Yarden Y (2010) Oncogenic mutant forms of EGFR: lessons in signal transduction and targets for cancer therapy. *FEBS Lett* 584(12):2699-2706.

32. Engelman JA, Luo J, & Cantley LC (2006) The evolution of phosphatidylinositol 3-kinases as regulators of growth and metabolism. *Nat Rev Genet* 7(8):606-619.

33. Cantley LC (2002) The phosphoinositide 3-kinase pathway. *Science* 296(5573):1655-1657.

34. Manning BD & Cantley LC (2007) AKT/PKB signaling: navigating downstream. *Cell* 129(7):1261-1274.

35. Huang J & Manning BD (2009) A complex interplay between Akt, TSC2 and the two mTOR complexes. *Biochem Soc Trans* 37(Pt 1):217-222.

36. Clerkin JS, Naughton R, Quiney C, & Cotter TG (2008) Mechanisms of ROS modulated cell survival during carcinogenesis. *Cancer Lett* 266(1):30-36.

37. He A, Liu X, Liu L, Chang Y, & Fang F (2007) How many signals impinge on GLUT4 activation by insulin? *Cell Signal* 19(1):1-7.

38. Yuan TL & Cantley LC (2008) PI3K pathway alterations in cancer: variations on a theme. *Oncogene* 27(41):5497-5510.

39. Nimnual A & Bar-Sagi D (2002) The two hats of SOS. *Sci STKE* 2002(145):pe36.

40. Hancock JF (2003) Ras proteins: different signals from different locations. *Nat Rev Mol Cell Biol* 4(5):373-384.

41. Gille H*, et al.* (1995) ERK phosphorylation potentiates Elk-1-mediated ternary complex formation and transactivation. *EMBO J* 14(5):951-962.

42. Chuang CF & Ng SY (1994) Functional divergence of the MAP kinase pathway. ERK1 and ERK2 activate specific transcription factors. *FEBS Lett* 346(2-3):229-234.

43. Miglarese MR, Richardson AF, Aziz N, & Bender TP (1996) Differential regulation of c-Myb-induced transcription activation by a phosphorylation site in the negative regulatory domain. *J Biol Chem* 271(37):22697-22705.

44. Burns KA & Vanden Heuvel JP (2007) Modulation of PPAR activity via phosphorylation. *Biochim Biophys Acta* 1771(8):952-960.

45. Marshall CJ (1995) Specificity of receptor tyrosine kinase signaling: transient versus sustained extracellular signal-regulated kinase activation. *Cell* 80(2):179-185.

46. Jongeward GD, Clandinin TR, & Sternberg PW (1995) sli-1, a negative regulator of let-23-mediated signaling in C. elegans. *Genetics* 139(4):1553-1566.

47. Hajnal A, Whitfield CW, & Kim SK (1997) Inhibition of Caenorhabditis elegans vulval induction by gap-1 and by let-23 receptor tyrosine kinase. *Genes Dev* 11(20):2715-2728.

48. Guan KL (1994) The mitogen activated protein kinase signal transduction pathway: from the cell surface to the nucleus. *Cell Signal* 6(6):581-589.

49. Modzelewska K*, et al.* (2007) An activating mutation in sos-1 identifies its Dbl domain as a critical inhibitor of the epidermal growth factor receptor pathway during Caenorhabditis elegans vulval development. *Mol Cell Biol* 27(10):3695-3707.

50. Dang CV & Semenza GL (1999) Oncogenic alterations of metabolism. *Trends Biochem Sci* 24(2):68-72.

51. Racker E, Resnick RJ, & Feldman R (1985) Glycolysis and methylaminoisobutyrate uptake in rat-1 cells transfected with ras or myc oncogenes. *Proc Natl Acad Sci U S A* 82(11):3535-3538.

52. Ramanathan A, Wang C, & Schreiber SL (2005) Perturbational profiling of a cell-line model of tumorigenesis by using metabolic measurements. *Proc Natl Acad Sci U S A* 102(17):5992-5997.

53. Chen C, Pore N, Behrooz A, Ismail-Beigi F, & Maity A (2001) Regulation of glut1 mRNA by hypoxia-inducible factor-1. Interaction between H-ras and hypoxia. *J Biol Chem* 276(12):9519-9525.

54. Sears R, Leone G, DeGregori J, & Nevins JR (1999) Ras enhances Myc protein stability. *Mol Cell* 3(2):169-179.

55. Adhikary S & Eilers M (2005) Transcriptional regulation and transformation by Myc proteins. *Nat Rev Mol Cell Biol* 6(8):635-645.

56. Wiesener MS*, et al.* (2003) Widespread hypoxia-inducible expression of HIF-2alpha in distinct cell populations of different organs. *FASEB J* 17(2):271-273.

57. Meyer N & Penn LZ (2008) Reflecting on 25 years with MYC. *Nat Rev Cancer* 8(12):976-990.

58. White RJ (2008) RNA polymerases I and III, non-coding RNAs and cancer. *Trends Genet* 24(12):622-629.

59. Amati B, Alevizopoulos K, & Vlach J (1998) Myc and the cell cycle. *Front Biosci* 3:d250-268.

60. Schmidt EV (1999) The role of c-myc in cellular growth control. *Oncogene* 18(19):2988-2996.

61. Kim JW*, et al.* (2004) Evaluation of myc E-box phylogenetic footprints in glycolytic genes by chromatin immunoprecipitation assays. *Mol Cell Biol* 24(13):5923-5936.

62. Gordan JD, Thompson CB, & Simon MC (2007) HIF and c-Myc: sibling rivals for control of cancer cell metabolism and proliferation. *Cancer Cell* 12(2):108-113.

63. Sans CL, Satterwhite DJ, Stoltzman CA, Breen KT, & Ayer DE (2006) MondoA-Mlx heterodimers are candidate sensors of cellular energy status: mitochondrial localization and direct regulation of glycolysis. *Mol Cell Biol* 26(13):4863-4871.

64. Stoltzman CA*, et al.* (2008) Glucose sensing by MondoA:Mlx complexes: a role for hexokinases and direct regulation of thioredoxin-interacting protein expression. *Proc Natl Acad Sci U S A* 105(19):6912-6917.

65. Tong X, Zhao F, Mancuso A, Gruber JJ, & Thompson CB (2009) The glucose-responsive transcription factor ChREBP contributes to glucose-dependent anabolic synthesis and cell proliferation. *Proc Natl Acad Sci U S A* 106(51):21660-21665.

66. Wise DR*, et al.* (2008) Myc regulates a transcriptional program that stimulates mitochondrial glutaminolysis and leads to glutamine addiction. *Proc Natl Acad Sci U S A* 105(48):18782-18787.

67. Gao P*, et al.* (2009) c-Myc suppression of miR-23a/b enhances mitochondrial glutaminase expression and glutamine metabolism. *Nature* 458(7239):762-765.

68. Hu CJ, Wang LY, Chodosh LA, Keith B, & Simon MC (2003) Differential roles of hypoxia-inducible factor 1alpha (HIF-1alpha) and HIF-2alpha in hypoxic gene regulation. *Mol Cell Biol* 23(24):9361-9374.

69. Lum JJ*, et al.* (2007) The transcription factor HIF-1alpha plays a critical role in the growth factor-dependent regulation of both aerobic and anaerobic glycolysis. *Genes Dev* 21(9):1037-1049.

70. Zhong H*, et al.* (2000) Modulation of hypoxia-inducible factor 1alpha expression by the epidermal growth factor/phosphatidylinositol 3-kinase/PTEN/AKT/FRAP pathway in human prostate cancer cells: implications for tumor angiogenesis and therapeutics. *Cancer Res* 60(6):1541-1545.

71. Laughner E, Taghavi P, Chiles K, Mahon PC, & Semenza GL (2001) HER2 (neu) signaling increases the rate of hypoxia-inducible factor 1alpha (HIF-1alpha) synthesis: novel mechanism for HIF-1-mediated vascular endothelial growth factor expression. *Mol Cell Biol* 21(12):3995-4004.

72. Kasuno K*, et al.* (2004) Nitric oxide induces hypoxia-inducible factor 1 activation that is dependent on MAPK and phosphatidylinositol 3-kinase signaling. *J Biol Chem* 279(4):2550-2558.

73. Kim SY, Suh HW, Chung JW, Yoon SR, & Choi I (2007) Diverse functions of VDUP1 in cell proliferation, differentiation, and diseases. *Cell Mol Immunol* 4(5):345-351.

74. Nishiyama A*, et al.* (1999) Identification of thioredoxin-binding protein-2/vitamin D(3) up-regulated protein 1 as a negative regulator of thioredoxin function and expression. *J Biol Chem* 274(31):21645-21650.

75. Junn E*, et al.* (2000) Vitamin D3 up-regulated protein 1 mediates oxidative stress via suppressing the thioredoxin function. *J Immunol* 164(12):6287-6295.

76. Jeon JH*, et al.* (2005) Tumor suppressor VDUP1 increases p27(kip1) stability by inhibiting JAB1. *Cancer Res* 65(11):4485-4489.

77. Shin D*, et al.* (2008) VDUP1 mediates nuclear export of HIF1alpha via CRM1-dependent pathway. *Biochim Biophys Acta* 1783(5):838-848.

78. Parikh H*, et al.* (2007) TXNIP regulates peripheral glucose metabolism in humans. *PLoS Med* 4(5):e158.

79. Nishinaka Y*, et al.* (2004) Loss of thioredoxin-binding protein-2/vitamin D3 up-regulated protein 1 in human T-cell leukemia virus type I-dependent T-cell transformation: implications for adult T-cell leukemia leukemogenesis. *Cancer Res* 64(4):1287-1292.

80. Han SH*, et al.* (2003) VDUP1 upregulated by TGF-beta1 and 1,25-dihydorxyvitamin D3 inhibits tumor cell growth by blocking cell-cycle progression. *Oncogene* 22(26):4035-4046.

81. Jeong M*, et al.* (2009) Thioredoxin-interacting protein regulates hematopoietic stem cell quiescence and mobilization under stress conditions. *J Immunol* 183(4):2495-2505.

82. Patwari P*, et al.* (2009) Thioredoxin-independent regulation of metabolism by the alpha-arrestin proteins. *J Biol Chem* 284(37):24996-25003.

83. Rohan JN & Weigel NL (2009) 1Alpha,25-dihydroxyvitamin D3 reduces c-Myc expression, inhibiting proliferation and causing G1 accumulation in C4-2 prostate cancer cells. *Endocrinology* 150(5):2046-2054.

84. Kaadige MR, Looper RE, Kamalanaadhan S, & Ayer DE (2009) Glutamine-dependent anapleurosis dictates glucose uptake and cell growth by regulating MondoA transcriptional activity. *Proc Natl Acad Sci U S A* 106(35):14878-14883.

85. Peterson CW, Stoltzman CA, Sighinolfi MP, Han KS, & Ayer DE (2010) Glucose controls nuclear accumulation, promoter binding, and transcriptional activity of the MondoA-Mlx heterodimer. *Mol Cell Biol* 30(12):2887-2895.

86. Alvarez CE (2008) On the origins of arrestin and rhodopsin. *BMC Evol Biol* 8:222.

87. Chen JL-Y*, et al.* (2010) Lactic acidosis triggers starvation response with paradoxical induction of TXNIP through MondoA. *PloS Genetics* In Press.

88. Butler LM*, et al.* (2002) The histone deacetylase inhibitor SAHA arrests cancer cell growth, up-regulates thioredoxin-binding protein-2, and down-regulates thioredoxin. *Proc Natl Acad Sci U S A* 99(18):11700-11705.

89. Deroo BJ, Hewitt SC, Peddada SD, & Korach KS (2004) Estradiol regulates the thioredoxin antioxidant system in the mouse uterus. *Endocrinology* 145(12):5485-5492.

90. Cadenas C*, et al.* (2010) Role of thioredoxin reductase 1 and thioredoxin interacting protein in prognosis of breast cancer. *Breast Cancer Res* 12(3):R44.

91. Jung YS, Qian Y, & Chen X (2010) Examination of the expanding pathways for the regulation of p21 expression and activity. *Cell Signal* 22(7):1003-1012.

92. Chutkow WA, Patwari P, Yoshioka J, & Lee RT (2008) Thioredoxin-interacting protein (Txnip) is a critical regulator of hepatic glucose production. *J Biol Chem* 283(4):2397-2406.

93. Billin AN & Ayer DE (2006) The Mlx network: evidence for a parallel Max-like transcriptional network that regulates energy metabolism. *Curr Top Microbiol Immunol* 302:255-278.

94. Billin AN, Eilers AL, Coulter KL, Logan JS, & Ayer DE (2000) MondoA, a novel basic helix-loop-helix-leucine zipper transcriptional activator that constitutes a positive branch of a max-like network. *Mol Cell Biol* 20(23):8845-8854.

95. Li MV*, et al.* (2010) Glucose-6-phosphate mediates activation of the carbohydrate responsive binding protein (ChREBP). *Biochem Biophys Res Commun* 395(3):395-400.

96. Uyeda K & Repa JJ (2006) Carbohydrate response element binding protein, ChREBP, a transcription factor coupling hepatic glucose utilization and lipid synthesis. *Cell Metab* 4(2):107-110.

97. Minn AH, Hafele C, & Shalev A (2005) Thioredoxin-interacting protein is stimulated by glucose through a carbohydrate response element and induces beta-cell apoptosis. *Endocrinology* 146(5):2397-2405.

98. Yamashita H*, et al.* (2001) A glucose-responsive transcription factor that regulates carbohydrate metabolism in the liver. *Proc Natl Acad Sci U S A* 98(16):9116-9121.

99. Zhang P*, et al.* (2010) c-Myc is required for the CHREBP-dependent activation of glucose-responsive genes. *Mol Endocrinol* 24(6):1274-1286.

CHAPTER 2

TRANSCRIPTIONAL AND TRANSLATIONAL DOWNREGULATION OF THIOREDOXIN INTERACTING PROTEIN DRIVES METABOLIC REPROGRAMMING DURING G_1

Chapter 2 is a manuscript currently under review by Genes & Cancer. Marc G. Elgort, John M. O'Shea, Yike Jiang and Donald E. Ayer are the authors on this manuscript. John M. O'Shea isolated T lymphocytes from murine spleens and performed the western blot and glucose uptake assay for Figure 2.1A and 2.1B. Yike Jiang performed the BrdU incorporation assays in wild type and TXNIP null MEFs for Figure 2.1C.

2.1 Abstract

Growth factor signaling drives increased glucose uptake and glycolysis - the Warburg effect - that supports macromolecular synthesis necessary for cell growth and proliferation. Thioredoxin interacting protein (TXNIP), a direct and glucose-induced transcriptional target of MondoA, is a potent negative regulator of glucose uptake and utilization. Thus, TXNIP may inhibit cell growth by restricting substrate availability for macromolecular synthesis. To determine TXNIP's contribution to metabolic reprogramming, we examined MondoA and TXNIP as cells exit quiescence and enter G_1. Serum stimulation of quiescent immortal diploid fibroblasts resulted in an acute upregulation of glucose uptake and glycolysis coinciding with downregulation of TXNIP expression. Ectopic expression of either MondoA or TXNIP restricted cell growth by blocking glucose uptake. Mechanistically, Ras-MAPK and PI3K/Akt signaling inhibit *TXNIP* translation and MondoA-dependent TXNIP transcription, respectively. We propose that the coordinated down regulation of MondoA transcriptional activity at the TXNIP promoter and inhibition of *TXNIP* translation are key components of metabolic reprogramming required for cells to exit quiescence.

2.2 Introduction

In metazoans, cell proliferation is required for normal organismal function as well as tumorigenesis. Cell proliferation requires increased aerobic glycolysis – the Warburg effect – for *de novo* synthesis of fatty acids, nucleic acids, proteins and energy required to increase biomass during the growth phase (G_1) of the cell cycle (1-4). Consistent with an increase in anabolic metabolism, extracellular nutrients such as glucose and amino acids are taken up at higher rates by growing cells to support the increased flux through the biosynthetic pathways that utilize them (5-7). Certain cell populations exist in a relatively metabolically inactive or quiescent state. Quiescent cells exhibit low flux of

glucose through glycolysis and primarily utilize β-oxidation of fatty acids and the tricarboxylic acid cycle (TCA) for survival (8, 9). However, when quiescent cells are stimulated to proliferate they increase flux through glycolysis while maintaining TCA activity through anapleurosis (2, 10). This reorganization of cellular metabolic programs is required to support biosynthetic processes necessary for cell growth and proliferation. Similarly, transformed cells also reprogram their metabolism to aerobic glycolysis to support their increased proliferation (11, 12). While signals that stimulate cell proliferation have been shown to orchestrate this metabolic reprogramming, little is known about the downstream effectors involved in this process (4).

Originally identified as a transcript induced by vitamin D_3, thioredoxin interacting protein (TXNIP) has been subsequently implicated in myriad cellular processes including proliferation, differentiation as well as disease (13-16). Considered a tumor suppressor, TXNIP levels are reduced in tumors and its over-expression causes cell cycle arrest (13, 17, 18). Consistent with these findings, high TXNIP expression portends a positive outcome in breast and gastric cancers (19-21). Some clues to how TXNIP might function to arrest cell growth come from studies in stem cells and those involving $p27^{Kip1}$; TXNIP expression is essential for maintaining hematopoietic stem cell (HSC) quiescence (22) and TXNIP stabilizes $p27^{Kip1}$ which is necessary for quiescence (23). Thus TXNIP's function as a tumor suppressor may be linked to its role in maintaining quiescence.

TXNIP negatively regulates glucose uptake and glycolysis, thus one way TXNIP may regulate cell growth is by restricting nutrient availability and utilization (24, 25). TXNIP may affect cell nutrient utilization in several ways. For example, murine embryonic fibroblasts (MEFs) from $TXNIP^{-/-}$ mice have increased glucose uptake and lactate production compared to their wild type counterparts. Thus deletion of TXNIP alone is sufficient to drive metabolic reprogramming toward aerobic glycolysis (24).

Furthermore, TXNIP destabilizes the hypoxia induced transcription factor, Hif1α, under normoxic growth conditions (21). HIF1α activates the transcription of most glycolytic target genes, thus TXNIP may downregulate a transcriptional program that drives glycolysis (26-28). Finally, TXNIP loss inactivates the PTEN lipid phosphatase by a REDOX-sensitive mechanism (29). PTEN negatively regulates glucose transporters and uptake by indirectly regulating the kinase activity of phosphoinositide 3-kinase (PI3K) (30, 31). Thus TXNIP may negatively regulate cell proliferation by controlling several of the core metabolic pathways required for cell proliferation.

Our lab is interested in how cells sense and respond transcriptionally to nutrients through the MondoA transcription factor. MondoA is a member of the basic helix-loop-helix leucine zipper (bHLHZIP) family of transcription factors and has superficial similarity to the Myc/Max/Mad family of transcriptional regulators (32-34). MondoA heterodimerizes with another bHLHZIP family member, Mlx, and MondoA:Mlx complexes are required for >75% of glucose-induced transcription in an epithelial cancer cell line model (35). Uniquely, MondoA:Mlx complexes reside at the outer mitochondrial membrane and translocate to the nucleus in response to elevated intracellular glucose-6-phosphate (G6P) concentrations, where they activate transcription of targets including TXNIP (35). Such a mechanism facilitates exchange of information about the bioenergetic state of the cell between the mitochondria and the nucleus. Thus, MondoA is a glucose sensor and its nuclear accumulation, promoter binding and transcriptional activity at glucose regulated targets reflects cellular nutrient status (36). MondoA binds directly to carbohydrate response elements (ChoRE) in the TXNIP promoter following elevations in G6P and MondoA knockout MEFs have no detectable TXNIP mRNA or protein expression (35, 36). Thus, TXNIP expression is entirely dependent on MondoA, suggesting a similarly pleiotropic role for MondoA in nutrient sensing and utilization.

Our current understanding of MondoA function suggests a key role in integrating and in coordinating signals from the two major circulating nutrients, glucose and glutamine. For glucose, we have established that MondoA transcriptional activity restricts glucose uptake in several cell lines, in part, through its transcriptional upregulation of TXNIP. Knockdown or knockout of MondoA increases glucose uptake in epithelial cells and ectopic TXNIP expression partially reverses this upregulation (35). Consistent with MondoA's negative regulation of glucose uptake, MondoA knockdown cells exhibit increased growth on plastic and in soft agar (37). Remarkably, glutamine converts MondoA from a glucose-dependent transcriptional activator of TXNIP to a potent histone deacetylase-dependent transcriptional repressor of TXNIP. Consistent with this molecular mechanism, glutamine-dependent repression of TXNIP by MondoA increases glucose uptake and proliferation (34, 37, 38). The glutamine effect on TXNIP expression requires glutamine metabolism *per se* and can be mimicked by TCA anapleurosis, suggesting that MondoA monitors glucose and glutamine-dependent signals that converge at the mitochondria.

MondoA has a paralog called the Carbohydrate Response Element Binding Protein (ChREBP), also known as MondoB. MondoA and ChREBP are most highly expressed in the post-mitotic tissues skeletal muscle and liver, respectively, suggesting they primarily regulate energy homeostasis in somatic tissues (33, 39). However, our studies and a recent report implicating ChREBP in anabolic synthesis and cell proliferation, suggest an important additional role for the Mondo family in regulating proliferative growth (40). Here, we investigate how *TXNIP* translation and MondoA-dependent TXNIP transcription are coordinately regulated to drive metabolic reprogramming as cells transition from quiescence into the growth phase of the cell cycle.

2.3 Results

2.3.1 TXNIP downregulation correlates with metabolic reprogramming and cell growth

Initially, to investigate whether TXNIP might be involved in metabolic reprogramming, we determined its levels in quiescent and activated T-lymphocytes. T-lymphocytes undergo a well characterized metabolic reprogramming following activation (4, 5, 7). Specifically, quiescent T-lymphocytes rely primarily on mitochondrial respiration for energy production, but following stimulation they dramatically increase glucose uptake and aerobic glycolysis (4, 7). As expected from these previous reports, glucose uptake was modestly increased in primary murine T-lymphocytes stimulated with α-CD3/α-CD28 for 4 hours; however, after 24 hours of activation, glucose uptake increased >5 fold over quiescent cells (Figure 2.1A). Consistent with TXNIP's negative regulation of glucose uptake, its levels decreased following 4 hours of activation and were undetectable after 24 hours (Figure 2.1B and data not shown). Thus, TXNIP downregulation correlates with metabolic reprogramming in activated T-lymphocytes.

To determine the necessity of TXNIP expression for cellular quiescence in other cell contexts, we utilized TXNIP-null murine embryonic fibroblasts (MEFs) (25, 41) and assessed growth arrest in the absence of serum. Compared to wild-type MEFs, TXNIP-null MEFs failed to arrest in response to 48 hours of serum deprivation, indicating that TXNIP is required for growth arrest in the absence of proliferative signals (Figure 2.1C). Taken together, our data from T-lymphocytes and TXNIP-null MEFs suggest that TXNIP downregulation may drive glucose repartitioning from oxidative metabolism to aerobic glycolysis as cells exit quiescence.

Since TXNIP is required for cellular quiescence, we determined whether TXNIP was downregulated in early G_1. For this study, we sought a tractable and well-

characterized system; normal diploid human BJ fibroblasts immortalized with human telomerase reverse transcriptase (BJ hTERT) (42). These cells can be synchronized in G_0 by serum withdrawal and stimulated by serum readdition to enter the cell cycle. Following 72 hours of serum starvation, quiescence in the BJ hTERTs was validated by stabilization of $p27^{Kip1}$ and accumulation of cells with 2N DNA content (43, 44). Following the readdition of serum, G_1/S progression was validated by $p27^{Kip1}$ loss by 4 hours, stabilization of cyclin A by 20 hours and DNA synthesis at 22 hours (Figure 2.1D and data not shown). TXNIP was upregulated in quiescent BJ hTERTs (Figure 2.1D), consistent with a role for TXNIP in β-oxidation of fatty acids (29). Within 4 hours of serum addition to quiescent BJ hTERTs, TXNIP loss was observed, suggesting that TXNIP downregulation was required for G_0 exit and G_1 entry. TXNIP protein returned by 12 hours post serum readdition, prior to the stabilization of cyclin A. TXNIP mRNA was also examined and like TXNIP protein downregulation, its mRNA was reduced >10 fold by 4 hours post serum addition (Figure 2.1E). Message increased by 12 hours and subsequently reached stable levels by 20 hours following serum addition. From these data, we conclude that TXNIP message and protein are coordinately downregulated as cells transition from G_0 into early G_1.

To determine whether metabolic reprogramming occurred in BJ hTERTs and correlated with TXNIP downregulation, glucose uptake and glycolytic flux were assayed. Glucose uptake nearly doubled within the first hour of serum readdition and reached maximal levels by 8-12 hours of G_1 progression (Figure 2.1F). As with glucose uptake, BJ hTERTs exhibited a >2-fold increase in glycolytic flux within 1 hour of serum readdition, which increased to >3-fold by 4 hours and subsequently plateaued by 8 hours (Figure 2.1G). Preliminary metabolomic studies revealed other indicators of increased glycolysis and no changes were observed in metabolites of TCA (not shown).

Figure 2.1 TXNIP downregulation correlates with metabolic reprogramming and cell growth (A) Increased glucose uptake in primary murine T-lymphocytes after 4 and 24 hours stimulation with α-CD3/α-CD28 (mean ± SD of duplicate biological samples) coincides with (B) TXNIP downregulation determined by western blotting. (C) BrdU incorporation was determined in immortalized wild-type and TXNIP-null MEFs growing asynchronously in complete media or serum-starved for 48 hours. Data are presented as percent of total BrdU incorporation relative to BrdU incorporation in asynchronous cells (mean ± SD of triplicate experiments). TXNIP expression and metabolic parameters were characterized during the G_0/G_1 transition in BJ hTERTs (D-F). (D) Expression of the indicated proteins was determined by western blotting. Serum withdrawal for 72 hours "Q" was sufficient to synchronize cells in G_0 ($p27^{Kip1}$ stabilization) and cyclin A stabilization at 20 hours post serum addition preceded S-phase at 22 hours (determined by BrdU labeling, not shown) (asynchronous cells, "A"). (E) Expression of TXNIP mRNA determined by RT-qPCR. Data are presented as fold change relative to expression in asynchronous cells "A" normalized to RPL19 mRNA (mean ± SD of triplicate samples). (F) Glucose uptake was determined in quiescent cells (G_0) and at the time points indicated following serum addition (G_1) (mean ± SD of triplicate biological samples). (G) Glycolytic flux was determined in G_0 and at the time points indicated (G_1) (mean ± SD of triplicate biological samples).

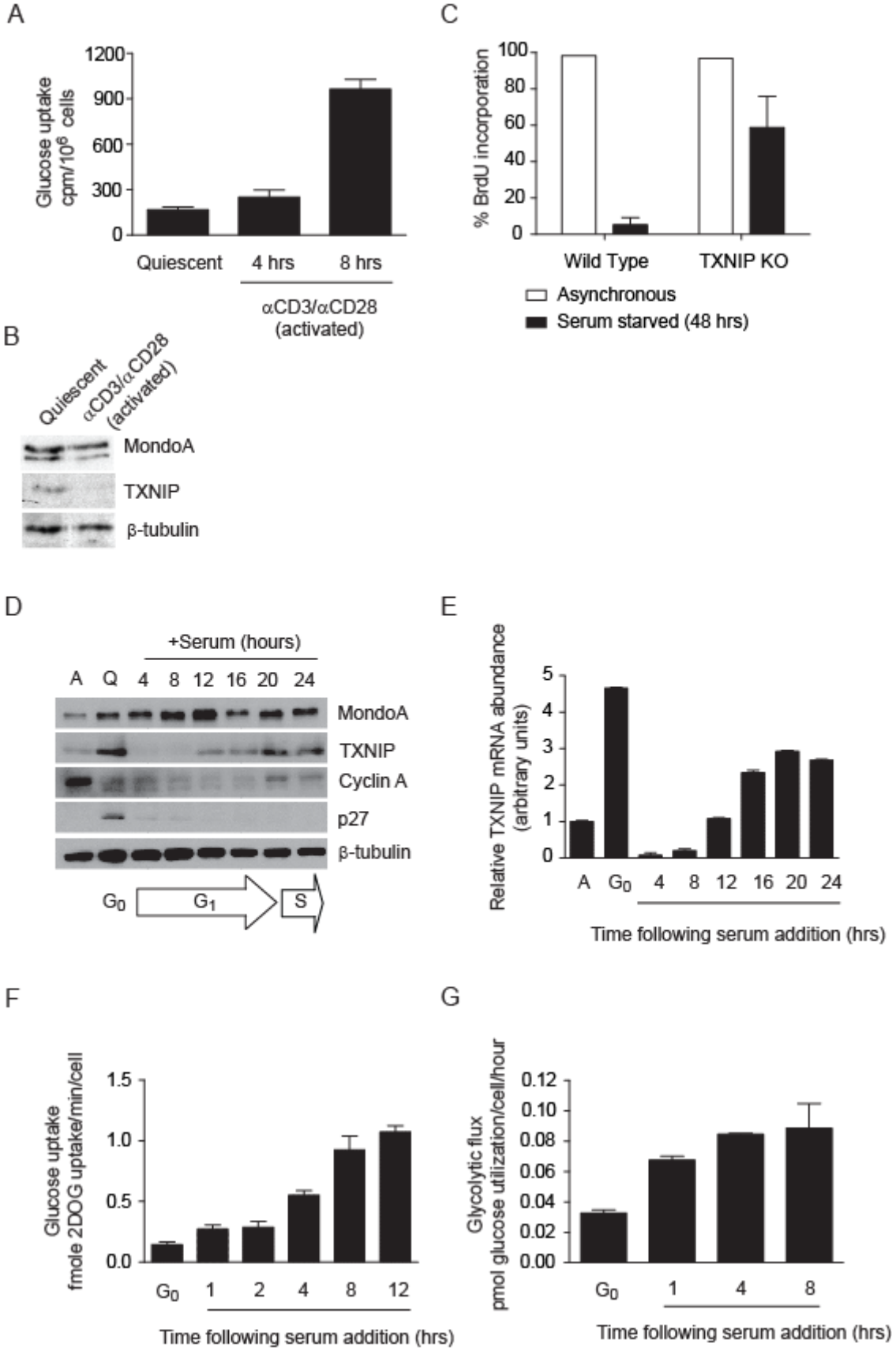
A
Glucose uptake cpm/10^6 cells
1200
900
600
300
0
Quiescent
4 hrs
8 hrs
αCD3/αCD28 (activated)
C
% BrdU incorporation
100
80
60
40
20
0
Wild Type
TXNIP KO
Asynchronous
Serum starved (48 hrs)
B
Quiescent
αCD3/αCD28 (activated)
MondoA
TXNIP
β-tubulin
D
+Serum (hours)
A Q 4 8 12 16 20 24
MondoA
TXNIP
Cyclin A
p27
β-tubulin
G0 G1 S
E
Relative TXNIP mRNA abundance (arbitrary units)
5
4
3
2
1
0
A G0 4 8 12 16 20 24
Time following serum addition (hrs)
F
Glucose uptake fmole 2DOG uptake/min/cell
1.5
1.0
0.5
0.0
G0 1 2 4 8 12
Time following serum addition (hrs)
G
Glycolytic flux pmol glucose utilization/cell/hour
0.12
0.10
0.08
0.06
0.04
0.02
0.00
G0 1 4 8
Time following serum addition (hrs)

Taken together, TXNIP downregulation in early G_1 mirrors the increase in glucose uptake and aerobic glycolysis.

2.3.2 Ectopic TXNIP expression restricts glucose uptake, glycolysis and blocks G_1 progression

To assess whether TXNIP downregulation in early G_1 was necessary for increased glucose uptake and ultilization, and consequently cell growth, TXNIP was ectopically expressed in BJ hTERTs (Figure 2.2A). Following serum addition, ectopic TXNIP-mCherry expression blocked the elevated glucose uptake and glycolytic flux observed in control cells (Figure 2.2B and C). Ultimately, failure to completely downregulate TXNIP in early G_1 resulted in a decrease in the number of cells that progressed to S-phase (Figure 2.2D). Unlike endogenous TXNIP, TXNIP-mCherry persisted in early G_1 which demonstrated that ectopic TXNIP protein levels could be maintained even though there was downregulation. Because the TXNIP-mCherry fusion only encodes the TXNIP open reading frame, it is likely that the stability of endogenous TXNIP is regulated by its coding sequence rather than by non-coding regions in its mRNA (Figure 2.2A) (see below). Interestingly, TXNIP-mCherry reduced endogenous TXNIP protein indicating that cells must tightly regulate TXNIP levels. From these data, we conclude that TXNIP over-expression can block metabolic reprogramming in early G_1 suggesting that TXNIP downregulation is necessary for cell growth.

2.3.3 Dominant-active MondoA blocks G_1 progression

We have previously demonstrated that TXNIP expression is strictly dependent on MondoA and glucose in a number of different cell types (35-37); paradoxically, both glucose and MondoA are replete in early G_1, but TXNIP protein and message are completely absent (Figure 2.1D and E and 2.2A). To further understand the regulation of

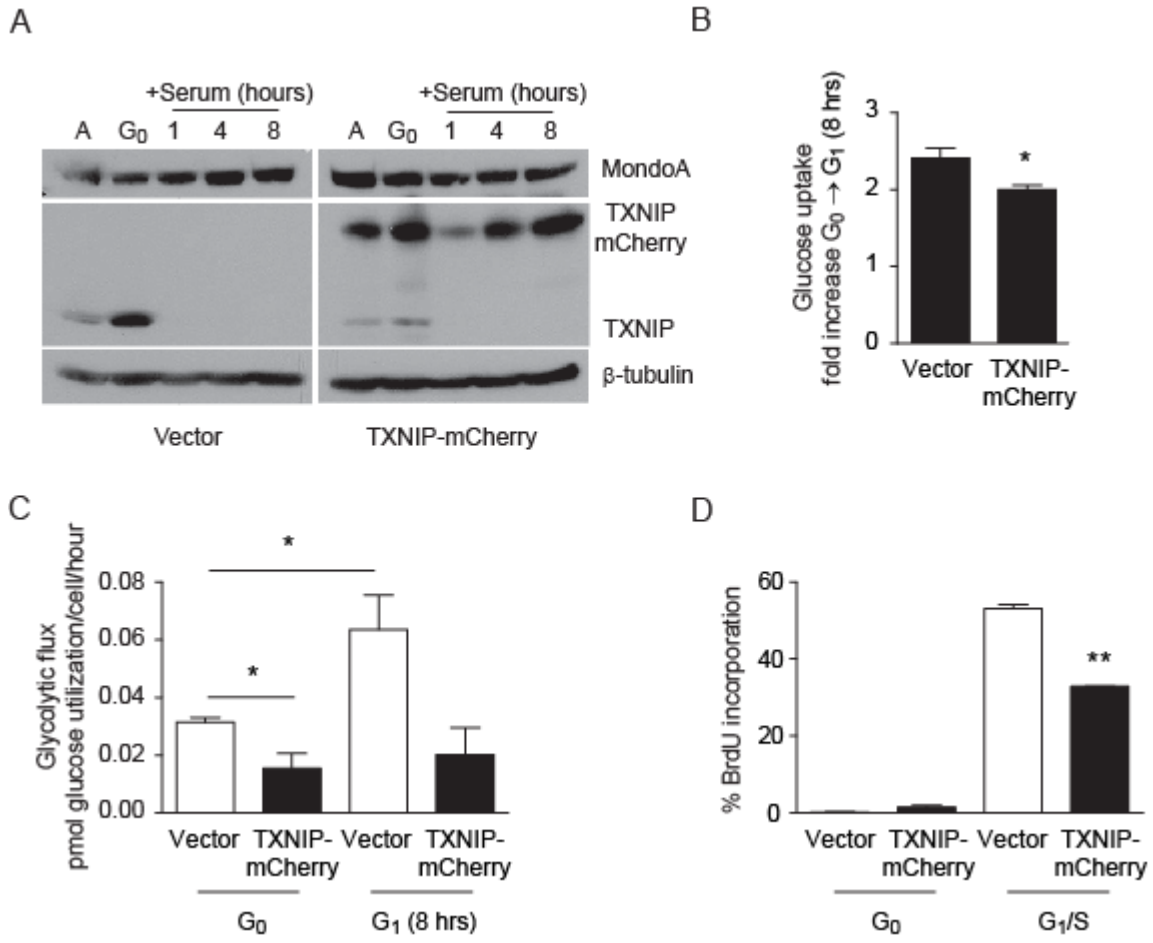

Figure 2.2 Ectopic TXNIP expression restricts glucose uptake, glycolysis and blocks G_1 progression (A) Expression of the indicated proteins in BJ hTERTs under indicated growth conditions determined by western blotting. (B) Glucose uptake was determined in control and TXNIP-mCherry infected BJ hTERTs in G_0 and following 8 hrs serum treatment. Data are presented as fold change relative to G_0 (mean ± SD. *, $P < 0.05$, paired student's t-test, n=3). (C) Glycolytic flux was measured for conditions as in (B). Each data point represents triplicate assay points from duplicate biological samples from 3 independent experiments (*, $P < 0.05$, paired student's t-test, n=3). (D) BrdU labeling of control or TXNIP-mCherry infected BJ hTERTs in G_0 and following 24 hour serum treatment (G_1/S). Data are presented as percent BrdU labeling relative to total cells counted. (mean ± SD. **, $P < 0.02$, paired student's t-test, n=3).

TXNIP expression by serum, we first established that its expression was MondoA-dependent in BJ hTERTs. Consistent with our published data, TXNIP levels were dramatically reduced in MondoA knockdown BJ hTERTs compared to control cells (Figure 2.3A), confirming that TXNIP expression is MondoA-dependent in this cell system.

To determine whether MondoA played a role in metabolic reprogramming in early G_1 and consequently G_1 progression, we ectopically expressed a constitutively active allele of MondoA, ΔN237NLSMondoA in BJ hTERTs (45). ΔN237NLSMondoA drove high TXNIP expression in both asynchronous and quiescent cells and importantly, partially blocked downregulation of TXNIP in early G_1 (Figure 2.3B). Additionally, ΔN237NLSMondoA expression in early G_1 resulted in a significant decrease in glucose uptake (Figure 2.3C). Most importantly, ΔN237NLSMondoA drove a significant decrease in the number of cells that reached S-phase (Figure 2.3E). Furthermore, Hif1α stabilization drives aerobic glycolysis (46) and, consistent with metabolic reprogramming, HIF1α was stabilized in early G_1 of control BJ hTERTs. Notably, ΔN237NLSMondoA expression resulted in loss of normoxic Hif1α expression in early G_1 (Figure 2.3B). Surprisingly, ΔN237NLSMondoA did not decrease glycolytic flux like TXNIP-mCherry and we attribute this disparity to constitutive activation or repression of other MondoA transcriptional targets (Figure 2.3D). We conclude that constitutive ectopic MondoA activity is sufficient to block cell growth, presumably by preventing TXNIP downregulation. These data suggest an important role for MondoA in regulating metabolic reprogramming in early G_1.

Figure 2.3 Dominant-active MondoA blocks G_1 progression (A) Determination of MondoA, TXNIP and β-tubulin expression in control and MondoA knockdown BJ hTERTs by western blotting. (B) Expression of TXNIP, MondoA, ΔN237NLSMondoA, Hif1α and β-tubulin in BJ hTERTs under indicated growth conditions determined by western blotting. (C) Glucose uptake was determined in control and ΔN237NLSMondoA expressing BJ hTERTs in G_0 and following 8 hrs serum treatment. Data are presented as fold change relative to G_0 (mean ± SD. *, $P < 0.05$, paired student's t-test, n=4). (D) Glycolytic flux was measured for conditions as in (C). Each data point represents triplicate assay points from duplicate biological samples from 3 independent experiments (mean ± SD). (E) BrdU labeling of control or ΔN237NLSMondoA expressing BJ hTERTs in G_0 and following 24 hour serum treatment (G_1/S). Data are presented as percent BrdU labeling relative to total cells counted. (mean ± SD. **, $P < 0.02$, paired student's t-test, n=3).

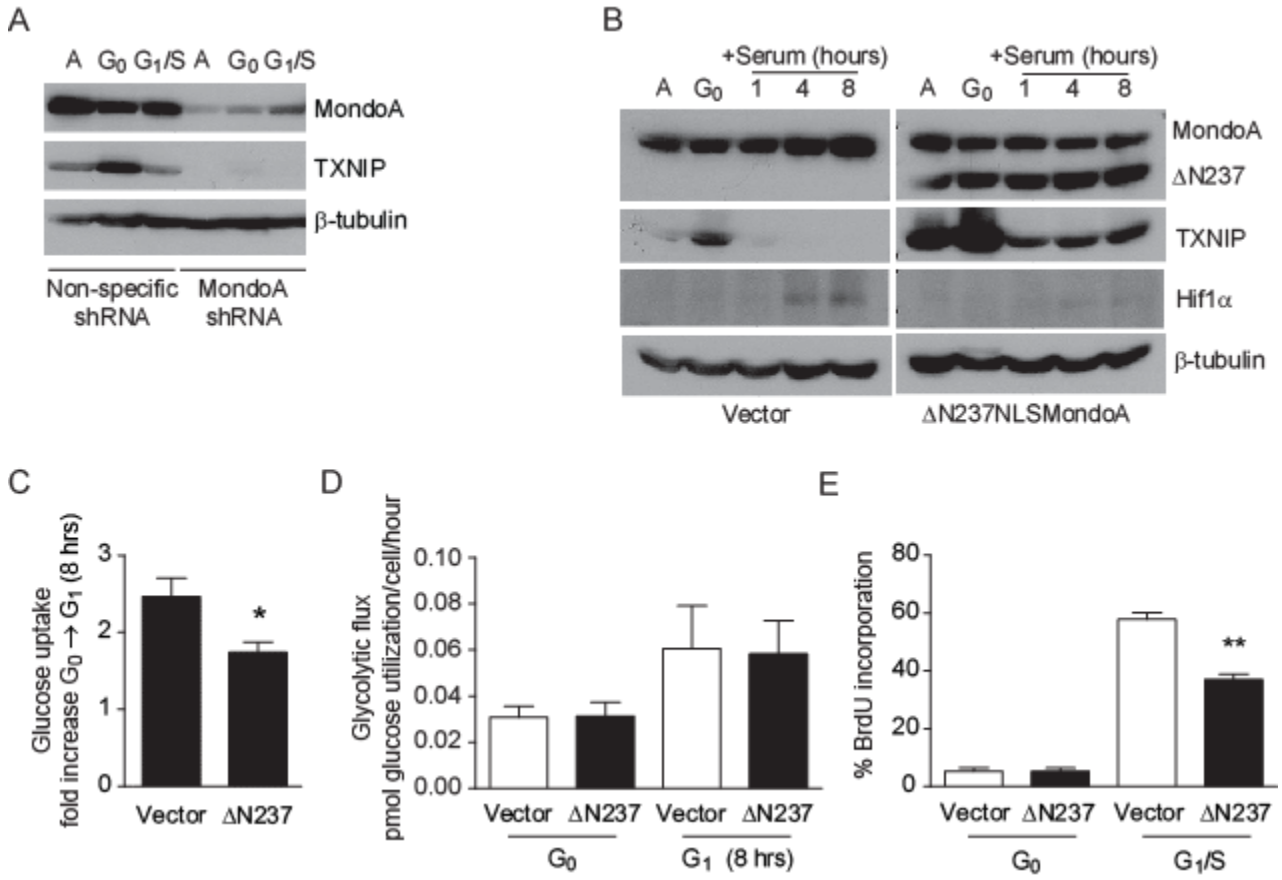
A
A G0 G1/S A G0 G1/S
MondoA
TXNIP
β-tubulin
Non-specific shRNA
MondoA shRNA
B
+Serum (hours)
+Serum (hours)
A G0 1 4 8
A G0 1 4 8
MondoA
ΔN237
TXNIP
Hif1α
β-tubulin
Vector
ΔN237NLSMondoA
C
Glucose uptake fold increase G0 → G1 (8 hrs)
3
2
1
0
*
Vector ΔN237
D
Glycolytic flux pmol glucose utilization/cell/hour
0.10
0.08
0.06
0.04
0.02
0.00
Vector ΔN237 Vector ΔN237
G0
G1 (8 hrs)
E
% BrdU incorporation
80
60
40
20
0
**
Vector ΔN237 Vector ΔN237
G0
G1/S

2.3.4 MondoA-dependent TXNIP transcription is acutely inhibited by serum

TXNIP expression was downregulated in early G_1 (Figure 2.1D and E) and ΔN237NLSMondoA partially blocked TXNIP downregulation in response to serum (Figure 2.3B). To determine whether TXNIP transcription was shut off by serum addition, we determined the half-life of TXNIP mRNA. We treated quiescent BJ hTERTs with the transcription inhibitor actinomycin D (Figure 2.4A). In G_0 cells, actinomycin D treatment revealed that TXNIP mRNA was quite stable, with an apparent half-life of ~150 minutes. Similarly, in early G_1 TXNIP mRNA had an apparent half-life of ~90 minutes. The slopes of the exponential portions of each decay curve were similar, indicating that the decay of mRNA following serum addition was comparable to its decay following transcriptional inhibition. These data support a model where serum addition shuts off TXNIP transcription acutely.

TXNIP mRNA can be upregulated by the histone deacetylase (HDAC) inhibitors TSA and SAHA (37, 47, 48). To determine whether TXNIP transcriptional downregulation in response to serum was a function of transcriptional repression, we treated quiescent and early G_1 cells with TSA. Consistent with published reports, TXNIP mRNA increased by ~50% in quiescent BJ hTERTs suggesting that TXNIP message levels here were modulated by an HDAC-dependent mechanism. However, in early G_1 TSA did not increase TXNIP message, indicating that TXNIP transcriptional downregulation by serum did not occur by an active HDAC-dependent repression mechanism (Figure 2.4B).

Given that MondoA is absolutely required for TXNIP transcription (Figure 2.3A) (35, 36), one mechanism of TXNIP mRNA downregulation may be that MondoA leaves the TXNIP promoter in response to serum. To investigate this, we determined MondoA

occupancy on the TXNIP promoter using chromatin immunoprecipitation (ChIP). In quiescent BJ hTERTs, MondoA occupied the carbohydrate response element (ChoRE) upstream of the TXNIP transcriptional start site (35, 49). Within 2 hours after serum addition, a time point where TXNIP transcription had ceased but mRNA persisted, MondoA occupancy was reduced at the ChoRE (Figure 2.4C). From these data, we conclude that MondoA leaves the TXNIP promoter as a rapid response to serum addition resulting in a shutdown of TXNIP transcription and decay of existing message.

MondoA-dependent TXNIP transcription can be upregulated by 2-deoxy-β-D-glucose (2DOG) (35). Given that TXNIP expression was absent in early G_1, we sought to determine whether this was reversible and establish the duration of transcriptional inhibition by serum. Quiescent and early G_1 BJ hTERTs were treated with 2DOG for 3 hours prior to the time points indicated in Figure 2.5. 2DOG increased both TXNIP protein and mRNA in quiescent cells; however, in serum treated cells neither TXNIP protein nor mRNA could be upregulated by 2DOG until 8 hours following serum addition (Figure 2.5A and B). Together these data indicate that during this window in early G_1, MondoA, while expressed, is refractory to stimuli - TSA and 2DOG - known to increase its activity at the TXNIP promoter during other phases of the cell cycle.

2.3.5 TXNIP translation is acutely inhibited by serum in early G_1

Following serum readdition, TXNIP protein was downregulated prior to its mRNA. TXNIP protein decreased to undetectable levels within 1 hour of serum readdition (Figure 2.2A and 2.3B) whereas TXNIP mRNA persisted for >2 hours (Figure 2.4A), suggesting that in addition to downregulation of TXNIP transcription, serum must also downregulate TXNIP protein more directly. To address this possibility, we examined the kinetics of TXNIP downregulation in response to serum. TXNIP protein was acutely

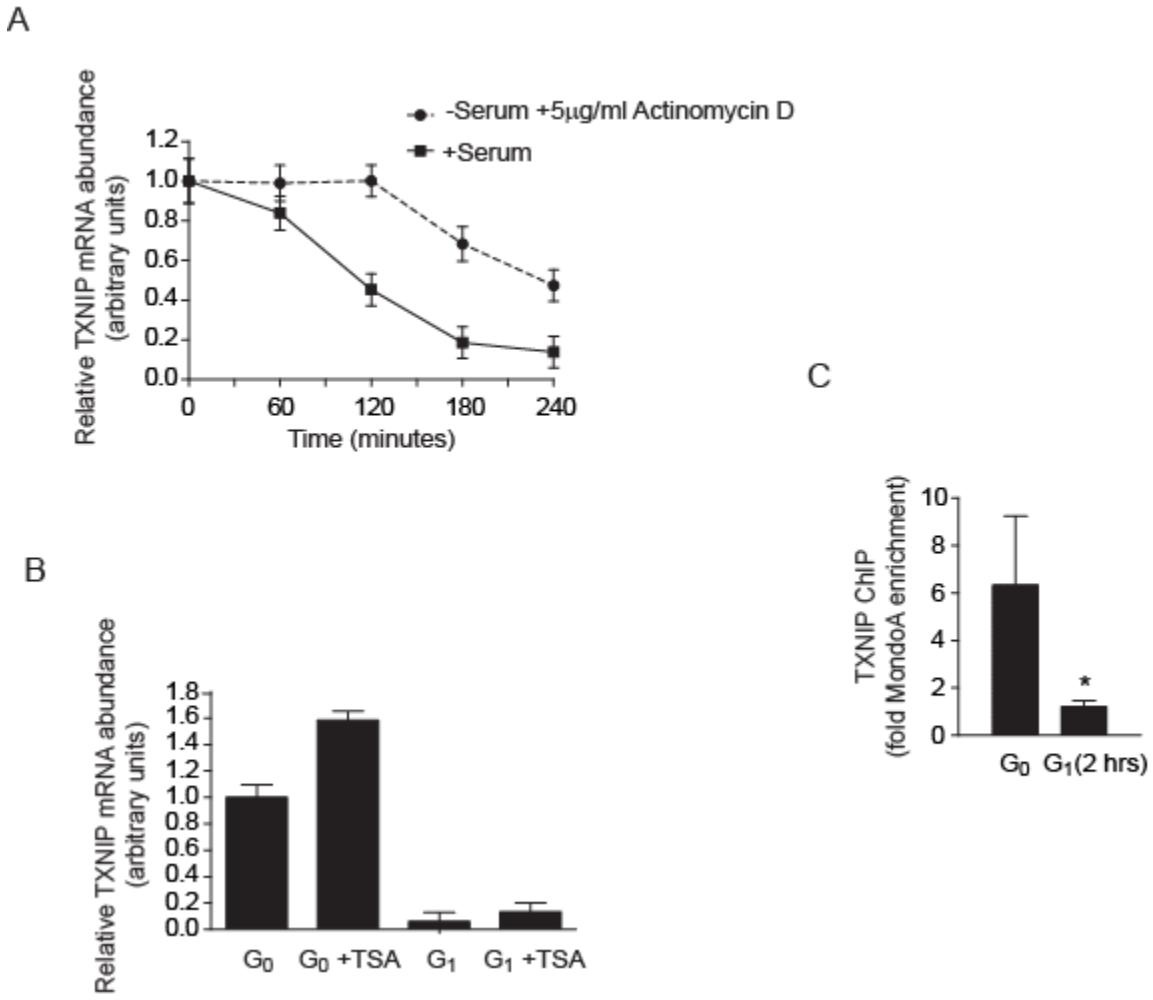

Figure 2.4 MondoA-dependent TXNIP transcription is acutely inhibited by serum
(A) Determination of TXNIP mRNA at the indicated times in G_0 in the presence of 5 μg/ml actinomycin D (●) or in the presence of serum (G_1) without actinomycin D (■) at the indicated time points by RT-qPCR. Data are presented as TXNIP message abundance relative to mRNA in G_0 (mean ± SD of triplicates from duplicate biological samples). Curve fitting in GraphPad Prism (plateau followed by one phase decay) revealed slopes for the exponential portion of each curve ($y=2.1139e^{-0.006x}$, ● and $y=1.8702e^{-0.013x}$, ■) which suggest comparable rates of decay. (B) TXNIP mRNA levels were determined by RT-qPCR after TSA treatment (100 ng/ml, 5 hours) (mean ± SD of triplicate assay points of biological duplicates). (C) ChIP was used to determine MondoA occupancy at the TXNIP promoter in BJ hTERTs under the indicated growth conditions. The data are presented as mean ± SD of three biological replicates (*, $P < 0.05$, student's t-test, n=3).

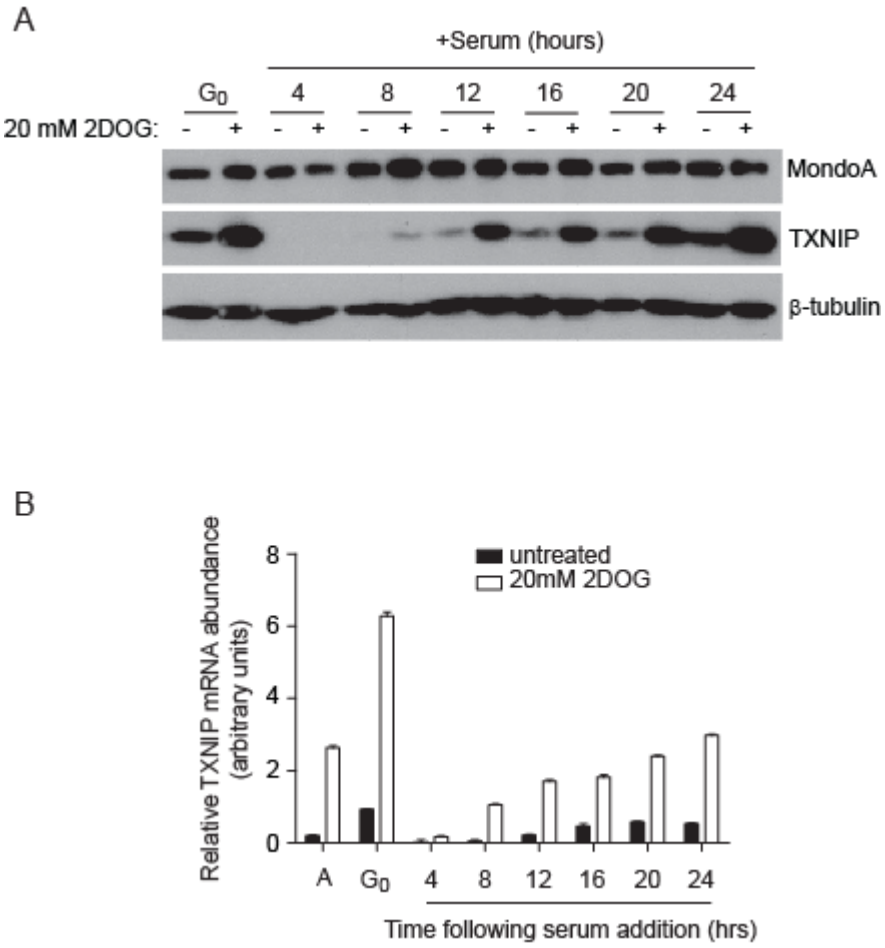

Figure 2.5 TXNIP expression is refractory to upregulation in early G_1 TXNIP, MondoA and β-tubulin expression was determined by western blotting (A) and RT-qPCR (B) following 2DOG treatment. 20 mM 2DOG was added to cells three hours prior to the time points indicated. Data in (A) are that of a representative experiment. Data in (B) are presented as fold change relative to expression in untreated quiescent cells normalized to RPL19 mRNA (mean ± SD of triplicate samples).

downregulated in early G_1 BJ hTERTs, and its levels were undetectable within ~10-15 minutes (Figure 2.6A and 2.7B). To assess whether the rapid decrease in TXNIP protein levels was due to inhibition of translation or increased degradation, we determined the apparent half-life of TXNIP in quiescent cells in the presence of the translation inhibitor cycloheximide. Strikingly, cycloheximide treatment revealed that TXNIP protein was labile, having an apparent half-life of ~10-15 minutes (Figure 2.6B and 2.7B). Given that TXNIP has the same half-life in G_0 and G_1, we conclude that the primary effect of serum is a blockade of TXNIP synthesis. Consistent with this, the proteasome inhibitors MG132 and lactacystin, which have been shown to stabilize TXNIP in other cell contexts (50, 51), did not increase TXNIP protein in early G_1 (not shown). Our data demonstrates that both TXNIP transcription and translation are immediately shut off by the addition of serum. Given the stability of TXNIP mRNA in the absence of active transcription (Figure 2.4A), inhibition of translation is sufficient to eliminate TXNIP in earliest stages of G_1.

2.3.6 Acute growth factor signaling downregulates TXNIP expression

The immediate nature of TXNIP downregulation suggested a role for active signaling by serum components. We examined the kinetics of TXNIP regulation in response to serum withdrawal and addition to determine whether the state of quiescence *per se* or dynamic signaling by serum withdrawal and subsequent readdition regulated TXNIP expression. TXNIP protein increased within 1 hour of serum removal, reached maximal levels by 4 hours post serum withdrawal and these elevated levels persisted out to 48 hours (Figure 2.7A). At all time points following serum removal, TXNIP protein levels dramatically decreased following 1 hour of serum readdition. The rapid regulation of TXNIP protein levels by serum suggests that a growth factor-regulated mechanism acutely targets TXNIP translation. To confirm that TXNIP downregulation was an

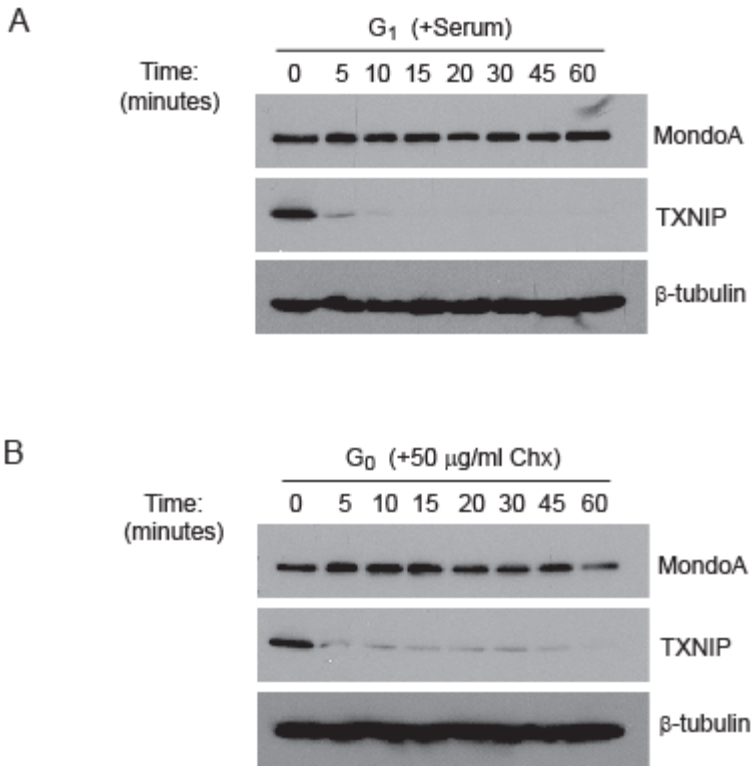

Figure 2.6 TXNIP translation is acutely inhibited by serum in early G_1 TXNIP, MondoA and β-tubulin levels in BJ hTERTs were determined following treatment of quiescent cells with 10% serum (A) or 50 μg/ml cycloheximide (B) for the time points indicated by western blotting.

immediate-early response to serum, we treated quiescent BJ hTERTs with both serum and cycloheximide, and found that TXNIP protein was still downregulated, indicating that new protein synthesis was not required for inhibition of TXNIP translation (Figure 2.7B). This is consistent with downregulation of TXNIP being an immediate-early consequence of signaling activated by serum components.

To investigate which serum components contributed to TXNIP downregulation, we treated quiescent BJ hTERTs for 30 minutes or 4 hours with serum, epidermal growth factor (EGF) or platelet derived growth factor (PDGF) (Figure 2.7C). After 30 minutes, all treatments downregulated TXNIP protein, but not TXNIP mRNA, suggesting that signaling through the receptor tyrosine kinases (RTK) EGFR and PDGFR inhibited TXNIP protein expression. After 4 hours of treatment, TXNIP protein returned to steady state levels in EGF-treated cells and was partially restored in PDGF-treated cells. As before (Figure 2.1D), TXNIP protein levels were not detectable following a 4 hour serum treatment. After 4 hours, EGF or PDGF treatment had no effect, or only modestly downregulated TXNIP message, respectively (Figure 2.7D). By contrast, TXNIP message remained low following 4 hours of serum treatment. Taken together, these data suggest that serum contains components capable of down-regulating both TXNIP transcription and translation, whereas isolated EGF- and PDGF- derived signals primarily inhibit TXNIP translation.

As both EGFR and PDGFR signal through PI3K and Ras (52), we next determined which pathway was necessary for downregulation of TXNIP translation. Inhibition of PI3K with wortmannin did not fully restore TXNIP protein following 30 minute treatments with EGF, PDGF or serum. By contrast, inhibition of MEK, a Ras effector upstream of MAPK, with u0126 restored TXNIP protein levels following 30 minute treatments with EGF, PDGF or serum. Thus the Ras-MAPK arm of the EGFR, PDGFR

Figure 2.7 Acute growth factor signaling downregulates TXNIP expression (A), (B) and (C) TXNIP, MondoA and β-tubulin levels were determined in BJ hTERTs by western blotting under the conditions indicated. In (C), 10 mM u0126 or 100 nM wortmannin were added where indicated and phospho-MAPK and phospho-Akt levels were also determined. (D) TXNIP mRNA levels were determined by RT-qPCR following 4 hours treatment under conditions indicated. Data are presented as fold change relative to expression in G_0 normalized to RPL19 mRNA (mean ± SD of triplicate samples of biological duplicates).

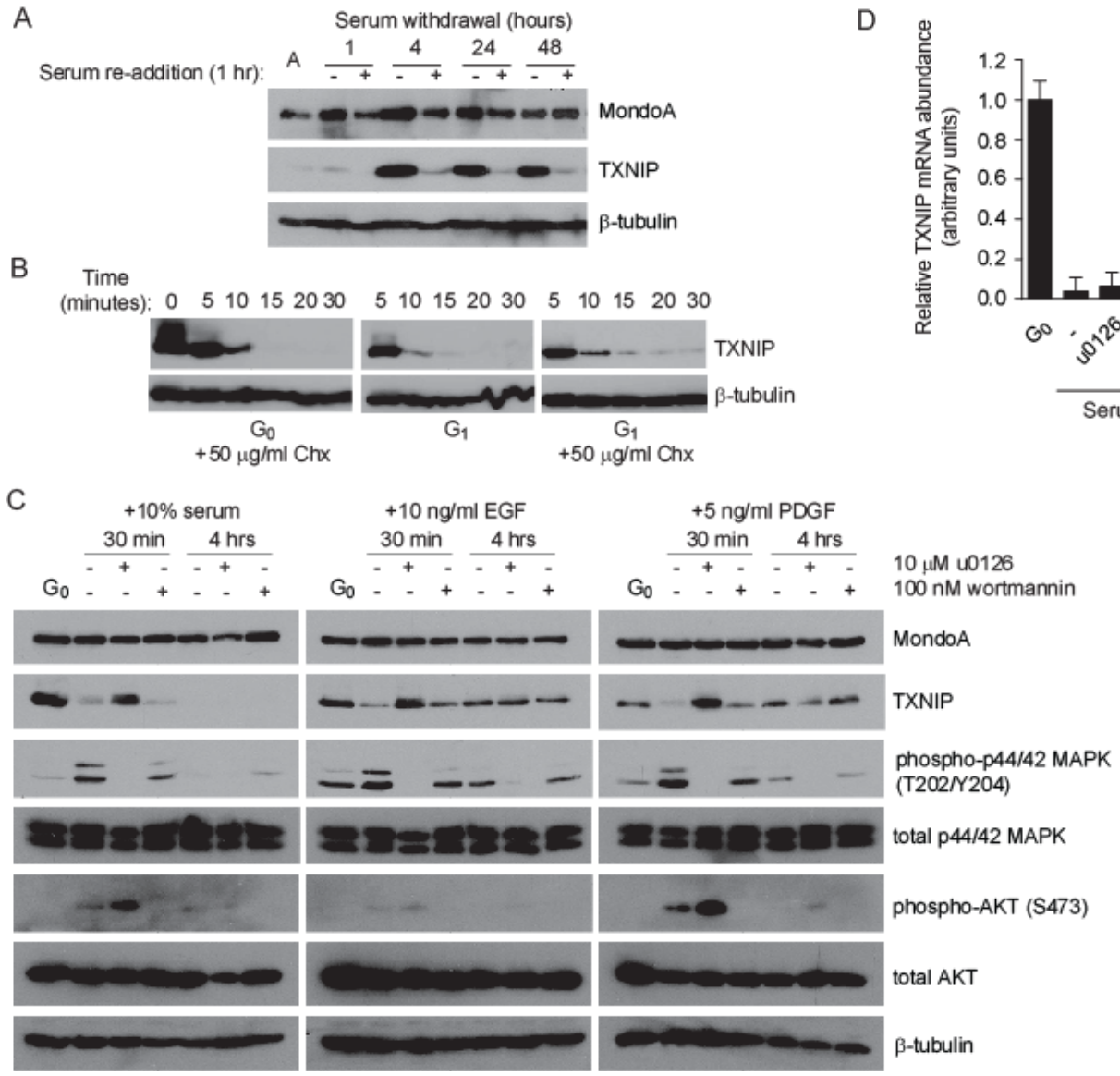
A
Serum withdrawal (hours)
Serum re-addition (1 hr):
A
1
4
24
48
MondoA
TXNIP
β-tubulin
B
Time (minutes): 0 5 10 15 20 30 5 10 15 20 30 5 10 15 20 30
TXNIP
β-tubulin
G0 +50 μg/ml Chx
G1
G1 +50 μg/ml Chx
C
+10% serum
+10 ng/ml EGF
+5 ng/ml PDGF
30 min
4 hrs
G0
10 μM u0126
100 nM wortmannin
MondoA
TXNIP
phospho-p44/42 MAPK (T202/Y204)
total p44/42 MAPK
phospho-AKT (S473)
total AKT
β-tubulin
D
Relative TXNIP mRNA abundance (arbitrary units)
1.2
1.0
0.8
0.6
0.4
0.2
0.0
G0
u0126
wort.
Serum
EGF
PDGF

and serum signaling pathways can drive inhibition of TXNIP translation (Figure 2.7C). After 4 hours of serum treatment, when TXNIP message is absent, u0126 did not restore TXNIP mRNA or protein, suggesting that Ras-MAPK signaling activated by serum did not regulate TXNIP transcription. By contrast, wortmannin restored TXNIP message in PDGF-treated cells but had no effect on serum-treated BJ hTERTs. Thus PI3K signaling downstream of PDGFR must partially block TXNIP transcription, which is consistent with one previous report (53). Further, the lack of effect of wortmannin on serum-dependent downregulation of TXNIP transcription suggests that other signaling pathways must regulate TXNIP transcription downstream of PI3K or in parallel with PI3K signaling.

2.3.7 Acute Ras-MAPK activation downregulates TXNIP translation

We next wished to determine whether Ras-MAPK signaling was sufficient to inhibit TXNIP translation. To simplify these experiments, they were conducted in the absence of serum to eliminate other signaling inputs. Since constitutive Ras activity in BJ hTERTs causes senescence (54, 55), we expressed a regulatable allele of activated oncogenic Ras. This allele expresses Ras^{G12V} as a fusion to the estrogen receptor (ER) ligand-binding domain that is stabilized and therefore activated by binding 4-hydroxytamoxifen (4OHT) (56, 57). Ras^{G12V}:ER stabilization with increasing concentrations of 4OHT resulted in dose-dependent MAPK phosphorylation which coincided with TXNIP downregulation when compared to control cells (Figure 2.8). From these data we conclude that Ras-MAPK signaling actively inhibits TXNIP translation, which is consistent with the immediate-early kinetics of TXNIP translational downregulation.

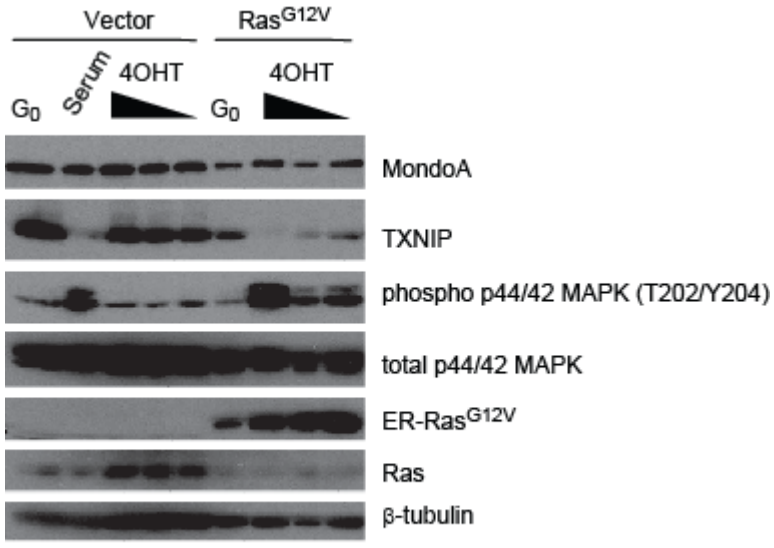

Figure 2.8 Acute Ras-MAPK activation downregulates TXNIP translation TXNIP, MondoA, phospho-MAPK and β-tubulin levels were determined in BJ hTERTs infected with pBABE-puro-ER (vector) and pBABE-puro-ER:Ras^{G12V} (Ras^{G12V}) by western blotting. Quiescent cells (G_0) were treated with 10% serum or increasing concentrations (64.5 nM, 645 nM and 6.45 μM) of 4-hydroxytamoxifen (4OHT) as indicated for 4 hours.

2.4 Discussion

As cells exit quiescence and enter the cell cycle, metabolic reprogramming in early G_1 drives biosynthesis of macromolecules necessary for cell growth prior to proliferation. Our data extend the current understanding of metabolic reprogramming by demonstrating the coordinated downregulation of TXNIP translation and MondoA-dependent TXNIP transcription as serum-starved cells exit quiescence and enter early G_1. Further, we directly link TXNIP downregulation to the signaling pathways commonly associated with metabolic reprogramming and growth, Ras-MAPK and PI3K/Akt (58-60). Because, constitutive MondoA or TXNIP expression blocks metabolic reprogramming in early G_1, we suggest that TXNIP downregulation not only correlates with metabolic reprogramming, but is a required event for cells to enter a productive cell cycle from quiescence. Finally, given the prevalence activating mutations in RTKs and their downstream effectors in cancer (52, 61, 62), we suggest that dysregulated TXNIP expression may be a relatively common driver contributing to the Warburg effect in tumorigenesis.

TXNIP has emerged as an interesting candidate in the regulation of cell growth and metabolism. Currently, literature suggests that TXNIP loss in early G_1 may drive metabolic reprogramming by one of several mechanisms or by a combination of these mechanisms. For example, T-lymphocytes upregulate GLUT-1 following stimulation in order to increase glucose consumption to support growth (2, 4), correlating with the downregulation of TXNIP we observed. Thus, it is possible that TXNIP regulates, directly or indirectly the expression level of the glucose transporters. Supporting a direct regulatory mechanism are findings demonstrating that TXNIP localizes to the nucleus and can interact with transcriptional corepressors (13, 63). A second possibility is that TXNIP loss leads to the stabilization of the HIF1α transcription factor that regulates the

expression of most glycolytic target genes. Finally, TXNIP loss leads to inactivation of PTEN (29) and the consequent activation of PI3K and its well-characterized functions in controlling both metabolic reprogramming and proliferation (64). As cells exit quiescence they must reorganize the machinery that directly regulates the transition into G_1, e.g. cyclins, cyclin-dependent kinases and cyclin-dependent kinase inhibitors. Our data suggests that reprogramming cellular metabolism in early G_1 is similarly complex and suggests a central role for TXNIP in orchestrating these growth-supporting metabolic changes. TXNIP also modulates levels of the cyclin-dependent kinase inhibitor $p27^{Kip1}$ (23), implying a function for TXNIP in linking cell cycle regulation directly to cellular metabolism.

Activation of many oncogenes can drive aerobic glycolysis and in many cases their regulation of metabolic reprogramming appears direct, implying that the Warburg effect contributes functionally to cancer cell growth rather than merely correlating with cancer cell growth (60, 65, 66). Interestingly, tumor cell models with activating Ras mutations have increased glucose uptake and glycolytic flux associated with the constitutive activation of Ras-MAPK signaling (67, 68). This effect of active Ras has been classically ascribed to its activation of cMyc and HIF1α (58, 69, 70). However, we demonstrate here a direct contribution of Ras-MAPK signaling to metabolic reprogramming via its acute inhibition of TXNIP translation in early G_1. This suggests that Ras-MAPK activation might regulate metabolic reprogramming by coordinating the activities of Myc/HIF1α and TXNIP. Myc and HIF1α regulate the transcription of genes encoding glycolytic and other biosynthetic targets (71, 72). Thus one simple model for how Ras-MAPK may coordinate metabolic reprogramming is that TXNIP downregulation allows uptake of glucose and potentially other “building blocks” required for cell growth and Myc/HIF1α upregulation controls flux of these nutrients into biosynthetic pathways.

As Myc-overexpressing cells can be addicted to glucose and/or glutamine (73-76), coordinating nutrient availability with nutrient utilization is clearly required for cellular homeostasis.

Recently, ChREBP (MondoB) was shown to be necessary for metabolic reprogramming in colorectal cancer cells and hepatoblastoma cells (40). For example, ChREBP knockdown cells shut down aerobic glycolysis, anabolic pathways and have reduced proliferation rates. Previously, we have shown that MondoA restricts glucose uptake (35) thus MondoA may act in opposition to ChREBP. In BJ hTERT cells ΔN237NLSMondoA upregulates TXNIP transcription and reduces glucose uptake as expected; however, ΔN237NLSMondoA does not inhibit glycolysis. By contrast TXNIP overexpression restricts both glucose uptake and glycolysis. Therefore, in addition to TXNIP, there must be other transcriptional targets of ΔN237NLSMondoA that oppose the negative activity of TXNIP on glycolysis. Identifying the direct MondoA-dependent transcriptome will likely provide insight into this important issue.

TXNIP expression is restored later in G_1 coinciding with a plateau in glucose uptake and utilization at about 12 hours following serum addition presumably when the biosynthetic needs of the cell are met. There may be two functional consequences to TXNIP upregulation later in G_1. First, TXNIP can bind to and inhibit thioredoxin resulting in increased intracellular reactive oxygen species (ROS) (77). ROS are required for G_1 progression and S-phase entry (78). Thus restoring TXNIP activity later in G_1 may contribute to increased ROS and subsequently G_1 progression and S-phase entry. Second, the restriction point (R) is defined as a point in G_1 where the cell assesses nutrient availability and can either arrest in order to survive under suboptimal growth conditions or proliferate when conditions are favorable (79). Thus it is possible that TXNIP upregulation occurs at a point that defines R in later G_1, after which the

commitment to undergo DNA replication and cell division no longer falls under nutrient control.

We show that TXNIP transcription is downregulated in early G_1 when MondoA leaves the TXNIP promoter. Additionally, wortmannin partially blocks TXNIP mRNA downregulation in early G_1 following PDGF but not serum addition. Thus there must be additional pathways within serum that bypass PI3K and regulate MondoA activation of the TXNIP promoter. It still remains to be determined how serum acutely and negatively regulates MondoA activity at the TXNIP promoter. ChREBP localization and activity are regulated by phosphorylation of key residues encompassing its DNA binding domain and nuclear localization sequence (80); however, these residues are not well conserved in MondoA. We cannot formally rule out the possibility that MondoA‘s activation of TXNIP transcription is directly modulated by post-translational modification in response to serum, yet the opposing roles for MondoA and ChREBP discussed above do not favor a unifying mechanism. A second interesting mechanistic possibility involves our recent demonstration that MondoA occupancy and activity at the TXNIP promoter is increased as intracellular pH drops (20). Previous studies have established that growth factor stimulation leads to a rapid – after approximately 2 minutes - increase in intracellular pH and this pH increase is required for cell division (81, 82). These findings support a model where intracellular alkalinization following growth factor stimulation drives MondoA off the TXNIP promoter accounting for the rapid transcriptional shut down of MondoA-dependent transcription of TXNIP we observed in response to serum.

The mechanism by which acute Ras signaling inhibits TXNIP translation is not completely understood. TXNIP-mCherry is destabilized by serum yet only has the coding sequence of the TXNIP message, eliminating translational regulation via its 5’ or 3’ UTRs as a possibility. MicroRNAs (miRNAs) typically inhibit translation by interacting

with the 3' UTR, yet there are examples of miRNAs targeting coding sequences (83, 84). Thus, we cannot completely rule out the involvement of miRNAs in regulating TXNIP translation. Furthermore, the rapid kinetics of TXNIP downregulation suggests a more direct mechanism that does not involve *de novo* RNA synthesis. With these caveats, it seems most likely that Ras-MAPK signaling targets preexisting components of the translational initiation machinery or, potentially, translating ribosomes. There are multiple examples of signaling cascades impinging directly on the translational initiation machinery supporting the former mechanism (85-87).

Our results establish the necessity of TXNIP downregulation for cells to escape quiescence and enter G_1. The fact that both TXNIP translation and TXNIP transcription are both inhibited by serum further underscores this point. Our data indicate that TXNIP transcription and translation are likely inhibited as acute immediate-early responses to serum addition. While activated simultaneously, each repression mechanism persists for a different length of time. EGF only effects translational inhibition of TXNIP. TXNIP protein returns normal levels after 4 hours of EGF treatment, defining the window of translational inhibition. The transient nature of TXNIP translational inhibition likely reflects the well-characterized transient signaling through the Ras-MAPK pathway (88, 89). By contrast, TXNIP transcription is shut off for a much longer time, not being inducible until 8-12 hours following serum addition. Thus, inhibition of TXNIP transcription reinforces the inhibition of TXNIP translation early in G_1. At 8-12 hours following serum addition, the translational inhibition mechanism is no longer in force and TXNIP protein levels appear to be primarily under the control of MondoA-dependent activation of TXNIP transcription. We have examined TXNIP regulation in subsequent G_1 phases of the cell cycle and find that TXNIP transcriptional and translational inhibition are restricted to the first G_1 phase following the release from quiescence (data not

shown). This finding is reminiscent of the peak of cMyc mRNA and protein observed only in the first G_1 following serum stimulation of quiescent cells (90, 91). We speculate that the restricted regulation of TXNIP and cMyc to the first G_1 after serum addition reflects increased metabolic requirements for cells to exit G_0 and that these metabolic demands must be relaxed during ensuing G_1 phases.

The switch to aerobic glycolysis supplies energy and biomolecules to support the high division rates of many cancer cells. Our work establishes an important role for TXNIP downregulation in metabolic reprogramming as cells exit quiescence and enter the first G_1 phase of the cell cycle. While not studied here broadly, we show that TXNIP is rapidly upregulated by serum withdrawal which may serve to downregulate nutrient uptake and utilization in response to reduced signaling from growth factors. Such a model implies that rapid metabolic reprogramming may also be an early event involved in establishing quiescence. Our work provides new insights into how growth factor signaling impacts transcriptional and translational regulation of TXNIP, and likely other targets, leading to cell growth and yields insights into how TXNIP dysregulation may contribute to tumorigenesis. As TXNIP is an attractive therapeutic target in cancer treatment (92), our work provides insight into the rational targeting of its upregulation through activation of MondoA.

2.5 Materials and Methods

2.5.1 Cell Culture and Conditions

BJ hTERTs (42) were maintained at 37°C in 5% CO_2 in Dulbecco modified Eagle medium (DMEM, HyClone) supplemented with 10% bovine calf serum (BCS, HyClone) and penicillin/streptomycin (pen/strep). For serum starvation (quiescence), cells were washed with PBS and incubated in DMEM containing 0.1% bovine serum albumin (BSA) and pen/strep for 72 hours. Serum starvation media was replaced with growth media to

release cells into the cell cycle for times indicated. For growth factor stimulation, 10 ng/ml EGF (Sigma-Aldrich) or 5 ng/ml PDGF (Sigma-Aldrich) were added to serum starvation media for times indicated. For MEK and PI3K inhibition, serum-starved cells were pretreated for 30 minutes with 10 μM u0126 (Cell Signaling Technology) or 100 nM wortmannin (Cell Signaling Technology), respectively, and were then treated with serum or growth factors in the presence of the inhibitors for times indicated. For mRNA and protein stability studies, cells were treated with 5 μg/ml actinomycin D (Sigma-Aldrich) or 50 μg/ml cycloheximide (Sigma-Aldrich), respectively under conditions and for times indicated. For HDAC studies, cells were treated with 100 ng/ml trichostatin A (TSA, BIOMOL) for 5 hours prior to mRNA isolation. Primary quiescent T-lymphocytes were isolated from murine spleen and purified via negative selection using the EasySep Mouse T Cell Enrichment Kit (STEMCELL Technologies) and cultured in RPMI 1640 (Cellgro) supplemented with 10% fetal bovine serum (FBS, Hyclone). Isolated T-lymphocytes were activated using Dynabeads Mouse T-Activator CD3/CD28 for cell expansion and activation (Invitrogen) for the indicated times. Wild-type and TXNIP-null MEFs (41) were immortalized by a 3T3 protocol (93) and maintained at 37°C in 5% CO_2 in DMEM supplemented with 10% FBS and pen/strep. For serum starvation, cells were washed with PBS and incubated with DMEM supplemented with 0.5% FBS and pen/strep for 48 hours. Cells were stimulated to enter the cell cycle by replacing serum starvation media with growth media for times indicated.

2.5.2 Western Blotting

Whole cell lysates were prepared in ice-cold RIPA (150 mM NaCl, 10 mM Tris-Cl [pH 7.4], 0.1% SDS, 1.0% triton X100, 1.0% Na-deoxycholate, 5 mM EDTA) containing protease and phosphatase inhibitors. Protein concentrations were determined by

Bradford Protein Assay (Bio-Rad). Following SDS-PAGE, proteins were transferred to PVDF membranes (PerkinElmer) and subsequently blocked in 5% nonfat dry milk-TBST (50 mM Tris-Cl [pH 8.0], 150 mM NaCl, 0.05% Tween 20) and probed with anti-MondoA (Stoltzman, et al., 2008, 1:500), anti-VDUP1(TXNIP) (MBL International, 1:1000); anti-tubulin (Sigma, 1:10000); anti-cyclin A, anti-p27 and anti-H-Ras (Santa Cruz); anti-Hif1α (BD Biosciences,1:1000); anti-phospho-p44/42 MAPK (T202/Y204), anti-p44/42 MAPK, anti-phospho-Akt (S473) and anti-Akt (Cell Signaling Technology) at 1:500 or 1:1000 or as otherwise indicated. The blots were developed using ECL Plus (Amersham).

2.5.3 Glucose Uptake Assays

BJ hTERTs were plated at 50,000 cells/well in 6-well dishes and treated as indicated. 10^6 quiescent or activated T-lymphocytes were used for assays at time points indicated. For all conditions, cells were washed with Krebs-Ringer-Phosphate-Hepes (KRPH, 5 mM Na-phosphate [pH 7.4], 20 mM Hepes [pH 7.4-7.9], 1 mM $MgSO_4$, 1 mM $CaCl_2$, 136 mM NaCl, 4.7 mM KCl) buffer and then incubated for 15 minutes in 1 ml KRPH containing 1 mM 2-deoxy-β-D-glucose (2DOG, Sigma-Aldrich) and 1 μCi 2-deoxy-D-[1,2-^{3}H(N)]-glucose (specific activity, 5-10 Ci/mmole; PerkinElmer) at 37°C/5% CO_2. Glucose uptake was terminated by removing the incubation solution and washing cells with ice cold KRPH. Cells were solubilized with 0.1% SDS over night at room temperature prior to scintillation counting to determine radiolabel incorporation. Assay results were normalized to cell number where indicated as described (35). All experiments were represented by three biological replicates and all data shown represent the results from at least three experiments.

2.5.4 Glycolytic Flux Assays

BJ hTERTs were plated at 50,000 cells/well in 6-well dishes and treated as indicated. For glycolysis assay, media was removed from cells and replaced with 0.5 ml media containing 10 μCi D-[5-^{3}H(N)]-glucose (specific activity 10-20 Ci/mmole, PerkinElmer) for 1 hour at 37°C/5% CO_2. The assay was terminated by addition of 0.5 ml 2N HCl. Triplicate 100 μl aliquots were transferred to capless 0.2 ml tubes and placed in sealed scintillation vials containing 0.5 ml H_2O for 48 hours at room temperature to allow for diffusion and equilibration of ^3H_2O. The 0.2 ml tubes were subsequently transferred to new scintillation vials and both diffused (^3H_2O) and unutilized D-[5-^{3}H(N)]-glucose were determined by scintillation counting. Controls for ^3H_2O diffusion included ^3H_2O standard and D-[5-^{3}H(N)]-glucose only. Data were analyzed by comparing diffused samples (reduced to ^{3}H2O by glycolysis) to undiffused samples and determining pmol glucose utilized per hour per cell as described (7, 35). Each experiment represents two biological replicates and all data shown represent the results from at least three experiments.

2.5.5 Viruses and Infections

Lentiviral pCDH-mCherry and pCDH-TXNIP-mCherry were a gift from W. Chutkow (25). pEIZ-Green was a gift from B. Welm. pEIZ-Green-ΔN237NLSMondoA was constructed by cloning ΔN237NLSMondoA as an XhoI/end-filled fragment from LXSH-ΔN237NLSMondoA (45) into the SmaI site of pEIZ-Green. Retroviral LMP vectors (Open Biosystems) containing nonsilencing (NS) and MondoA specific shRNA (M2) sequences were as described (35). Retroviral construct pBABE-puro-ER:Ras^{G12V} was a gift from C. Counter (56) and pBABE-puro was as described (94). Stable cell lines containing nonsilencing shRNA, MondoA shRNA, pBABE-puro and ER:Ras^{G12V} were made by infecting BJ hTERTs with retrovirus generated from each construct in HEK293T

cells (95) and subsequent selection in 2 μg/ml puromycin. For experiments utilizing BJ hTERT:pBABE-puro and BJ hTERT:pBABE-puro-ER:Ras^{G12V}, cells were plated and serum starved as above and subsequently treated with vehicle (0.1% ethanol) or indicated concentrations of 4-hydroxytamoxifen for 4 hours in starvation media prior to analysis. Transient infections with pCDH-mCherry, pCDH-TXNIP-mCherry, pEIZ-Green and pEIZ-Green-ΔN237NLSMondoA were performed with lentivirus generated from each construct in HEK 293T as described (96). Briefly, BJ hTERTs were infected over night with lentivirus from each construct and allowed to recover from infection for 24 hours. Asynchronous cells were subsequently serum starved for 72 hours and then released into G_1 by serum addition. Relative infection efficiency for each experiment was determined by mCherry fluorescence (pCDH) or GFP fluorescence (pEIZ).

2.5.6 BrdU Labeling and Immunofluorescence

BJ hTERTs or MEFs were plated at subconfluent density on cover slips and treated as indicated. For MEFs, cells were incubated for 24 hours in media containing 10 μM 5-bromo-2'-deoxyuridine (BrdU, Roche) prior to analysis for all conditions tested. For BJ hTERTs, G_1 cells, following 22 hours in media supplemented with serum, were incubated in media containing 10 μM BrdU for 4 hours and quiescent cells received 10 μM BrdU in media lacking serum for 4 hours. Following BrdU labeling, cells were washed with PBS then fixed in ice-cold methanol for 10 minutes and DNA was denatured with 2N HCl for 1 hour at 37°C. Cover slips were subsequently neutralized by 20 minute incubation in 0.1M sodium borate pH 8.5 and subsequently washed with PBS. Cover slips were blocked in PBS containing 0.1 % BSA, then incubated with 1 μg/ml anti-fluorescein-BrdU (Roche) for 1 hour and subsequently washed with PBS. Following 10 minute incubation with 1 μg/ml DAPI (Sigma-Aldrich), cover slips were washed and

mounted using Prolong Gold (Invitrogen). Total cell number was determined by counting nuclei (DAPI) and BrdU incorporation by counting fluorescein labeled cells. For each experiment 200-500 total cells per cover slip were counted and three cover slips per condition were evaluated. Each data point shown represents the average of three independent experiments.

2.5.7 Chromatin Immunoprecipitation (ChIP)

1.8×10^6 BJ hTERTs on 15 cm dishes (3 dishes per point) for all conditions indicated were washed with PBS and fixed/cross-linked for 10 minutes with 1% formaldehyde. Cross-linking was stopped with 0.125M glycine for 10 minutes and cells were washed with PBS and harvested by scraping and incubation in cell lysis buffer (10 mM Tris-Cl [pH 7.4], 10 mM NaCl, 3 mM $MgCl_2$, 0.5% NP40). After washing, cell pellets were sonicated at 4°C in 0.5 ml nuclear lysis buffer (50 mM Tris-Cl [pH 8.0], 10mM EDTA, 5 mM EGTA, 1% SDS) for 20 rounds of 25 second cycles (0.9 sec on/0.1 sec off) on a Misonix Ultrasonic Processor, setting 3 (Misonix Incorporated). The extent of chromatin shearing was determined by reversing the cross-links on an aliquot and examination by agarose gel electrophoresis. Sonicated lysates were per-cleared by incubation with Dynabeads (Sheep anti-rabbit M-280, Invitrogen) at 4°C in ChIP dilution buffer (20 mM Tris [pH 8.0], 2 mM EDTA, 150 mM NaCl, 1% Triton X-100, 2 mg/ml BSA, 100 μg/ml ssDNA) and immunoprecipitated over night with 2 μg anti-MondoA or 2 μg normal rabbit IgG (Santa Cruz) at 4°C. Beads were isolated by magnetic separation and washed once with wash I (20 mM Tris-Cl [pH 8.0], 2 mM EDTA, 1% Triton X-100, 150 mM NaCl, 1 mM PMSF) then twice with wash II (wash I with 0.1 % SDS, 500 mM NaCl) and finally once with wash III (20 mM Tris-Cl [pH 8.0], 1mM EDTA, 250 mM LiCl, 0.5% NP40, 0.5% sodium deoxycholate). Beads were resuspended in 50 μl 10 mM Tris-Cl [pH 8.0], 1 mM EDTA (TE) and incubated with 200 ng/ml RNase A (Qiagen) for 20 minutes

at 37°C. Proteinase K and SDS were added to final concentrations of 200 μg/ml and 0.5 %, respectively, and beads were incubated at 55°C for 3 hours. Subsequently, immunoprecipitations were incubated over night at 65°C to reverse cross links. Samples were phenol-chloroform extracted and further processed by the Qiaquick PCR Purification Kit (Qiagen) prior to qPCR. For experiments shown, specific MondoA DNA binding was determined by normalizing to IgG controls and MondoA enrichment at the TXNIP locus was determined at all conditions by normalizing qPCR to the MondoA off-target loci PFKFB3 or Bcl2 (35, 36) (primer sequences available upon request). DNA quantities were determined from standard curves for all primer sets. Data represented are from 3 independent experiments.

2.5.8 Reverse Transcription Quantitative PCR (RT-qPCR)

For expression analysis, total RNA was extracted from cells using RNeasy Mini Kit (Qiagen) and cDNA was generated from 250-500 ng RNA using Superscript III RT system (oligo dT, Invitrogen). cDNAs were mixed with TXNIP or RPL19 primers (sequences available upon request) and IQ SYBR Green Supermix (Bio-Rad) and qPCR reactions were performed on the iCycler (Bio-Rad) as follows: one cycle of 95°C for 2.5 min.; 40 cycles of 95°C for 30 sec., 55°C for 30 sec., one cycle of 72°C for 35 sec.; 72°C for 2.5 min.; 77 cycles 72°C-95°C for 10 sec. at each temperature. Relative mRNA quantities were determined from standard curves for each primer set and TXNIP mRNA quantities were normalized to RPL19 expression. For each experiment, triplicate reactions were run from a minimum of two biological replicates.

2.6 Acknowledgements

We thank W. Chutkow for wild type and TXNIP null MEFs, M. Topham and the Ayer lab for reviewing the manuscript. NIH grants GM55668 and GM60387 (D.E.A.) and

the Huntsman Cancer Foundation supported this work. DNA sequencing and oligonucleotide synthesis were supported by the Cancer Center Support Grant 2P30 CA42014.

2.7 References

1. Bauer DE*, et al.* (2004) Cytokine stimulation of aerobic glycolysis in hematopoietic cells exceeds proliferative demand. *Faseb J* 18(11):1303-1305.

2. Brand K (1985) Glutamine and glucose metabolism during thymocyte proliferation. Pathways of glutamine and glutamate metabolism. *Biochem J* 228(2):353-361.

3. Vander Heiden MG, Cantley LC, & Thompson CB (2009) Understanding the Warburg effect: the metabolic requirements of cell proliferation. *Science* 324(5930):1029-1033.

4. Frauwirth KA*, et al.* (2002) The CD28 signaling pathway regulates glucose metabolism. *Immunity* 16(6):769-777.

5. Bruszewski WB*, et al.* (1984) Early mitogen-induced metabolic events essential to proliferation of human T lymphocytes: dependence of specific events on the influence of adherent accessory cells. *J Immunol* 132(6):2837-2843.

6. Frauwirth KA & Thompson CB (2004) Regulation of T lymphocyte metabolism. *J Immunol* 172(8):4661-4665.

7. Vander Heiden MG*, et al.* (2001) Growth factors can influence cell growth and survival through effects on glucose metabolism. *Mol Cell Biol* 21(17):5899-5912.

8. MacIver NJ*, et al.* (2008) Glucose metabolism in lymphocytes is a regulated process with significant effects on immune cell function and survival. *J Leukoc Biol* 84(4):949-957.

9. Rathmell JC, Vander Heiden MG, Harris MH, Frauwirth KA, & Thompson CB (2000) In the absence of extrinsic signals, nutrient utilization by lymphocytes is insufficient to maintain either cell size or viability. *Mol Cell* 6(3):683-692.

10. DeBerardinis RJ*, et al.* (2007) Beyond aerobic glycolysis: transformed cells can engage in glutamine metabolism that exceeds the requirement for protein and nucleotide synthesis. *Proc Natl Acad Sci U S A* 104(49):19345-19350.

11. Elstrom RL*, et al.* (2004) Akt stimulates aerobic glycolysis in cancer cells. *Cancer Res* 64(11):3892-3899.

12. Warburg O (1956) On the origin of cancer cells. *Science* 123(3191):309-314.

13. Han SH, *et al.* (2003) VDUP1 upregulated by TGF-beta1 and 1,25-dihydorxyvitamin D3 inhibits tumor cell growth by blocking cell-cycle progression. *Oncogene* 22(26):4035-4046.

14. Kim SY, Suh HW, Chung JW, Yoon SR, & Choi I (2007) Diverse functions of VDUP1 in cell proliferation, differentiation, and diseases. *Cell Mol Immunol* 4(5):345-351.

15. Lee KN, *et al.* (2005) VDUP1 is required for the development of natural killer cells. *Immunity* 22(2):195-208.

16. Parikh H, *et al.* (2007) TXNIP regulates peripheral glucose metabolism in humans. *PLoS Med* 4(5):e158.

17. Dutta KK, *et al.* (2005) Two distinct mechanisms for loss of thioredoxin-binding protein-2 in oxidative stress-induced renal carcinogenesis. *Lab Invest* 85(6):798-807.

18. Goldberg SF, *et al.* (2003) Melanoma metastasis suppression by chromosome 6: evidence for a pathway regulated by CRSP3 and TXNIP. *Cancer Res* 63(2):432-440.

19. Cadenas C, *et al.* (2010) Role of thioredoxin reductase 1 and thioredoxin interacting protein in prognosis of breast cancer. *Breast Cancer Res* 12(3):R44.

20. Chen JL-Y, *et al.* (2010) Lactic acidosis triggers starvation response with paradoxical induction of TXNIP through MondoA. *PloS Genetics* In Press.

21. Shin D, *et al.* (2008) VDUP1 mediates nuclear export of HIF1alpha via CRM1-dependent pathway. *Biochim Biophys Acta* 1783(5):838-848.

22. Jeong M, *et al.* (2009) Thioredoxin-interacting protein regulates hematopoietic stem cell quiescence and mobilization under stress conditions. *J Immunol* 183(4):2495-2505.

23. Jeon JH, *et al.* (2005) Tumor suppressor VDUP1 increases p27(kip1) stability by inhibiting JAB1. *Cancer Res* 65(11):4485-4489.

24. Hui TY, *et al.* (2004) Mice lacking thioredoxin-interacting protein provide evidence linking cellular redox state to appropriate response to nutritional signals. *J Biol Chem* 279(23):24387-24393.

25. Patwari P, *et al.* (2009) Thioredoxin-independent regulation of metabolism by the alpha-arrestin proteins. *J Biol Chem* 284(37):24996-25003.

26. Firth JD, Ebert BL, & Ratcliffe PJ (1995) Hypoxic regulation of lactate dehydrogenase A. Interaction between hypoxia-inducible factor 1 and cAMP response elements. *J Biol Chem* 270(36):21021-21027.

27. Obach M*, et al.* (2004) 6-Phosphofructo-2-kinase (pfkfb3) gene promoter contains hypoxia-inducible factor-1 binding sites necessary for transactivation in response to hypoxia. *J Biol Chem* 279(51):53562-53570.

28. Riddle SR*, et al.* (2000) Hypoxia induces hexokinase II gene expression in human lung cell line A549. *Am J Physiol Lung Cell Mol Physiol* 278(2):L407-416.

29. Hui ST*, et al.* (2008) Txnip balances metabolic and growth signaling via PTEN disulfide reduction. *Proc Natl Acad Sci U S A* 105(10):3921-3926.

30. Jia S*, et al.* (2008) Essential roles of PI(3)K-p110beta in cell growth, metabolism and tumorigenesis. *Nature* 454(7205):776-779.

31. Luo J*, et al.* (2005) Modulation of epithelial neoplasia and lymphoid hyperplasia in PTEN+/- mice by the p85 regulatory subunits of phosphoinositide 3-kinase. *Proc Natl Acad Sci U S A* 102(29):10238-10243.

32. Billin AN & Ayer DE (2006) The Mlx network: evidence for a parallel Max-like transcriptional network that regulates energy metabolism. *Curr Top Microbiol Immunol* 302:255-278.

33. Billin AN, Eilers AL, Coulter KL, Logan JS, & Ayer DE (2000) MondoA, a novel basic helix-loop-helix-leucine zipper transcriptional activator that constitutes a positive branch of a max-like network. *Mol Cell Biol* 20(23):8845-8854.

34. Kaadige MR, Elgort MG, & Ayer DE (2010) Coordination of glucose and glutamine utilization by an expanded Myc network. *Transcription* In Press.

35. Stoltzman CA*, et al.* (2008) Glucose sensing by MondoA:Mlx complexes: a role for hexokinases and direct regulation of thioredoxin-interacting protein expression. *Proc Natl Acad Sci U S A* 105(19):6912-6917.

36. Peterson CW, Stoltzman CA, Sighinolfi MP, Han KS, & Ayer DE (2010) Glucose controls nuclear accumulation, promoter binding, and transcriptional activity of the MondoA-Mlx heterodimer. *Mol Cell Biol* 30(12):2887-2895.

37. Kaadige MR, Looper RE, Kamalanaadhan S, & Ayer DE (2009) Glutamine-dependent anapleurosis dictates glucose uptake and cell growth by regulating MondoA transcriptional activity. *Proc Natl Acad Sci U S A* 106(35):14878-14883.

38. Sloan EJ & Ayer DE (2010) Myc, Mondo and Metabolism. *Genes & Cancer* In Press.

39. Yamashita H*, et al.* (2001) A glucose-responsive transcription factor that regulates carbohydrate metabolism in the liver. *Proc Natl Acad Sci U S A* 98(16):9116-9121.

40. Tong X, Zhao F, Mancuso A, Gruber JJ, & Thompson CB (2009) The glucose-responsive transcription factor ChREBP contributes to glucose-dependent

anabolic synthesis and cell proliferation. *Proc Natl Acad Sci U S A* 106(51):21660-21665.

41. Chutkow WA, Patwari P, Yoshioka J, & Lee RT (2008) Thioredoxin-interacting protein (Txnip) is a critical regulator of hepatic glucose production. *J Biol Chem* 283(4):2397-2406.

42. Jiang XR*, et al.* (1999) Telomerase expression in human somatic cells does not induce changes associated with a transformed phenotype. *Nat Genet* 21(1):111-114.

43. Eblen ST, Fautsch MP, Anders RA, & Leof EB (1995) Conditional binding to and cell cycle-regulated inhibition of cyclin-dependent kinase complexes by p27Kip1. *Cell Growth Differ* 6(8):915-925.

44. Reynisdottir I, Polyak K, Iavarone A, & Massague J (1995) Kip/Cip and Ink4 Cdk inhibitors cooperate to induce cell cycle arrest in response to TGF-beta. *Genes Dev* 9(15):1831-1845.

45. Sans CL, Satterwhite DJ, Stoltzman CA, Breen KT, & Ayer DE (2006) MondoA-Mlx heterodimers are candidate sensors of cellular energy status: mitochondrial localization and direct regulation of glycolysis. *Mol Cell Biol* 26(13):4863-4871.

46. Lum JJ*, et al.* (2007) The transcription factor HIF-1alpha plays a critical role in the growth factor-dependent regulation of both aerobic and anaerobic glycolysis. *Genes Dev* 21(9):1037-1049.

47. Butler LM*, et al.* (2002) The histone deacetylase inhibitor SAHA arrests cancer cell growth, up-regulates thioredoxin-binding protein-2, and down-regulates thioredoxin. *Proc Natl Acad Sci U S A* 99(18):11700-11705.

48. Deroo BJ, Hewitt SC, Peddada SD, & Korach KS (2004) Estradiol regulates the thioredoxin antioxidant system in the mouse uterus. *Endocrinology* 145(12):5485-5492.

49. Minn AH, Hafele C, & Shalev A (2005) Thioredoxin-interacting protein is stimulated by glucose through a carbohydrate response element and induces beta-cell apoptosis. *Endocrinology* 146(5):2397-2405.

50. Shao W, Yu Z, Fantus IG, & Jin T (2010) Cyclic AMP signaling stimulates proteasome degradation of thioredoxin interacting protein (TxNIP) in pancreatic beta-cells. *Cell Signal* 22(8):1240-1246.

51. Zhang P*, et al.* (2010) The ubiquitin ligase itch regulates apoptosis by targeting thioredoxin-interacting protein for ubiquitin-dependent degradation. *J Biol Chem* 285(12):8869-8879.

52. Lemmon MA & Schlessinger J (2010) Cell signaling by receptor tyrosine kinases. *Cell* 141(7):1117-1134.

53. Schulze PC*, et al.* (2004) Hyperglycemia promotes oxidative stress through inhibition of thioredoxin function by thioredoxin-interacting protein. *J Biol Chem* 279(29):30369-30374.

54. Hahn WC*, et al.* (1999) Creation of human tumour cells with defined genetic elements. *Nature* 400(6743):464-468.

55. Serrano M, Lin AW, McCurrach ME, Beach D, & Lowe SW (1997) Oncogenic ras provokes premature cell senescence associated with accumulation of p53 and p16INK4a. *Cell* 88(5):593-602.

56. Lim KH & Counter CM (2005) Reduction in the requirement of oncogenic Ras signaling to activation of PI3K/AKT pathway during tumor maintenance. *Cancer Cell* 8(5):381-392.

57. Littlewood TD, Hancock DC, Danielian PS, Parker MG, & Evan GI (1995) A modified oestrogen receptor ligand-binding domain as an improved switch for the regulation of heterologous proteins. *Nucleic Acids Res* 23(10):1686-1690.

58. Dang CV & Semenza GL (1999) Oncogenic alterations of metabolism. *Trends Biochem Sci* 24(2):68-72.

59. Wieman HL, Wofford JA, & Rathmell JC (2007) Cytokine stimulation promotes glucose uptake via phosphatidylinositol-3 kinase/Akt regulation of Glut1 activity and trafficking. *Mol Biol Cell* 18(4):1437-1446.

60. DeBerardinis RJ, Lum JJ, Hatzivassiliou G, & Thompson CB (2008) The biology of cancer: metabolic reprogramming fuels cell growth and proliferation. *Cell Metab* 7(1):11-20.

61. Gazdar AF (2009) Activating and resistance mutations of EGFR in non-small-cell lung cancer: role in clinical response to EGFR tyrosine kinase inhibitors. *Oncogene* 28 Suppl 1:S24-31.

62. Lievre A, Blons H, & Laurent-Puig P (2010) Oncogenic mutations as predictive factors in colorectal cancer. *Oncogene* 29(21):3033-3043.

63. Perrone L, Devi TS, Hosoya K, Terasaki T, & Singh LP (2009) Thioredoxin interacting protein (TXNIP) induces inflammation through chromatin modification in retinal capillary endothelial cells under diabetic conditions. *J Cell Physiol* 221(1):262-272.

64. Jiang BH & Liu LZ (2009) PI3K/PTEN signaling in angiogenesis and tumorigenesis. *Adv Cancer Res*), Vol 102, pp 19-65.

65. Morrish F, Isern N, Sadilek M, Jeffrey M, & Hockenbery DM (2009) c-Myc activates multiple metabolic networks to generate substrates for cell-cycle entry. *Oncogene* 28(27):2485-2491.

66. Wallace DC (2005) Mitochondria and cancer: Warburg addressed. *Cold Spring Harb Symp Quant Biol* 70:363-374.

67. Racker E, Resnick RJ, & Feldman R (1985) Glycolysis and methylaminoisobutyrate uptake in rat-1 cells transfected with ras or myc oncogenes. *Proc Natl Acad Sci U S A* 82(11):3535-3538.

68. Ramanathan A, Wang C, & Schreiber SL (2005) Perturbational profiling of a cell-line model of tumorigenesis by using metabolic measurements. *Proc Natl Acad Sci U S A* 102(17):5992-5997.

69. Chen C, Pore N, Behrooz A, Ismail-Beigi F, & Maity A (2001) Regulation of glut1 mRNA by hypoxia-inducible factor-1. Interaction between H-ras and hypoxia. *J Biol Chem* 276(12):9519-9525.

70. Sears R, Leone G, DeGregori J, & Nevins JR (1999) Ras enhances Myc protein stability. *Mol Cell* 3(2):169-179.

71. Hu CJ, Wang LY, Chodosh LA, Keith B, & Simon MC (2003) Differential roles of hypoxia-inducible factor 1alpha (HIF-1alpha) and HIF-2alpha in hypoxic gene regulation. *Mol Cell Biol* 23(24):9361-9374.

72. Kim JW*, et al.* (2004) Evaluation of myc E-box phylogenetic footprints in glycolytic genes by chromatin immunoprecipitation assays. *Mol Cell Biol* 24(13):5923-5936.

73. Gao P*, et al.* (2009) c-Myc suppression of miR-23a/b enhances mitochondrial glutaminase expression and glutamine metabolism. *Nature* 458(7239):762-765.

74. Shim H, Chun YS, Lewis BC, & Dang CV (1998) A unique glucose-dependent apoptotic pathway induced by c-Myc. *Proc Natl Acad Sci U S A* 95(4):1511-1516.

75. Wise DR*, et al.* (2008) Myc regulates a transcriptional program that stimulates mitochondrial glutaminolysis and leads to glutamine addiction. *Proc Natl Acad Sci U S A* 105(48):18782-18787.

76. Yuneva M, Zamboni N, Oefner P, Sachidanandam R, & Lazebnik Y (2007) Deficiency in glutamine but not glucose induces MYC-dependent apoptosis in human cells. *J Cell Biol* 178(1):93-105.

77. Li X*, et al.* (2009) Up-regulation of thioredoxin interacting protein (Txnip) by p38 MAPK and FOXO1 contributes to the impaired thioredoxin activity and increased ROS in glucose-treated endothelial cells. *Biochem Biophys Res Commun* 381(4):660-665.

78. Havens CG, Ho A, Yoshioka N, & Dowdy SF (2006) Regulation of late G1/S phase transition and APC Cdh1 by reactive oxygen species. *Mol Cell Biol* 26(12):4701-4711.

79. Pardee AB (1974) A restriction point for control of normal animal cell proliferation. *Proc Natl Acad Sci U S A* 71(4):1286-1290.

80. Uyeda K & Repa JJ (2006) Carbohydrate response element binding protein, ChREBP, a transcription factor coupling hepatic glucose utilization and lipid synthesis. *Cell Metab* 4(2):107-110.

81. Cassel D, Rothenberg P, Zhuang YX, Deuel TF, & Glaser L (1983) Platelet-derived growth factor stimulates Na+/H+ exchange and induces cytoplasmic alkalinization in NR6 cells. *Proc Natl Acad Sci U S A* 80(20):6224-6228.

82. Escobedo JA, Keating MT, Ives HE, & Williams LT (1988) Platelet-derived growth factor receptors expressed by cDNA transfection couple to a diverse group of cellular responses associated with cell proliferation. *J Biol Chem* 263(3):1482-1487.

83. Pan W, Xin P, & Clawson GA (2010) MicroRNAs align with accessible sites in target mRNAs. *J Cell Biochem* 109(3):509-518.

84. Qin W*, et al.* (2010) miR-24 regulates apoptosis by targeting the open reading frame (ORF) region of FAF1 in cancer cells. *PLoS One* 5(2):e9429.

85. Hotamisligil GS (2010) Endoplasmic reticulum stress and the inflammatory basis of metabolic disease. *Cell* 140(6):900-917.

86. Monick MM*, et al.* (2006) Active ERK contributes to protein translation by preventing JNK-dependent inhibition of protein phosphatase 1. *J Immunol* 177(3):1636-1645.

87. Thiaville MM*, et al.* (2008) MEK signaling is required for phosphorylation of eIF2alpha following amino acid limitation of HepG2 human hepatoma cells. *J Biol Chem* 283(16):10848-10857.

88. Sun P*, et al.* (2006) Sustained activation of M-Ras induced by nerve growth factor is essential for neuronal differentiation of PC12 cells. *Genes Cells* 11(9):1097-1113.

89. Tan PB & Kim SK (1999) Signaling specificity: the RTK/RAS/MAP kinase pathway in metazoans. *Trends Genet* 15(4):145-149.

90. Blanchard JM*, et al.* (1985) c-myc gene is transcribed at high rate in G0-arrested fibroblasts and is post-transcriptionally regulated in response to growth factors. *Nature* 317(6036):443-445.

91. Walker W, Zhou ZQ, Ota S, Wynshaw-Boris A, & Hurlin PJ (2005) Mnt-Max to Myc-Max complex switching regulates cell cycle entry. *J Cell Biol* 169(3):405-413.

92. Watanabe R, Nakamura H, Masutani H, & Yodoi J (2010) Anti-oxidative, anti-cancer and anti-inflammatory actions by thioredoxin 1 and thioredoxin-binding protein-2. *Pharmacol Ther* 127(3):261-270.

93. Todaro GJ & Green H (1963) Quantitative studies of the growth of mouse embryo cells in culture and their development into established lines. *J Cell Biol* 17:299-313.

94. Morgenstern JP & Land H (1990) Advanced mammalian gene transfer: high titre retroviral vectors with multiple drug selection markers and a complementary helper-free packaging cell line. *Nucleic Acids Res* 18(12):3587-3596.

95. Gavrilescu LC & Van Etten RA (2007) Production of replication-defective retrovirus by transient transfection of 293T cells. *J Vis Exp* (10):550.

96. Tiscornia G, Singer O, & Verma IM (2006) Production and purification of lentiviral vectors. *Nat Protoc* 1(1):241-245.

CHAPTER 3

SUMMARY

Proliferating cells are required not only to replicate their genomes during each passage through the cell cycle, but additionally they must duplicate all macromolecular components prior to mitosis and cytokinesis. This presents proliferating cells with significant metabolic challenges as they must increase nutrient uptake and metabolic activity to accommodate increases in biosynthetic activities. To accomplish this, the metabolism of proliferating cells is significantly different from that of nonproliferating cells. Proliferating cells engage in aerobic glycolysis which drives cytoplasmic ATP production and diverts metabolites from glycolysis and the TCA cycle to biosynthetic reactions including protein, lipid and nucleotide biosynthesis (1, 2). Non-proliferating cells primarily engage in glycolysis, but principally to generate pyruvate which feeds the TCA cycle in the mitochondria where the majority of ATP synthesis occurs by oxidative phosphorylation (3).

As outlined in Chapter 1, quiescent cells can be stimulated to proliferate and a component of entry into the cell cycle is metabolic reprogramming from oxidative metabolism to aerobic glycolysis (2). Growth factor signaling pathways drive increased glucose uptake as well as uptake of other nutrients required for cell growth (4, 5). Additionally, these pathways upregulate transcriptional programs that increase glycolytic flux and nutrient uptake (6-10). PI3K/Akt and Ras-MAPK signaling downstream of growth factor receptors directly drive metabolic reprogramming by increasing GLUT trafficking and activating Myc and HIF which directly increase the transcription of

glycolytic targets. Additionally, Myc directly drives mitochondrial biogenesis and glutaminolysis necessary for utilization of TCA cycle intermediates for biosynthetic reactions. Clearly, regulation of metabolic reprogramming is a highly complex and orchestrated process, not unlike the cell cycle itself.

Chapter 2 introduces two new regulators of metabolic reprogramming, the transcription factor MondoA and the tumor suppressor TXNIP. Data from TXNIP$^{-/-}$ mice suggests that TXNIP downregulation supports growth and proliferation as well as increasing aerobic glycolysis and nutrient uptake (11, 12). MondoA directly regulates *TXNIP* transcription and restricts glucose uptake, in part, through TXNIP protein (13). Additionally, MondoA knockdown drives increased proliferation and glucose uptake in certain cellular contexts and MondoA$^{-/-}$ have no detectable TXNIP expression and high rates of glucose uptake (14, 15). Taken together, these data suggest that MondoA and TXNIP might regulate cell growth and proliferation through their negative regulation of glucose availability and glycolysis. Thus, MondoA and TXNIP regulation in cells transitioning from quiescence (G_0) into the growth phase (G_1) of the cell cycle is examined in Chapter 2.

As TXNIP activity is required for cellular quiescence (16, 17), it is no surprise that it is highly upregulated in BJ hTERT cells quiesced by serum starvation. TXNIP protein and mRNA are both acutely downregulated by the readdition of serum which releases cells into G_1. Concomitant with TXNIP downregulation is the upregulation of glucose uptake and glycolysis which are hallmarks of metabolic reprogramming from oxidative phosphorylation in G_0 to aerobic glycolysis in G_1. As cells progress through G_1, both glucose uptake and glycolysis plateau, presumably as the cells metabolic needs have been met, and TXNIP transcription and translation are upregulated. We show that ectopic expression of TXNIP in early G_1 restricts glucose uptake, glycolysis and S-phase entry, suggesting that downregulation of TXNIP is necessary for metabolic

reprogramming and cell growth (Figure 3.1). We ultimately show that TXNIP transcription and translation are inhibited by Ras-MAPK and PI3K/Akt signaling downstream of EGF and PDGF receptor signals.

While MondoA appears to be ubiquitously present throughout G_0 and G_1, its transcriptional activity at the *TXNIP* promoter as well as another arrestin protein, *ARRDC4* (18) is highly regulated. We show that *TXNIP* transcription is downregulated when MondoA leaves the *TXNIP* promoter, likely concomitantly, with serum addition to quiescent BJ hTERTs. Expression of a constitutively active allele of MondoA, ΔN237NLSMondoA, in early G_1 restricts glucose uptake and S-phase entry but not glycolysis. As MondoA has been shown to upregulate the glycolytic genes *HKII*, *PKFB3* and *LDHA* (19), it is likely that constitutive activation of these targets, and likely other yet characterized targets, is in direct opposition to TXNIP downregulation of glycolysis and the net effect is no change in glycolytic rate. PDGF stimulation of BJ hTERTs modestly downregulated MondoA-dependent TXNIP transcription through a PI3K dependent mechanism; however, inhibition of PI3K was not sufficient to restore TXNIP mRNA in serum-treated cells. This suggests that signaling pathways parallel to PI3K must also regulate MondoA-dependent TXNIP transcription. Preliminary studies with lysophosphatidic acid (LPA) which signals through multiple networks including PI3K and Ras (20), demonstrate that TXNIP mRNA is downregulated by one or more of these pathways (Figure 3.2). Not surprisingly, the phorbol ester, phorbol-12-myristate-13-acetate (PMA), which is a potent tumor promoter that activates Raf directly through protein kinase C (PKC) (21), also downregulates MondoA-dependent TXNIP transcription and this is not reversed with PI3K inhibition by wortmannin (Figure 3.2). Clearly, regulation of MondoA-dependent TXNIP transcription by growth factor signaling is complex and remains an open question.

Figure 3.1 MondoA and TXNIP regulation during the G_0/G_1 transition. During quiescence, MondoA and TXNIP activities are regulated by glucose and the absence of extracellular signaling. MondoA-dependent TXNIP transcription and TXNIP translation are robust, thus restricting glucose uptake and glycolysis and preventing cell growth. Upon serum or growth factor addition, MondoA leaves the TXNIP promoter preventing TXNIP transcription and TXNIP translation is inhibited by a Ras-MAPK dependent mechanism. Growth factor signaling increases glucose uptake and glycolysis, in part, by downregulation of MondoA transcriptional activity and TXNIP. As MondoA and TXNIP are no longer regulated by glucose, high glucose uptake and glycolytic flux drives growth and cell proliferation.

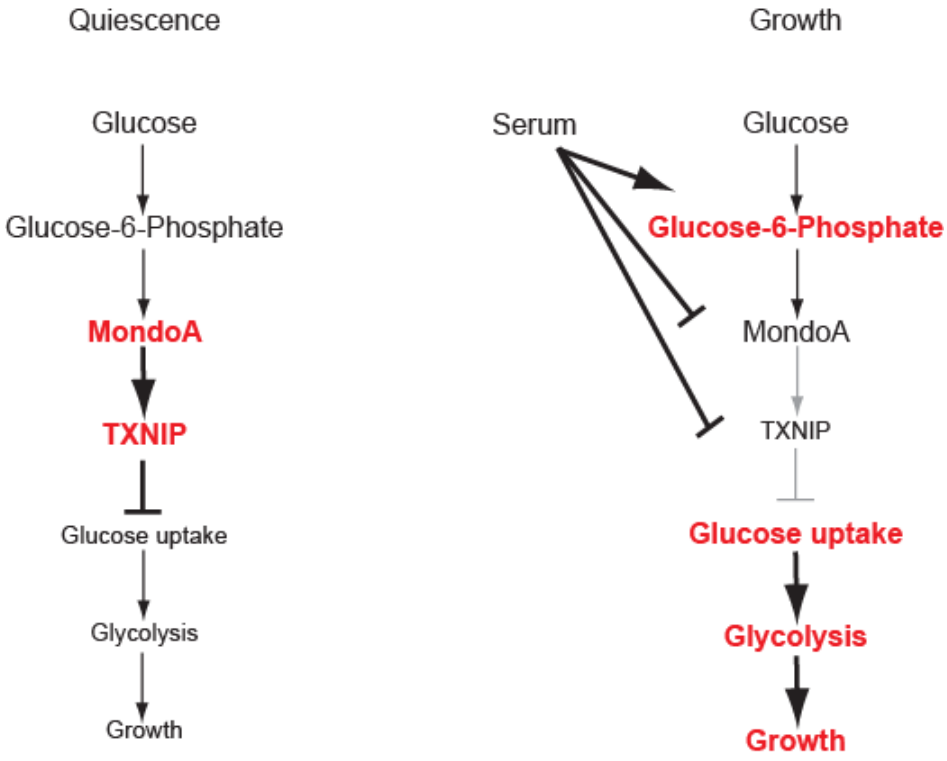
Quiescence
Glucose
Glucose-6-Phosphate
MondoA
TXNIP
Glucose uptake
Glycolysis
Growth
Growth
Serum
Glucose
Glucose-6-Phosphate
MondoA
TXNIP
Glucose uptake
Glycolysis
Growth

Figure 3.2 Lysophosphatidic acid (LPA) and phorbol-12-myristate-13-acetate (PMA) downregulate TXNIP mRNA. RT-qPCR reactions on mRNA isolated 4 hours after serum, PDGF, LPA, PMA and EGF addition to quiescent BJ hTERT cells. Serum maximally downregulates TXNIP mRNA and this is not reversible by u0126 (MEK), wortmannin (PI3K) or PKC inhibition. PDGF modestly downregulates TXNIP mRNA and this is reversible by wortmannin treatment suggesting PI3K signaling downregulates TXNIP mRNA upon PDGF stimulation. LPA downregulation of TXNIP mRNA is not reversible by PI3K inhibition suggesting a parallel pathway is involved, however, the complexity of LPA signaling limits study of this. PMA potently downregulates TXNIP mRNA as well, and only PKC inhibition reverses this, consistent with PMA activating PKC. EGF has no effect on TXNIP mRNA. Serum, EGF and PDGF regulation of TXNIP transcription are discussed in Chapter 2.

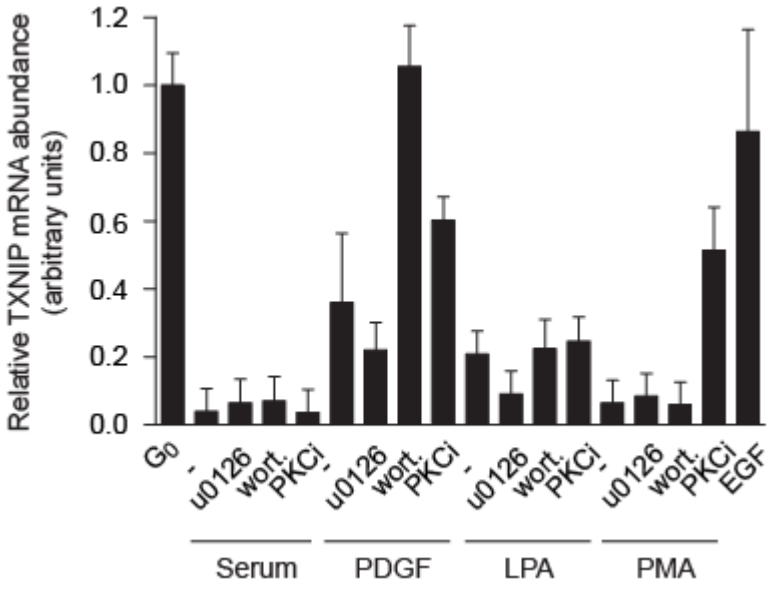
Relative TXNIP mRNA abundance
(arbitrary units)
1.2
1.0
0.8
0.6
0.4
0.2
0.0
G0
-
u0126
wort.
PKCi
-
u0126
wort.
PKCi
-
u0126
wort.
PKCi
-
u0126
wort.
PKCi
EGF
Serum
PDGF
LPA
PMA

Two important mechanistic questions arise from the work in Chapter 2. First, we have shown that TXNIP is highly regulated by both MondoA and glucose (13), however, in early G_1, MondoA and glucose are replete and yet there is no TXNIP transcription or translation. As we show MondoA leaves the TXNIP promoter upon serum re-addition, one likely explanation is that MondoA is modified, for example by phosphorylation, and its nuclear entry is restricted or it is alternatively localized. ChREBP subcellular localization and transcriptional activity have been shown to be regulated by phosphorylation of key residues encompassing its DNA binding domain and nuclear localization sequence (22); however, these residues are not conserved in MondoA. Additionally, preliminary immunofluorescence experiments examining MondoA subcellular localization in response to serum and PDGF, in the presence and absence of wortmannin, reveal no significant changes in MondoA localization and more importantly, cytoplasmic-nuclear shuttling does not appear to change. While we cannot formally rule out post-translational modification of MondoA, a more tractable model explaining how MondoA leaves the TXNIP promoter comes from recent work showing that lactic acidosis increases TXNIP transcription by increasing MondoA occupancy at the *TXNIP* promoter (23). As growth factor stimulation acutely increases intracellular pH (24, 25) it is certainly possible that as pH decreases from lactic acidosis increase MondoA occupancy on the *TXNIP* promoter, pH increases resulting from RTK signaling could reduce MondoA occupancy accounting for the acute downregulation of TXNIP mRNA. However, to fully gain an understanding of how serum might regulate MondoA activity, we must also understand how MondoA is regulated at other target promoters. While *HKII* and *LDHA* are directly regulated by MondoA (19), this activity does not appear to be glucose regulated. As such, we are currently trying to acquire more glucose and constitutive MondoA targets by chromatin immunoprecipitation sequencing (ChIP Seq)

(26, 27). Still, regulation of MondoA-dependent *TXNIP* transcription in G_1 remains an open question.

An alternative mechanism for downregulation of MondoA promoter occupancy at *TXNIP* comes from the observation that Mnt (figure 1.4) can dimerize with Mlx (28). Mnt:Max heterodimers occupy Myc transcriptional targets regulating growth and proliferation during quiescence and subsequently repress their transcription (29). Upon growth factor stimulation, Myc is upregulated and Myc:Max heterodimers dominate occupancy of Myc transcriptional targets (29). The Myc:Max heterodimers form at the expense of Mnt:Max complexes, yet Mnt expression is transiently stable (29). It is therefore conceivable that Mnt:Mlx heterodimers form during this period at the expense of MondoA:Mlx complexes, either reducing the number of MondoA:Mlx heterodimers available to activate MondoA targets like *TXNIP* or simply, Mnt:Mlx complexes displace MondoA at targets like *TXNIP* and repress their transcription. Certainly, looking at Mnt occupancy at the *TXNIP* promoter would resolve this issue, however, given the potential cooperativity of Myc superfamily members (30), a more comprehensive strategy would be to examine Myc, Mnt, MondoA and ChREBP occupancy at multiple targets during the G_0/G_1 transition by ChIP Seq.

The second important mechanistic question raised in Chapter 2 is how TXNIP translation is downregulated by growth factor signaling in early G_1. We demonstrate that TXNIP translation is acutely downregulated by MAPK activation directly downstream of Ras activation (Figure 2.8). TXNIP-mCherry is clearly regulated by serum (Figure 2.2A) suggesting that TXNIP is likely downregulated at the level of translation or by its coding sequence, as TXNIP-mCherry contains only the open reading frame of *TXNIP* (18). If eiF2α, shown to regulate the translation of other stress induced proteins, like ATF4, is responsible for TXNIP translation in G_0, its MAPK induced dephosphorylation upon serum addition would explain the acute downregulation in G_1 (31-34). However, the

mechanism of phosphorylated eiFα-mediated translation elongation relies on it scanning the 5' untranslated region (UTR) of its targets for alternate open reading frames (33-35). TXNIP contains a minimal 5' UTR with no alternate translation start sites and TXNIP-mCherry does not contain the TXNIP 5' UTR; thus, this it is unlikely that TXNIP translation is regulated in this way. Alternatively, there are other examples of signaling cascades directly impinging on the translation machinery supporting a mechanism inhibiting TXNIP translation at this level (32, 36). Alternatively, there is recent evidence supporting TXNIP downregulation by microRNA (miRNA) (37), and while we suggest in Chapter 2 that the kinetics of TXNIP downregulation in response to serum are incompatible with new transcription, we cannot formally rule this out as a potential mechanism.

The data presented in Chapter 2 establishes the necessity of TXNIP downregulation for cells to enter the cell cycle from a quiescent state. The fact that both TXNIP transcription and translation are downregulated further underscores this point. Our data indicate that TXNIP transcription and translation are inhibited as acute immediate-early responses to growth factor signaling. However, each mechanism persists for different durations (Figure 2.5). This suggests a mechanism where TXNIP translation is inhibited for a time necessary to allow sufficient mRNA decay and subsequently transcriptional inhibition reinforces TXNIP downregulation. This appears to be the case as EGF stimulation only downregulates TXNIP translation and not mRNA, and TXNIP expression is restored early (Figure 2.7). While growth factor signaling has been shown to regulate metabolic reprogramming (1, 2, 38) mechanistically, however, it is not clear how this is accomplished directly. It is clear from this work that MondoA and TXNIP represent important downstream effectors.

The switch to aerobic glycolysis supplies both energy and macromolecules to support cell proliferation and as such understanding how this is accomplished at a

mechanistic level is important in understanding the pathogenesis of disease involving proliferation, namely cancer. Data in Chapter 2 identify the necessity of downregulation of TXNIP translation and MondoA-dependent TXNIP transcription for metabolic reprogramming and growth, however, it still remains unclear how these proteins negatively regulate glucose uptake and glycolysis. This work provides further insight into the regulation of metabolic reprogramming presented in Chapter 1 and lays the ground work for additional studies in the regulation of cell growth and metabolism by MondoA and TXNIP.

3.1 References

1. DeBerardinis RJ, Lum JJ, Hatzivassiliou G, & Thompson CB (2008) The biology of cancer: metabolic reprogramming fuels cell growth and proliferation. *Cell Metab* 7(1):11-20.

2. Fox CJ, Hammerman PS, & Thompson CB (2005) Fuel feeds function: energy metabolism and the T-cell response. *Nat Rev Immunol* 5(11):844-852.

3. Frauwirth KA & Thompson CB (2004) Regulation of T lymphocyte metabolism. *J Immunol* 172(8):4661-4665.

4. Frauwirth KA*, et al.* (2002) The CD28 signaling pathway regulates glucose metabolism. *Immunity* 16(6):769-777.

5. Wieman HL, Wofford JA, & Rathmell JC (2007) Cytokine stimulation promotes glucose uptake via phosphatidylinositol-3 kinase/Akt regulation of Glut1 activity and trafficking. *Mol Biol Cell* 18(4):1437-1446.

6. Chen C, Pore N, Behrooz A, Ismail-Beigi F, & Maity A (2001) Regulation of glut1 mRNA by hypoxia-inducible factor-1. Interaction between H-ras and hypoxia. *J Biol Chem* 276(12):9519-9525.

7. Racker E, Resnick RJ, & Feldman R (1985) Glycolysis and methylaminoisobutyrate uptake in rat-1 cells transfected with ras or myc oncogenes. *Proc Natl Acad Sci U S A* 82(11):3535-3538.

8. Ramanathan A, Wang C, & Schreiber SL (2005) Perturbational profiling of a cell-line model of tumorigenesis by using metabolic measurements. *Proc Natl Acad Sci U S A* 102(17):5992-5997.

9. Sears R, Leone G, DeGregori J, & Nevins JR (1999) Ras enhances Myc protein stability. *Mol Cell* 3(2):169-179.

10. Dang CV & Semenza GL (1999) Oncogenic alterations of metabolism. *Trends Biochem Sci* 24(2):68-72.

11. Hui ST*, et al.* (2008) Txnip balances metabolic and growth signaling via PTEN disulfide reduction. *Proc Natl Acad Sci U S A* 105(10):3921-3926.

12. Hui TY*, et al.* (2004) Mice lacking thioredoxin-interacting protein provide evidence linking cellular redox state to appropriate response to nutritional signals. *J Biol Chem* 279(23):24387-24393.

13. Stoltzman CA*, et al.* (2008) Glucose sensing by MondoA:Mlx complexes: a role for hexokinases and direct regulation of thioredoxin-interacting protein expression. *Proc Natl Acad Sci U S A* 105(19):6912-6917.

14. Kaadige MR, Looper RE, Kamalanaadhan S, & Ayer DE (2009) Glutamine-dependent anapleurosis dictates glucose uptake and cell growth by regulating MondoA transcriptional activity. *Proc Natl Acad Sci U S A* 106(35):14878-14883.

15. Peterson CW, Stoltzman CA, Sighinolfi MP, Han KS, & Ayer DE (2010) Glucose controls nuclear accumulation, promoter binding, and transcriptional activity of the MondoA-Mlx heterodimer. *Mol Cell Biol* 30(12):2887-2895.

16. Jeon JH*, et al.* (2005) Tumor suppressor VDUP1 increases p27(kip1) stability by inhibiting JAB1. *Cancer Res* 65(11):4485-4489.

17. Jeong M*, et al.* (2009) Thioredoxin-interacting protein regulates hematopoietic stem cell quiescence and mobilization under stress conditions. *J Immunol* 183(4):2495-2505.

18. Patwari P*, et al.* (2009) Thioredoxin-independent regulation of metabolism by the alpha-arrestin proteins. *J Biol Chem* 284(37):24996-25003.

19. Sans CL, Satterwhite DJ, Stoltzman CA, Breen KT, & Ayer DE (2006) MondoA-Mlx heterodimers are candidate sensors of cellular energy status: mitochondrial localization and direct regulation of glycolysis. *Mol Cell Biol* 26(13):4863-4871.

20. Yart A, Chap H, & Raynal P (2002) Phosphoinositide 3-kinases in lysophosphatidic acid signaling: regulation and cross-talk with the Ras/mitogen-activated protein kinase pathway. *Biochim Biophys Acta* 1582(1-3):107-111.

21. Liu WS & Heckman CA (1998) The sevenfold way of PKC regulation. *Cell Signal* 10(8):529-542.

22. Uyeda K & Repa JJ (2006) Carbohydrate response element binding protein, ChREBP, a transcription factor coupling hepatic glucose utilization and lipid synthesis. *Cell Metab* 4(2):107-110.

23. Chen JL-Y*, et al.* (2010) Lactic acidosis triggers starvation response with paradoxical induction of TXNIP through MondoA. *PloS Genetics* In Press.

24. Cassel D, Rothenberg P, Zhuang YX, Deuel TF, & Glaser L (1983) Platelet-derived growth factor stimulates Na+/H+ exchange and induces cytoplasmic alkalinization in NR6 cells. *Proc Natl Acad Sci U S A* 80(20):6224-6228.

25. Escobedo JA, Keating MT, Ives HE, & Williams LT (1988) Platelet-derived growth factor receptors expressed by cDNA transfection couple to a diverse group of cellular responses associated with cell proliferation. *J Biol Chem* 263(3):1482-1487.

26. Park PJ (2009) ChIP-seq: advantages and challenges of a maturing technology. *Nat Rev Genet* 10(10):669-680.

27. Farnham PJ (2009) Insights from genomic profiling of transcription factors. *Nat Rev Genet* 10(9):605-616.

28. Meroni G*, et al.* (2000) Mlx, a new Max-like bHLHZip family member: the center stage of a novel transcription factors regulatory pathway? *Oncogene* 19(29):3266-3277.

29. Walker W, Zhou ZQ, Ota S, Wynshaw-Boris A, & Hurlin PJ (2005) Mnt-Max to Myc-Max complex switching regulates cell cycle entry. *J Cell Biol* 169(3):405-413.

30. Zhang P*, et al.* (2010) c-Myc is required for the CHREBP-dependent activation of glucose-responsive genes. *Mol Endocrinol* 24(6):1274-1286.

31. Kilberg MS, Shan J, & Su N (2009) ATF4-dependent transcription mediates signaling of amino acid limitation. *Trends Endocrinol Metab* 20(9):436-443.

32. Monick MM*, et al.* (2006) Active ERK contributes to protein translation by preventing JNK-dependent inhibition of protein phosphatase 1. *J Immunol* 177(3):1636-1645.

33. Bi M*, et al.* (2005) ER stress-regulated translation increases tolerance to extreme hypoxia and promotes tumor growth. *EMBO J* 24(19):3470-3481.

34. Harding HP*, et al.* (2000) Regulated translation initiation controls stress-induced gene expression in mammalian cells. *Mol Cell* 6(5):1099-1108.

35. Ron D & Walter P (2007) Signal integration in the endoplasmic reticulum unfolded protein response. *Nat Rev Mol Cell Biol* 8(7):519-529.

36. Thiaville MM*, et al.* (2008) MEK signaling is required for phosphorylation of eIF2alpha following amino acid limitation of HepG2 human hepatoma cells. *J Biol Chem* 283(16):10848-10857.

37. Zhuo DX*, et al.* (2010) Vitamin D3 up-regulated protein 1 (VDUP1) is regulated by FOXO3A and miR-17-5p at the transcriptional and posttranscriptional levels, respectively, in senescent fibroblasts. *J Biol Chem*.

38. Vander Heiden MG*, et al.* (2001) Growth factors can influence cell growth and survival through effects on glucose metabolism. *Mol Cell Biol* 21(17):5899-5912.

APPENDIX A

AN ACTIVATING MUTATION IN *SOS-1* IDENTIFIES ITS DBL DOMAIN AS A CRITICAL INHIBITOR OF THE EPIDERMAL GROWTH FACTOR RECEPTOR PATHWAY DURING *CAENORHABDITIS ELEGANS* VULVAL DEVELOPMENT

Appendix A is a manuscript published in Molecular and Cellular Biology in May, 2007. It is reprinted here with permission from the publisher and the authors. Briefly, it describes an activating mutation in the Ras-GEF Sos that results in sustained MAPK activation in the presence of EGFR signaling. This work was done in the laboratory of Nadeem Moghal. Katarzyna Modzelewska and Marc G. Elgort are co-first authors on the manuscript and contributed equally to the research along with the writing of the discussion under the guidance of Nadeem Moghal. Marc G. Elgort recapitulated the Cdc25 mutations in human Sos and performed the experiments shown in Figure 4 of the published manuscript.

MOLECULAR AND CELLULAR BIOLOGY, May 2007, p. 3695–3707 Vol. 27, No. 10
0270-7306/07/$08.00+0 doi:10.1128/MCB.01630-06

An Activating Mutation in *sos-1* Identifies Its Dbl Domain as a Critical Inhibitor of the Epidermal Growth Factor Receptor Pathway during *Caenorhabditis elegans* Vulval Development[▽]

Katarzyna Modzelewska,[1]† Marc G. Elgort,[1]† Jingyu Huang,[1] Gregg Jongeward,[2]‡ Amara Lauritzen,[1] Charles H. Yoon,[2]§ Paul W. Sternberg,[2] and Nadeem Moghal[1]*

Department of Oncological Sciences, Huntsman Cancer Institute, University of Utah, 2000 Circle of Hope, Room 3242, Salt Lake City, Utah 84112-5550,[1] and Howard Hughes Medical Institute and Division of Biology, California Institute of Technology, Pasadena, California 91125[2]

Received 1 September 2006/Returned for modification 7 November 2006/Accepted 15 February 2007

Proper regulation of receptor tyrosine kinase (RTK)–Ras–mitogen-activated protein kinase (MAPK) signaling pathways is critical for normal development and the prevention of cancer. SOS is a dual-function guanine nucleotide exchange factor (GEF) that catalyzes exchange on Ras and Rac. Although the physiologic role of SOS and its CDC25 domain in RTK-mediated Ras activation is well established, the in vivo function of its Dbl Rac GEF domain is less clear. We have identified a novel gain-of-function missense mutation in the Dbl domain of *Caenorhabditis elegans* SOS-1 that promotes epidermal growth factor receptor (EGFR) signaling in vivo. Our data indicate that a major developmental function of the Dbl domain is to inhibit EGF-dependent MAPK activation. The amount of inhibition conferred by the Dbl domain is equal to that of established *trans*-acting inhibitors of the EGFR pathway, including c-Cbl and RasGAP, and more than that of MAPK phosphatase. In conjunction with molecular modeling, our data suggest that the *C. elegans* mutation, as well as an equivalent mutation in human SOS1, activates the MAPK pathway by disrupting an autoinhibitory function of the Dbl domain on Ras activation. Our work suggests that functionally similar point mutations in humans could directly contribute to disease.

Receptor tyrosine kinase (RTK)–Ras–mitogen-activated protein kinase (MAPK) signaling pathways play profound roles in development and, when improperly regulated, can contribute to oncogenesis (8). Although most of the core components of RTK-Ras-MAPK pathways were discovered a decade ago, the diverse mechanisms for positive and negative regulation are still being elucidated. Genetic model organisms, such as *Caenorhabditis elegans* and *Drosophila melanogaster*, have been invaluable for the study of the regulation of these pathways. In the *C. elegans* hermaphrodite, a single epidermal growth factor (EGF)-like ligand and a single EGF receptor (EGFR) family member are required for normal development and behavior (61). A canonical EGFR-Grb2-SOS-Ras-Raf-Mek-MAPK pathway is essential for viability past the first larval stage and for development of the vulva, while an EGF-dependent inositol (1,4,5)-trisphosphate (IP3) pathway that is Ras independent controls ovulation behavior. The vulva develops through the induction of vulval cell fates in three out of six progenitor cells. The initiating events are the production of LIN-3 (EGF) from the anchor cell in the somatic gonad and its stimulation of LET-23 (EGFR) on the underlying P6.p progenitor cell. In the presence of sufficient levels of EGFR signaling and a cooperating signal from a Wnt pathway, *Notch* receptor ligands are upregulated and stimulate LIN-12 (*Notch*) on the adjacent P5.p and P7.p progenitors (17). Ultimately, eight progeny are produced from P6.p and seven each from P5.p and P7.p to form a mature 22-cell vulva. The remaining progenitor cells, P3.p, P4.p, and P8.p, fuse with an underlying hypodermal syncytium and do not adopt vulval fates.

Vulval development is well suited for studying EGFR-Ras-MAPK pathway regulation, since small deviations in signaling intensity quantifiably affect vulval development. Too little signaling results in fewer than three progenitor cells adopting vulval fates (vulvaless [Vul]), while excessive signaling results in more than three progenitor cells adopting vulval fates (multivulva [Muv]). Using various genetically defined sensitized backgrounds of either too little or too much signaling, a variety of mechanisms have been identified that regulate output or responsiveness to EGFR-Ras-MAPK signaling (61). These mechanisms include cell-autonomous *trans*-acting factors, such as SLI-1 (c-Cbl) (45, 96), KSR-1 (54, 87), and GAP-1 (Ras GAP) (37); cell-autonomous intramolecular constraints, such as autoinhibitory determinants within the EGFR (50, 62); and non-cell-autonomous pathways involving heterologous signals from surrounding neurons and muscles (60).

Here, we describe the isolation of a novel gain-of-function mutation in the guanine nucleotide exchange factor (GEF) SOS-1. SOS is a multidomain protein (see Fig. 2B) that in vitro catalyzes exchange on Ras through its CDC25 domain (16, 28) and exchange on Rac through its Dbl domain (65). In *Drosophila* (9, 75), *C. elegans* (15), and mouse (69, 92), SOS is

* Corresponding author. Mailing address: Department of Oncological Sciences, Huntsman Cancer Institute, University of Utah, 2000 Circle of Hope, Room 3242, Salt Lake City, UT 84112-5550. Phone: (801) 585-1358. Fax: (801) 587-9415. E-mail: nadeem.moghal@hci.utah.edu.

‡ Present address: Department of Biological Sciences, University of the Pacific, 3601 Pacific Ave., Stockton, CA 95211.

§ Present address: Department of Surgery, Columbia Presbyterian Medical Center, 177 Fort Washington Avenue, New York, NY 10032.

† K. Modzelewska and M. G. Elgort contributed equally.

▽ Published ahead of print on 5 March 2007.

essential for development. Whereas it is clear that SOS and its CDC25 domain are crucial for RTK-mediated Ras signaling (9, 15, 69, 75, 92) and that perturbation of this function leads to developmental defects (9, 15, 75), it is less clear to what extent its Dbl domain is also required for normal development. Recent studies have demonstrated that a variety of signals, including phosphatidylinositides (65), protein phosphorylation (82), and protein interactions (80), can regulate SOS Rac GEF activity, suggesting the catalytic activity of the Dbl domain may also be important for development. We found that our gain-of-function mutation in *sos-1*, which strongly affects an EGFR-Ras-MAPK pathway, lies in the Dbl domain rather than the CDC25 domain. Genetic analysis indicated that the activated mutant SOS-1 predominantly signals through Ras, rather than Rac, suggesting that the Dbl domain has an inhibitory function in Ras signaling that is separate from its catalytic activity on Rac proteins. Molecular modeling further suggested that our mutation may disrupt a recently described in vitro autoinhibitory function of the Dbl domain on CDC25 Ras GEF activity (84). We also found that human SOS1 (hSOS1) can be activated by an equivalent mutation. Together, our data demonstrate a crucial role of the Dbl domain in inhibiting EGFR pathway activity in vivo and suggest that analogous mutations in hSOS1 may contribute to disease.

MATERIALS AND METHODS

Strains. *C. elegans* was cultured at 20°C (13) unless otherwise indicated. The alleles used were *let-23(sy1)* and *let-23(sy16)* (2) and *rol-6(e187)* (21) on LGII; *pha-1(e2123ts)* (34) on LGIII; *ced-10(n1993)* (29), *lip-1(zh15)* (7), *lin-45(sy96)* (41), *unc-24(e138)* (72), *lin-3(n378)* (30), *let-60(n1876)* (5), *let-60(sy95)* (40, 42), *let-60(n1531)* (5), *let-60(sy101)* (40, 42), *let-60(n1046)* (5, 30), *dpy-20(e1282)* (43), *unc-22(s7)* (59), and *rac-2(ok326)* on LGIV; *let-341/sos-1(s1031)* (44) and *unc-46(e177)* (13) on LGV; and *sli-1(sy143)* (45), *gap-1(n1691)* (37), *unc-2(e55)* (13), and *mig-2(mu28)* (98) on LGX.

Isolation, mapping, and molecular identification of the *sy262* mutation. To identify new recessive alleles of the *sli-1* locus, an F1 noncomplementation screen was performed. *let-23(sy1)* males were mutagenized with ethanemethylsulfonate (13) and crossed into marked *let-23(sy1); sli-1(sy143)* hermaphrodites. The *sy262* mutation was discovered as a dominant *let-23(sy1)* suppressor that was unlinked to the *sli-1* locus. Standard genetic approaches assigned linkage to chromosome V. Mapping relative to *let-341* (now known to be *sos-1*) and *unc-46* was carried out by crossing *let-23(sy1); sy262* males into heterozygous *sos-1(s1031) unc-46(e177)* hermaphrodites. From *let-23(sy1)/+; sos-1 unc-46/sy262* heterozygotes, 12 Unc non-Let recombinants were picked. After homozygosing *let-23(sy1)* and the recombinant chromosome, it was determined that 12/12 recombinants picked up *sy262*, indicating *sy262* is to the left of *unc-46* and close to or to the left of *sos-1*. Single-nucleotide polymorphism (SNP) mapping (94) was performed by crossing CB4856 Hawaiian *C. elegans* males into hermaphrodites derived from Bristol, England, carrying *let-23(sy1)* and the linked *sy262* and *unc-46* mutations. After homozygosing the *let-23* mutation, Unc non-*sy262* recombinants were picked. Five out of nine recombinants did not pick up the Hawaiian SNP located at position 9725 of cosmid F41F3, indicating that *sy262* is to the left of cosmid F41F3. However, all of the recombinants picked up the SNP in yeast artificial chromosome (YAC) Y61A9LA, which is next to the *sos-1* gene. Since we did not find recombinants that crossed over between *sy262* and the SNP in Y61A9LA, we speculated that *sy262* must be close to the *sos-1* locus. Based on these mapping data and our genetic data showing that *sy262* suppresses a dominant-negative Ras mutation, but not a Raf reduction-of-function [(rf)] mutation, we speculated that *sy262* was a gain-of-function mutation in *sos-1*. The entire coding regions of the *sos-1* cDNAs derived from either wild-type or *sy262* mutant worms were sequenced. A single G-to-A transition mutation was found in the *sy262 sos-1* cDNA, changing codon 322 from GGA to AGA. The presence of this mutation in *sy262* genomic DNA was confirmed by PCR amplifying and sequencing exon 6 from wild-type and *sy262* mutant worms.

Vulval induction and gonad ablations. Vulval development was scored during the L4 stage under Nomarski optics (86). The number of vulval nuclei was used to extrapolate how many of the vulval progenitor cells (VPCs) were induced to adopt vulval fates. A VPC that gave rise to seven or eight great-granddaughters and no hyp7 tissue was scored as 1.0 cell induction. A VPC in which one daughter fused with hyp7 and the other daughter divided to generate three or four great-granddaughter cells was scored as 0.5 cell induction. In wild-type animals, P5.p, P6.p, and P7.p each undergo 1.0 cell induction, whereas the other Pn.p cells do not adopt vulval fates, resulting in a total of 3.0 cell inductions. Animals displaying more than 3.0 cell inductions are Muv, and animals with less than 3.0 cell inductions are Vul. Gonad cells (Z1, Z2, Z3, and Z4) were ablated with a laser microbeam during the L1 stage (4).

RNAi. *Escherichia coli* HT115 bacteria containing the respective RNA interference (RNAi) clones were obtained from the Ahringer bacterial feeding library (48). The bacteria were grown overnight in LB with 50 μg/ml ampicillin and then spotted onto NG plates containing 1 mM IPTG (isopropyl-β-D-thiogalactopyranoside) and 50 μg/ml ampicillin to make RNAi plates. The next day, Po L4 stage worms were seeded onto the plates. After 2 days, the Po worms were transferred to fresh RNAi plates, and progeny were scored 4 to 7 days later.

Plasmid constructions. A 4,002-bp cDNA encoding isoform 1 of hSOS1 (GenBank accession number L13857) was used in all experiments. A C-terminally FLAG-tagged expression construct was generated by first cloning an N-terminal BamHI/KpnI fragment spanning nucleotides 1 to 3146 into the BglII/KpnI sites of p3XFLAG-CMV-14 (Sigma). A C-terminal fragment spanning nucleotides 3146 to 4000 that replaced the stop codon with an XbaI site was generated by PCR using oligonucleotides hSOS1-1 (5′-AAC TTG AAT CCG ATG GGA AAT AGC-3′) and hSOS1-2 (5′-CTA GCC TAG TCT AGA GGA AGA ATG GGC ATT CTC CAA CAG-3′). This fragment was then ligated to the N-terminal hSOS1 fragment in the FLAG vector via KpnI/XbaI digestion. Site-directed mutagenesis using oligonucleotides hSOS1-3 (5′-C CAT CCA CTA GTA GGA AGC CGC TTT GAA GAC TTA GCA GAG-3′), hSOS1-4 (5′-CTC TGC TAA GTC TTC AAA GCG GCT TCC TAC TAG TGG ATG G-3′), and Accuprime *Pfx* DNA Polymerase (Invitrogen) was performed on an XhoI hSOS1 subfragment spanning nucleotides 112 to 896 that had been cloned into pBluescript (Stratagene). The mutagenesis changed codon 282 from TGC (Cys) to CGC (Arg). The mutagenized fragment was then used to replace the corresponding region in the wild-type FLAG-tagged construct via XhoI digestion. All constructs were verified by sequencing them.

Transient transfections, growth factor stimulations, and Western blotting. NIH 3T3 and HEK 293 EBNA cells were grown in Dulbecco's modified Eagle's medium (DMEM) supplemented with 10% fetal bovine serum, penicillin, streptomycin, and glutamine and maintained in a 5% CO_2 incubator. The NIH 3T3 cells were plated at 5×10^5 cells/60-mm dish 12 to 24 h prior to transfection. For NIH 3T3 cell transfection, 25 μl of Lipofectamine (Invitrogen) was combined with 300 μl DMEM and 8 μg total DNA and incubated for 30 min at room temperature. Complexes were added to the cells in the presence of 2.4 ml DMEM for 5 hours. The transfected cells were washed once with DMEM or phosphate-buffered saline (PBS) and then starved for an additional 15 to 20 h in serum-free DMEM. HEK 293 EBNA cells were plated at 1.2×10^6 cells/60-mm dish 12 to 24 h prior to transfection. For HEK 293 EBNA cell transfection, 30 μl polyethylenimine (1 mg/ml) was combined with 1.5 ml DMEM and 6.5 μg total DNA and incubated for 15 to 30 min at room temperature. Complexes were added to the cells in a total of 4 ml of DMEM and incubated for 16 h at 37°C. The cells were recovered in complete medium for 8 hours before being starved in serum-free DMEM for 18 to 24 h.

Transfected cells were stimulated with 10 ng/ml human EGF (BD Biosciences) and lysed in NP-40 lysis buffer (1% Nonidet P40, 150 mM NaCl, 50 mM Tris-Cl [pH 8.0]) containing 1 μg/ml antipain, 1 μg/ml aprotinin, 10 μg/ml leupeptin, 1 μg/ml pepstatin A, 20 μg/ml phenylmethylsulfonyl fluoride, 20 mM NaF, 2 mM sodium orthovanadate, and 20 mM beta-glycerophosphate. Protein concentrations were determined by the bicinchoninic acid assay (Pierce).

Following sodium dodecyl sulfate-polyacrylamide gel electrophoresis, proteins were transferred to Immobilon-P membranes (Millipore) in transfer buffer (50 mM Tris-base, 40 mM glycine, 0.04% sodium dodecyl sulfate, 10% methanol) using a semidry transfer apparatus (Owl). The blots were blocked in 5% nonfat dry milk-TBST (50 mM Tris-Cl, 150 mM NaCl, 0.05% Tween-20 [pH 8.0]) and probed with anti-phospho-p44/42 MAPK (Cell Signaling, no. 9101; 1:1,000), anti-FLAG (Sigma, no. F1804; 1:2,000), or anti-p44/42 MAPK (Cell Signaling, no. 9102; 1:2,000). The blots were developed using ECL Plus (Amersham), and the intensities of the bands were determined by densitometric scanning, followed by quantification using ImageJ software (NIH).

SWISS-MODEL. The three-dimensional structure of the *C. elegans* SOS-1 Dbl-PH-REM-CDC25 domains was modeled using the crystal structure of the Dbl-PH-REM-CDC25 domains of hSOS1 (crystal structure coordinates 1xd4A.pdb) and the optimize mode of SWISS-MODEL (36, 67, 79), an Internet-based automated comparative protein-modeling server (http://www

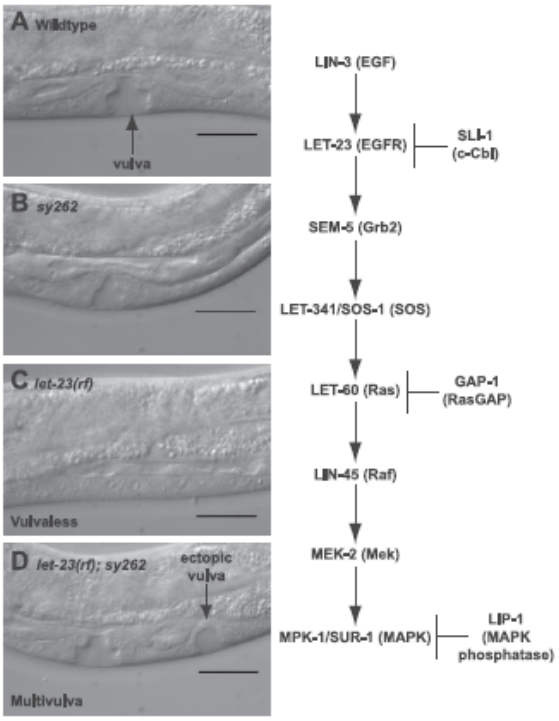

FIG. 1. The *sy262* mutation suppresses the Vul phenotype of a reduction-of-function mutation in *let-23* (EGFR). The animals were photographed during the mid-L4 larval stage using Nomarski optics. (A) Wild type. (B) Homozygous *sy262* mutant. (C) Homozygous *let-23(sy1)* reduction-of-function mutant. (D) Homozygous *let-23(sy1); sy262* double mutant. Scale bars = 20 μm. On the right, the names of the *C. elegans* and human (in parentheses) components of the EGFR pathway are indicated.

.expasy.ch/swissmod/SWISS-MODEL.html). In the optimize mode, the SOS -1 protein sequence was aligned with that of hSOS1 using BLAST (http://www .ncbi.nlm.nih.gov/BLAST/).

RESULTS

The *sy262* mutation acts at the level of Ras and upstream of Raf. The *sy262* mutation was discovered in a *sli-1* (c-Cbl) F1 noncomplementation screen (see Materials and Methods) as a novel mutation that was unlinked to the *sli-1* locus but could still strongly suppress a *let-23* (EGFR) reduction-of-function mutation (Fig. 1 and Table 1). To determine how the *sy262* mutation interacts with the EGFR pathway, we performed a genetic epistasis analysis using standard reduction-of-function mutations in the EGFR-Ras-MAPK pathway (Fig. 1 and Table 1). By itself, the *sy262* mutation does not alter vulval development. However, the *sy262* mutation strongly suppresses a reduction-of-function mutation in *lin-3* (EGF), which likely affects EGF processing, and a mutation in *let-23* (EGFR), which affects EGFR localization (47, 56). The *sy262* mutation also suppresses a weak dominant-negative S89F mutation in *let-60* (Ras) but does not suppress stronger *let-60* (Ras) dominant-negative mutations (G10R and G15D) or a relatively weak reduction-of-function mutation in *lin-45* (Raf) (40–42). These data suggest that the *sy262* locus normally acts upstream of Raf and possibly on Ras.

The *sy262* mutation maps to the Dbl domain of the Ras/Rac GEF SOS-1. We used three-factor mapping to place *sy262* to the left of *unc-46* and close to or to the left of *let-341* (now known to be *sos-1*) (see Materials and Methods) on chromosome V. We then used SNPs to determine that *sy262* was to the left of cosmid F41F3 and close to the YAC Y61A9LA, which includes the *sos-1* locus (Fig. 2A). There are 22 predicted genes between the SNP in F41F3 and *sos-1*. Given our genetic

TABLE 1. The *sy262* mutation acts at the level of Ras and upstream of Raf

Genotype[a]	Vulval induction[b]	% Muv[c]	% Vul[d]	*n*[e]	*P* value[f]
Wild type	3.00	0	0	24	
sy262	3.00	0	0	20	
lin-3(rf)	1.40	0	95	21	
lin-3(rf); sy262	2.93	0	10	20	<0.00001 to *lin-3(rf)*
let-23(rf)	0.23	0	100	20	
let-23(rf); sy262	3.80	68	0	22	<0.00001 to *let-23(rf)*
let-23(rf); sy262/+	2.95	35	20	20	<0.00001 to *let-23(rf)*
let-60(S89Fdn)/+	1.55	0	81	21	
let-60(S89Fdn)/+; sy262	2.80	0	18	22	0.0001 to *let-60(S89Fdn)/+*
let-60(G10Rdn)/+	0.25	0	100	20	
let-60(G10Rdn)/+; sy262	0.40	0	100	20	0.42 to *let-60(G10Rdn)/+*
let-60(G15Ddn)/+	0.08	0	100	20	
let-60(G15Ddn)/+; sy262	0.04	0	100	27	0.64 to *let-60(G15Ddn)/+*
lin-45(rf)	2.10	0	70	20	
lin-45(rf); sy262	2.14	0	67	21	0.88 to *lin-45(rf)*

[a] The complete genotypes are as follows: (i) *sy262* = *sy262 him-5(e1490)*, (ii) *lin-3(rf)* = *lin-3(n378); unc-46(e177)*, (iii) *lin-3(rf); sy262* = *lin-3(n378); sy262 unc-46(e177)*, (iv) *let-23(rf)* = *let-23(sy1)*, (v) *let-23(rf); sy262* = *let-23(sy1); sy262 him-5(e1490)*, (vi) *let-23(rf); sy262/+* = *let-23(sy1); sy262 unc-46(e177)/+*, (vii) *let-60(S89Fdn)/+* = *unc-24(e138) let-60(sy95)/dpy-20(e1282)*, (viii) *let-60(S89Fdn)/+; sy262* = *unc-24(e138) let-60(sy95)/dpy-20(e1282); sy262 unc-46(e177)*, (ix) *let-60(G10Rdn)/+* = *let-60(sy101) dpy-20(e1282)/ unc-24(e138) unc-22(s7); unc-46(e177)*, (x) *let-60(G10Rdn)/+; sy262* = *let-60(sy101) dpy-20(e1282)/unc-24(e138) unc-22(s7); sy262 unc-46(e177)*, (xi) *let-60(G15Ddn)/+* = *let-60(n1531) unc-22(s7)/dpy-20(e1282); unc-46(e177)*, (xii) *let-60(G15Ddn)/+; sy262* = *let-60(n1531) unc-22(s7)/dpy-20(e1282); sy262 unc-46(e177)*, (xiii) *lin-45(rf)* = *unc-24(e138) lin-45(sy96)*, and (xiv) *lin-45(rf); sy262* = *unc-24(e138) lin-45(sy96); sy262 unc-46(e177)*.

[b] Average number of vulval progenitor cells adopting vulval fates. Wild type is three. The maximum is six.

[c] The percentage of animals that have more than three vulval progenitor cells adopting vulval fates.

[d] The percentage of animals that have fewer than three vulval progenitor cells adopting vulval fates.

[e] *n*, number of animals examined.

[f] Statistical significance of the vulval induction value as determined by a two-tailed Student's *t* test.

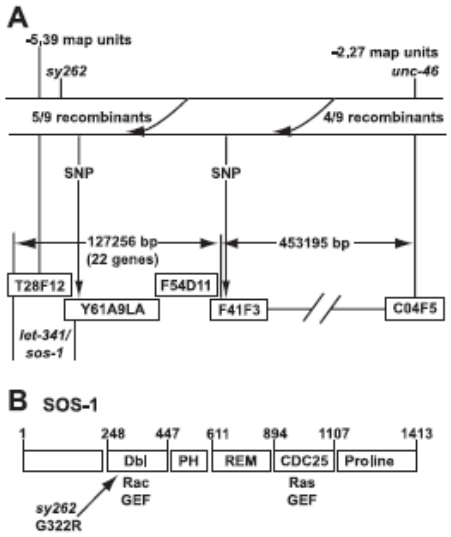

FIG. 2. The *sy262* mutation maps to the Dbl domain of SOS-1. (A) SNP mapping of *sy262*. Five out of nine Unc non-*sy262* recombinants did not pick up the SNP located at position 9725 of cosmid F41F3, indicating that *sy262* is to the left of cosmid F41F3. All the recombinants picked up the SNP at 14897 in the YAC Y61A9LA, which is next to the *sos-1* gene. Thus, the *sy262* mutation is close to the *sos-1* locus. (B) Architecture of the *C. elegans* SOS-1 protein (GenBank accession number AF251308) and location of the *sy262* mutation. The numbers refer to amino acid positions. Domain boundaries were determined by SMART (http://smart.embl-heidelberg.de/), except for the REM domain, whose position was determined by a BLAST (http://www.ncbi.nlm.nih.gov/BLAST/) alignment with hSOS1.

epistasis results showing that *sy262* acts at the level of Ras and upstream of Raf, we hypothesized that the *sy262* mutation was a gain-of-function mutation in *sos-1*. After sequencing the entire coding region of the *sos-1* cDNA derived from *sy262* mutant animals, we found a single G-to-A mutation in codon 322 that results in a substitution of Arg for Gly in the Dbl domain (Fig. 2B). The presence of the mutation was also confirmed in *sy262* genomic DNA.

The *sy262* (G322R) mutation predominantly affects Ras signaling. SOS-1 and its *Drosophila* and mammalian orthologs are multidomain proteins best characterized for their critical biological roles as Ras GEFs (Fig. 2B) (9, 15, 16, 28, 69, 92). However, in addition to containing a CDC25 Ras GEF domain, SOS-1 also possesses a Dbl domain, which allows the mammalian protein to function as a Rac GEF (65). The location of the *sy262* mutation in the Dbl domain suggests at least two models for the way in which the change may create a gain-of-function protein. In one model, the *sy262* mutation may relieve one of several previously described forms of inhibition on SOS Rac GEF activity (23, 65, 80–83). For example, the *sy262* mutation might disrupt autoinhibition by the PH domain on the Rac GEF activity of the Dbl domain (23, 65, 83). In this model, elevated Rac signaling might bypass some of the requirement for Ras signaling during vulval development. In the second model, the *sy262* mutation might relieve inhibition of Ras GEF activity. The second model is particularly appealing, since recent X-ray crystallographic studies of hSOS1 have uncovered an autoinhibitory function of the Dbl domain on CDC25 Ras GEF activity (84).

To distinguish between these models, we examined the sensitivity of *sy262* mutant SOS-1 to further mutations in either Ras or Rac (Table 2). For these experiments, we used a background in which the *sy262* mutation suppressed a reduction-of-function mutation in *let-23* (EGFR). When we additionally lowered Ras levels through a heterozygous strong reduction-of-function mutation in *let-60* (Ras), *sy262* activity was strongly reduced to only 29% of that seen in the presence of two copies of wild-type Ras. Thus, the activity of SOS-1 G322R is critically dependent on the amount of Ras. This observation is also consistent with the failure of *sy262* to suppress strong domi-

TABLE 2. The *sy262* mutation predominantly acts through Ras rather than Rac

Genotype[a]	Vulval induction[b]	% Muv[c]	% Vul[d]	*n*[e]	*P* value[f]
Wild type	3.00	0	0	24	
sy262	3.00	0	0	20	
let-23(rf)	0.23	0	100	20	
let-23(rf); sy262	3.80	68	0	22	
let-60(rf)/+	3.00	0	0	20	
let-23(rf); let-60(rf)/+; sy262	1.25	0	80	22	<0.00001 to *let-23(rf); sy262*
rac-2(null)	3.00	0	0	20	
let-23(rf); rac-2(null); sy262	3.65	60	0	20	0.50 to *let-23(rf); sy262*
ced-10(rf)	3.00	0	0	20	
let-23(rf); ced-10(rf); sy262	3.90	70	5	20	0.68 to *let-23(rf); sy262*
mig-2(null)	3.00	0	0	20	
let-23(rf); sy262; mig-2(null)	2.85	25	25	20	0.002 to *let-23(rf); sy262*
let-23(rf); rac-2(RNAi); sy262; mig-2(null)	2.83	30	30	18	0.97 to *let-23(rf); sy262; mig-2(null)*
let-23(rf); ced-10(RNAi); sy262; mig-2(null)	2.55	21	47	19	0.45 to *let-23(rf); sy262; mig-2(null)*
let-23(rf); ced10(RNAi); rac-2(RNAi); sy262; mig-2(null)	2.68	30	40	20	0.64 to *let-23(rf); sy262; mig-2(null)*

[a] *let-23(rf)* = *let-23(sy1)*, *let-60(rf)/+* = *let-60(n1876) unc-22(s7)/dpy-20(e1282)*, *rac-2(null)* = *rac-2(ok326)*, *ced-10(rf)* = *ced-10(n1993)*, and *mig-2(null)* = *mig-2(mu28)*. In the *mig-2(null)* strains, *sy262* was linked to *unc-46(e177)*. In all other strains, *sy262* was linked to *him-5(e1490)*. By themselves, the *unc-46* and *him-5* mutations do not affect vulval development in *let-23(rf)* animals.

[b] Average number of vulval progenitor cells adopting vulval fates. Wild type is three. The maximum is six.

[c] The percentage of animals that have more than three vulval progenitor cells adopting vulval fates.

[d] The percentage of animals that have fewer than three vulval progenitor cells adopting vulval fates.

[e] *n*, number of animals examined.

[f] Statistical significance of the vulval induction value as determined by a two-tailed Student's *t* test.

TABLE 3. The *sy262* mutation is strongly dependent on upstream signaling by EGF

Genotype[a]	Gonad[b]	Vulval Induction[c]	% Mut[d]	% Vul[e]	*n*[f]	*P* value[g]
Wild type	+	3.00	0	0	24	
Wild type	−	0.00	0	100	14	
let-23(rf); sy262	+	3.80	68	0	22	
let-23(rf); sy262	−	0.00	0	100	19	
let-23(rf); let-60(gf)/+	+	4.58	100	0	20	
let-23(rf); let-60(gf)	+	5.38	100	0	20	
let-23(rf); let-60(gf)	−	1.17	12	88	16	0.01 to wild type gonad ablated

[a] *let-23(rf)* = *let-23(sy1)*, *let-60(gf)* = *let-60(n104gf)*, and *sy262* was linked to *him-5(e1490)*.
[b] The gonadal primordium, which gives rise to the EGF-producing anchor cell, is either present (+) or removed by laser ablation (−).
[c] Average number of vulval progenitor cells adopting vulval fates. Wild type is three. The maximum is six.
[d] The percentage of animals that have more than three vulval progenitor cells adopting vulval fates.
[e] The percentage of animals that have fewer than three vulval progenitor cells adopting vulval fates.
[f] *n*, number of animals examined.
[g] Statistical significance of the vulval induction value as determined by a two-tailed Student's *t* test.

nant-negative mutations in Ras (Table 1). *C. elegans* has three Rac genes: *rac-2* (57), *ced-10* (71), and *mig-2* (98). Although nonnull mutations in *let-60* (Ras) by themselves can reduce vulval induction (5, 40) (Table 1), single null mutations in either *rac-2* or *mig-2* or a single strong reduction-of-function mutation in *ced-10* has no effect on vulval development (Table 2). Thus, unlike the requirement for Ras, vulval development is not normally dependent on any single Rac gene. Furthermore, in the sensitized background of *sy262* suppression of the *let-23* (EGFR) reduction-of-function mutation, *rac-2* and *ced-10* mutations still have no effect on vulval development. However, a null mutation in *mig-2* partially reduced *sy262*-suppressing activity to 73% of that seen in the presence of MIG-2. The effect of the *mig-2* mutation was not enhanced by additional reduction of *rac-2* and *ced-10* through RNAi. Given that a partial reduction of Ras levels, which by itself is not even sufficient to weaken Ras activity in its known biological pathways (viability, vulval development, and fertility), has a more profound effect on *sy262* activity than null mutations and reductions in function of the three Rac genes (1.25 cells induced versus 2.68 cells induced, respectively), it is likely that SOS-1 G322R exerts most of its effect through the Ras pathway (see Discussion).

The Dbl domain mutation increases the sensitivity of the Ras pathway to upstream signaling. Although a precise mechanism has not yet been defined, it has been suggested that SOS catalytic activity toward the Ras-MAPK pathway might be positively regulated by growth factor signaling (14, 70). To determine if the G322R change increases SOS-1 basal activity and converts it into a constitutively active GEF, we examined whether the gain-of-function phenotype was still manifested in the complete absence of upstream signaling from EGF and the EGFR. We first tested whether the *sy262* mutation could still suppress the Vul phenotype of a *let-23* (EGFR) reduction-of-function mutation in the absence of the EGF-producing anchor cell. In wild type animals, laser ablation of the gonadal primordium, which gives rise to the anchor cell prior to the onset of vulval induction, results in 100% of the animals having absolutely no vulval induction (Table 3). Although a control G13E gain-of-function change in *let-60* (Ras) was still able to promote some vulval induction in this background, the SOS-1 G322R could not promote vulval development in the complete absence of EGF (Table 3). Thus, in this assay, SOS-1 G322R does not appear to be constitutively active.

In another assay, we examined the ability of the *sy262* mutation to suppress the lethality conferred by a homozygous *let-23* (EGFR) null mutation. Due to the 100% penetrant lethality of this mutation, we initially constructed a strain in which the *sy262* mutation was homozygous but the *let-23* (EGFR) null mutation was maintained in a heterozygous state. The *let-23* (EGFR) null mutation was linked to a recessive mutation in the *rol-6* gene. Thus, in the absence of suppression, 25% of the progeny die as L1 larvae, and adult rolling animals are never seen. If there is 100% suppression of *let-23(null)* lethality, 25% of the progeny will appear as adult rolling animals, since this is the expected Mendelian frequency of homozygosing the mutant *let-23* (EGFR) chromosome from heterozygous animals. In the presence of a homozygous *let-60* (Ras) G13E gain-of-function mutation, 26% of the progeny were adult rollers (Table 4). This frequency indicates that the Ras mutation can suppress 100% of the lethality associated with complete loss of the EGFR. These rollers were 100% sterile, since an EGF-dependent IP3 pathway, rather than Ras, is required for hermaphrodite fertility (19). The Ras mutation was also able to drive excessive vulval induction. Almost 100% of the animals had all six progenitor cells adopting vulval fates, rather than the normal three. In contrast to the gain-of-function Ras mutation, the *sy262* mutation resulted in only 1.5% of total progeny from heterozygous mothers appearing as adult rollers (Table 4). This translates into a rescue frequency of only 6%, compared to a rescue frequency of 100% for the G13E Ras mutation. The rescued *sy262* mutant animals were not rare recombinants, since all were sterile, and on average, only one progenitor cell was induced to adopt a vulval fate. Failure of the *sy262* mutation to rescue the sterility defect of *let-23* (EGFR) null animals also provides further evidence that the Ras effector arm of the EGFR pathway is specifically affected by the *sy262* mutation. Rescue of the EGFR (null)-induced lethality and defective vulval induction was weak but statistically significant. Together, these data indicate that the G322R change only weakly increases the basal activity of SOS-1. However, since SOS-1 G322R has strong rescuing activity in the presence of nonnull mutations in the EGFR pathway (which allows low levels of signaling) (Table 1), we infer

TABLE 4. The *sy262* mutation displays very weak activity in the absence of functional EGFRs

Genotype[a]	% Suppression of *let-23(null)*-induced lethality[b]	*P* value[c]	% Suppression of *let-23(null)*-induced sterility[d]	Vulval induction[f]	% Muv[h]	% Vul[i]	*n*[j]	*P* value[k]
let-23(null)	0 (1,091)		NA[e]	NA[g]	NA[g]	NA[g]	NA[g]	
let-23(null); *sy262*	6 (1,372)	<0.001	0 (16)	0.98	0	91	11	0.013
let-23(null); *let-60(gf)*	100 (324)	<0.0001	0 (44)	5.73	100	0	11	<0.00001

[a] The complete genotype of *let-23(null)* was *rol-6(e187) let-23(sy16); let-60(gf)* = *let-60(n1046gf); sy262* was linked to *him-5(e1490)*.
[b] Suppression of lethality was calculated from strains that were homozygous for the *sy262* or *let-60* mutation but heterozygous for the *rol-6(e187) let-23(sy16)* chromosome. In the absence of suppression, rolling adults never appear. In the presence of complete suppression, 25% of total descendants from the *rol-6(e187) let-23(sy16)* heterozygous parents would be rolling; 100% suppression is normalized to the generation of 25% rollers relative to total progeny. The number in parentheses refers to the total number of progeny examined from *rol-6(e187) let-23(sy16)* heterozygous parents.
[c] The statistical significance of the observed frequency of viable animals was determined by comparison with *let-23(null)* animals alone and using a chi square test.
[d] Animals suppressed for *let-23(null)*-induced lethality were picked as L4 larvae and examined for progeny 4 days later. The number in parentheses refers to the total number of animals examined.
[e] NA, not applicable. Due to the 100% penetrant lethality conferred by the homozygous *let-23(null)* mutation, these animals could not be examined for sterility; 100% sterility, however, is inferred from reduction-of-function mutations in *lin-3* and LET-23 structure-function studies.
[f] Average number of vulval progenitor cells adopting vulval fates. Wild type is three. The maximum is six.
[g] NA, not applicable. Due to the 100% penetrant lethality conferred by the homozygous *let-23(null)* mutation, these animals could not be examined for vulval induction. However, based on certain combinations of *let-23* alleles, it could be inferred that the vulval induction of these animals would be 0.00 and that 0% of the animals would be Muv.
[h] Percentage of animals with more than three vulval progenitor cells adopting vulval fates.
[i] Percentage of animals with fewer than three vulval progenitor cells adopting vulval fates.
[j] *n*, number of animals examined for vulval induction.
[k] The statistical significance of the vulval induction value was determined by comparison with gonad-ablated wild-type animals and use of a two-tailed Student's *t* test.

that G322R acts by increasing the responsiveness of SOS-1 to upstream signaling.

The SOS-1 Dbl domain is a critical developmental inhibitor of Ras signaling. Our data suggest that during *C. elegans* vulval development, a major function of the Dbl domain is to prevent excessive Ras activation by the CDC25 Ras GEF domain. To determine the importance of this negative regulatory mechanism relative to that of established *trans*-acting inhibitors of the EGFR-Ras-MAPK pathway, we compared *sy262* suppression of a reduction-of-function mutation in *let-23* (EGFR) to that conferred by loss-of-function mutations in *sli-1* (c-Cbl) (96), *gap-1* (RasGAP) (37), and *lip-1* (MAPK phosphatase) (7). We found that the *sy262* mutation was a better suppressor of the *let-23* (EGFR) mutation than a likely null mutation in *lip-1* (MAPK phosphatase) and equivalent in strength to null mutations in either *sli-1* (c-Cbl) or *gap-1* (RasGAP) (Table 5). To further determine the importance of the Dbl domain for inhibition of the EGFR-Ras-MAPK signaling pathway, we constructed a double mutant harboring the *sy262* mutation and a null mutation in *gap-1* (RasGAP). Together, these mutations should increase GTP loading on Ras while reducing its GTPase activity. Individually, these single mutations do not disrupt vulval development. However, 25% of double-mutant animals displayed excessive vulval differentiation (Table 5). Thus, the SOS-1 Dbl domain helps provide a critical balance between the opposing GEF and GAP activities that regulate Ras.

A mutation equivalent to *sy262* G322R activates hSOS1. To further study the molecular mechanism of action of the *sy262* G322R mutation and to determine whether hSOS1 might be regulated in a similar manner, we sought to introduce the equivalent activating mutation into the hSOS1 cDNA. We used the solved X-ray crystal structure of the Dbl-PH-REM-CDC25 domains of hSOS1 and SWISS-MODEL modeling software (36, 67, 79) to generate a structural model of *C. elegans* SOS-1 (Fig. 3). In this model, G322 lies in the H3 helix of the Dbl domain. The equivalent residue in hSOS1 appears

TABLE 5. Magnitude of inhibition of the SOS-1 Dbl domain, c-Cbl, RasGAP, and MAPK phosphatase on the EGFR pathway

Genotype[a]	Vulval induction[b]	% Muv[c]	% Vul[d]	*n*[e]	*P* value[f]
let-23(rf)	0.23	0	100	20	
sli-1(null)	3.00	0	0	24	
let-23(rf); *sli-1(null)*	3.57	60	17	30	<0.00001 to *let-23(rf)*
gap-1(null)	3.00	0	0	36	
let-23(rf); *gap-1(null)*	3.74	71	0	21	<0.00001 to *let-23(rf)*
lip-1(null)	3.00	0	0	20	
let-23(rf); *lip-1(null)*	2.10	0	52	21	<0.00001 to *let-23(rf)*
sy262	3.00	0	0	24	
let-23(rf); *sy262*	3.80	68	0	22	0.34 to *let-23(rf)*; *sli-1(null)*, 0.80 to *let-23(rf)*; *gap-1(null)*, and <0.00001 to *let-23(rf)*; *lip-1(null)*
sy262; *gap-1(null)*	3.26	26	0	35	0.004 to *gap-1(null)* and *sy262*

[a] *let-23(rf)* = *let-23(sy1)*, and *sli-1(null)* = *sli-1(sy143)*. The complete genotype of *gap-1(null)* is *gap-1(n1691) unc-2(e55). lip-1(null)* = *lip-1(zh15); sy262* was linked to *him-5(e1490)*.
[b] Average number of vulval progenitor cells adopting vulval fates. Wild type is three. The maximum is six.
[c] Percentage of animals with more than three vulval progenitor cells adopting vulval fates.
[d] Percentage of animals with fewer than three vulval progenitor cells adopting vulval fates.
[e] *n*, number of animals examined.
[f] The statistical significance for the vulval induction value was determine using a two-tailed Student's *t* test.

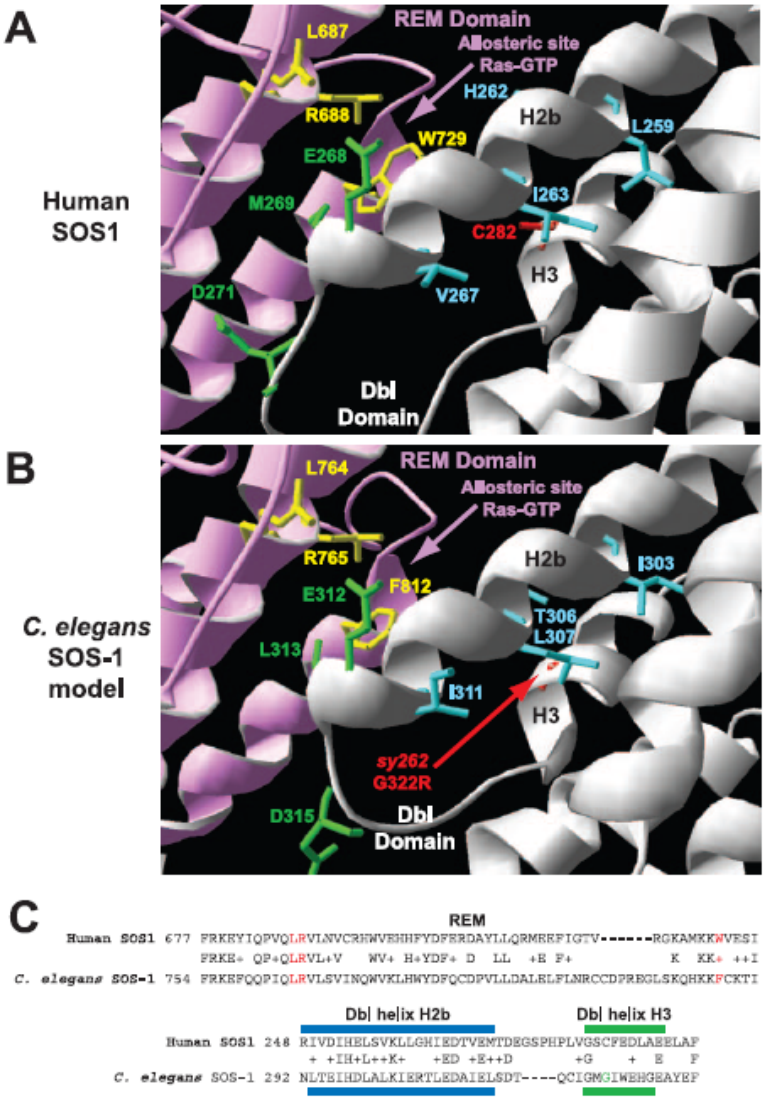

FIG. 3. Conservation of the Dbl and REM domains between human and *C. elegans* SOS proteins. (A) Crystal structure of the Dbl-PH-REM-CDC25 domains from hSOS1 at 3.62 Å (84). The yellow residues (L687, R688, and W729) indicate amino acids in the REM domain that interact with Ras-GTP and are important for Ras-GTP-dependent allosteric stimulation of CDC25 activity. The green residues in the Dbl helix H2b (E268 and M269) and loop (D271) contribute to autoinhibition of the REM domain. Substitution mutations converting all three green amino acids to alanines result in a protein that is hypersensitive to allosteric activation (84). The blue residues (L259, H262, I263, and V267) in helix H2b point toward the surface of helix H3. C282 in helix H3 is in the position analogous to that of the *sy262* G322R mutation in the *C. elegans* Dbl domain. SWISS-MODEL modeling suggested that a C282R change might not be compatible with the normal geometry of the blue residues in helix H2b. (B) SWISS-MODEL of the *C. elegans* Dbl-PH-REM-CDC25 domains from SOS-1. Note the conservation of the yellow residues (L764, R765, and F812) in the REM domain for allosteric stimulation of CDC25 activity by Ras-GTP, conservation of the green residues (E312, L313, and D315) in the Dbl domain for potential autoinhibition of the REM domain, and conservation of the blue bulky/hydrophobic residues (I303, T306, L307, and I311) that face the surface of Dbl helix H3. SWISS-MODEL modeling suggests that the G322R change in helix H3 may not be compatible with the predicted geometry of the blue residues in helix H2b. (C) BLAST alignments of relevant portions of the REM and Dbl domains between human and *C. elegans* SOS proteins. The red amino acids in the REM domain are important for binding Ras-GTP. The blue bar indicates the position of Dbl helix H2b (predicted in *C. elegans*), and the green bar indicates the position of Dbl helix H3 (predicted in *C. elegans*). The green amino acid is the locations of the *sy262* mutation. Plusses indicate conservative amino acid changes between the human and *C. elegans* proteins.

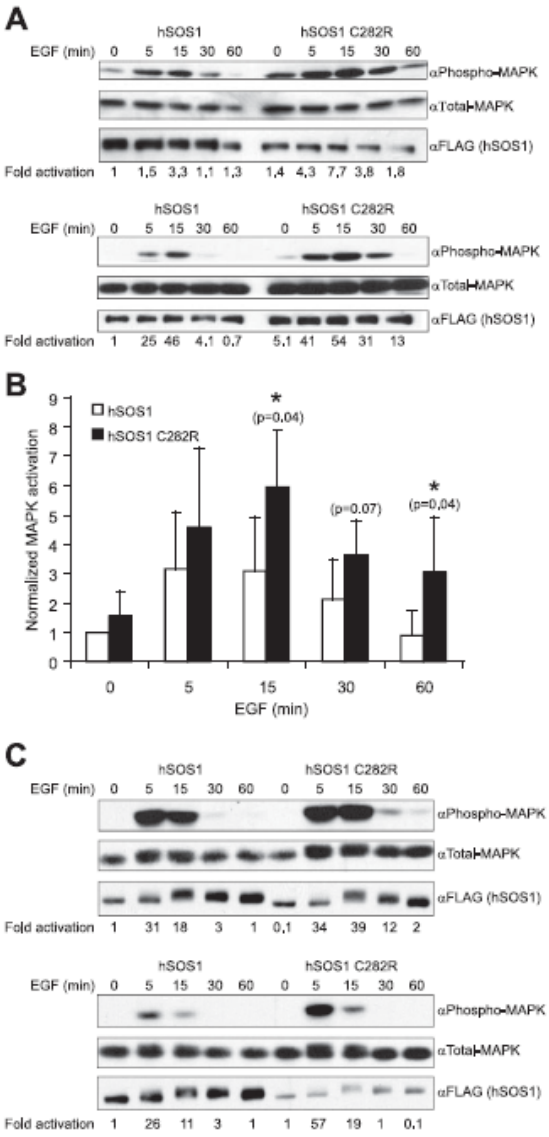

FIG. 4. A C282R mutation in hSOS1 is functionally equivalent to the *sos-1(sy262)* G322R mutation in *C. elegans* SOS-1. (A) hSOS1 C282R promotes EGF-dependent MAPK activation in NIH 3T3 cells. The cells were transfected with 2 to 4 μg of FLAG-tagged hSOS1 expression vector and 4 μg of HA-ERK1 (MAPK) expression vector. After serum starvation and stimulation with EGF for the indicated times, whole-cell lysates were prepared and analyzed by Western blotting with the indicated antibodies. Phosphorylated and total transfected MAPKs were distinguished from endogenous MAPK by a mobility shift caused by the HA tag on the MAPK in the transfection construct. Representative blots from two independent experiments are shown. Activation (*n*-fold) was calculated by dividing the α-phospho-MAPK signal by the α-total-MAPK signal and then adjusting the values to that observed with wild-type hSOS1 at the zero time point. (B) Mean results from four independent experiments in NIH 3T3 cells, where the wild-type and mutant hSOS1 constructs were similarly expressed and the control wild-type hSOS1 construct caused similar levels of MAPK activation between experiments. Normalized activation (*n*-fold) is as described for panel A, except that α-phospho-MAPK/α-total MAPK ratios were also adjusted for slight differences in transfected hSOS1 expression. Statistical significance was assessed using a one-tailed Student's *t* test. (C) hSOS1 C282R promotes EGF-dependent MAPK activation in HEK 293 EBNA cells. The cells were transfected with 2 to 4 μg of FLAG-tagged hSOS1 expression vector and 2.5 μg of HA-ERK1 (MAPK) expression vector. After serum starvation and stimulation with EGF for the indicated times, whole-cell lysates were prepared and analyzed by Western blotting as described for panel A. Representative blots from two independent experiments are shown.

to be C282, which is not disulfide bonded in the crystal structure. In both the human and *C. elegans* proteins, these residues appear to be essential to accommodate the bulky side chains from residues in the nearby H2b helix. It is thus conceivable that the G322R change in *C. elegans* SOS-1 is incompatible with the normal positioning of the H2b helix and that a similar effect might be obtained by a C282R change in hSOS1.

Since *C. elegans* SOS-1 G322R predominantly acts by enhancing the signal-dependent output of an EGFR-Ras-MAPK pathway, we examined the ability of transfected hSOS1 C282R to enhance EGF-dependent MAPK activation in serum-starved mammalian cell lines (Fig. 4). In NIH 3T3 cells, compared to transfection of wild-type hSOS1, hSOS1 C282R was able to enhance the amplitude and duration of MAPK activation (Fig. 4A). Although from experiment to experiment there was variability in the extent to which MAPK was activated, we were able to establish statistical significance ($P < 0.05$) for differences in MAPK activation at 15 and 60 min following EGF stimulation (Fig. 4B). On average, the differences between the activities of the wild-type and mutant proteins were two- to threefold. To further validate this result, we also performed the same experiment in HEK 293 EBNA cells. Once again, we found that compared to wild-type hSOS1, hSOS1 C282R was more potent at promoting EGF-dependent MAPK activation (Fig. 4C). Compared to NIH 3T3 cells, in HEK 293 EBNA cells, the time points at which differences in activity were manifested were more variable. Thus, it was harder to establish statistical significance. Nevertheless, in every experiment we found that at some time point, hSOS1 C282R displayed two- to fourfold more activity than wild-type hSOS1. In conjunction with our genetic data, these data suggest that the G322R change in *C. elegans* SOS-1, as well as the equivalent C282R change in hSOS1, does indeed enhance EGF-dependent MAPK activation. Thus, it is likely that the Dbl domain normally acts to dampen the amount of EGF-dependent MAPK activation and that the structural mechanism by which this is accomplished is conserved across species.

DISCUSSION

Although SOS is an evolutionarily conserved critical regulator of RTK-Ras-MAPK signaling, the key mechanisms that regulate its biologic activity in vivo are not well-defined. It was initially thought that RTK-dependent translocation of SOS to its substrate Ras at the plasma membrane was the key mechanism that controlled Ras-MAPK activation (3). However, sev-

eral lines of evidence have suggested that control of SOS activity in the Ras-MAPK pathway might be more complex. First, in *Drosophila melanogaster*, in the absence of the SEVENLESS RTK or Grb2, SOS still localizes to the plasma membrane, yet Ras signaling is impaired (9, 49). Second, SOS structure-function studies have identified autoinhibitory effects of the N and C termini (20, 51, 93) and have suggested that growth factor signaling might be required to relieve these or other inhibitory mechanisms (14, 70). Third, although their developmental significance is not yet clear, a number of modifications/protein-protein interactions have been described that can alter the activities of either the Rac or Ras GEF domains of SOS. For example, Rac GEF activity of the Dbl domain is autoinhibited through interactions with the PH domain and is relieved by PI3 kinase signaling (23, 65, 83). Rac GEF activity also can be stimulated by protein interactions with Eps8 and Abi-1 (80, 81), as well as tyrosine phosphorylation by Abl (82). Finally, Ras GEF activity is allosterically stimulated through a positive feedback mechanism involving the binding of Ras-GTP to the REM domain (58). A two-pronged mechanism for controlling SOS activity, involving both translocation and signaling-dependent modifications/protein-protein interactions, would be consistent with emerging data regarding regulation of other GEFs. In a basal state, the Rho family GEF Vav is autoinhibited by the insertion of Tyr 174 from the N-terminal acidic region into the Dbl domain active site (1). This autoinhibition can be further compounded by PIP2-dependent interactions between the PH and Dbl domains (39). Signaling leading to phosphorylation of Tyr 174 and the generation of PIP3 disrupts both inhibitory mechanisms and increases Vav catalytic activity (1, 22, 25, 38, 39). Similarly, the catalytic activity of the Ral GEF Ral-GDS is inhibited via its N-terminal REM domain (77). In this case, signaling resulting in PI3 kinase activation promotes the association of another protein, PDK1, with the REM domain and relieves this inhibition (91).

We have discovered a novel gain-of-function mutation in the *sos-1* gene that increases EGFR-Ras-MAPK pathway output during *C. elegans* vulval development. The localization of this mutation to the Dbl domain (G322R) implies that this domain normally confers some type of inhibition on EGFR signaling. SOS-1 G322R restores signaling to animals defective in EGF processing and EGFR localization and overcomes inhibition by one class of dominant-negative Ras protein (Table 1). Given that SOS possesses both Rac and Ras GEF activities and that the *sy262* mutation lies within the Rac GEF Dbl domain, it is possible that the mutation acts through one or both of the GTPases. We favor a model in which the predominant effect of the G322R change is on Ras activation. First, SOS-1 G322R does not appear to act through any of the canonical mechanisms implicated in Rac-dependent MAPK activation. Current models involve activation of Pak by Rac and subsequent phosphorylation of either Raf or Mek. Pak can directly phosphorylate Raf on S338 (52), which is an activating modification, or it can phosphorylate Mek and enhance its binding to Raf and MAPK (27, 33, 97). *C. elegans* Raf has an aspartate residue at the analogous position of S338. Thus, the importance of an acidic charge is conserved, but not the use of protein phosphorylation at this position. Furthermore, our genetic epistasis results indicated that SOS-1 G322R acts upstream of Mek and Raf and possibly Ras activation (Table 1). Second, further genetic analysis indicated that SOS-1 G322R is more sensitive to reductions in Ras than in Rac levels (Table 2). Homozygous null and severe reduction-of-function mutations in two of the three *C. elegans* Rac genes (*rac-2* and *ced-10*) had no effect on SOS-1 G322R activity, while a null mutation in the third Rac gene, *mig-2*, had only a partial effect. In fact, even a homozygous null mutation in *mig-2* coupled with RNAi-induced reductions in the other Rac genes still allowed SOS-1 G322R to have 69% of its normal activity. In contrast, animals heterozygous for a strong reduction-of-function mutation in Ras retained only 29% of SOS-1 G322R activity. This result is even more striking considering that, by itself, the heterozygous state of the Ras(rf) mutation does not impair any known Ras-dependent pathway, while the homozygous state of the *mig-2(null)* mutation disrupts Q-cell descendant migration in 85% of animals (98). Finally, by itself, a null mutation in *mig-2* (Rac) has no effect on vulval development (Table 2), while reduction-of-function mutations in Ras severely impair vulval development; furthermore, an activated Ras mutant almost fully restores wild-type vulval development to *sos-1(null)* animals (5, 15, 40). These data suggest that Ras is the key GTPase normally downstream of SOS-1 during vulval development. However, it remains possible that MIG-2 (Rac) partially contributes to the effect of SOS-1 G322R through a novel mechanism or that it functions through an independent pathway parallel to SOS-1 G322R. For example, the Rho family GEF UNC-73 (Trio) acts on MIG-2 (Rac) to regulate vulval cell divisions and cell migrations (53, 85). Furthermore, MIG-2 (Rac) is expressed in cell types other than the VPCs, including neurons (98), which can indirectly regulate vulval development (60).

The Dbl domain could control Ras-MAPK signaling through several mechanisms. Regulatory proteins could constitutively bind to the Dbl domain and sterically interfere with CDC25 Ras GEF activity. Alternatively, the Dbl domain could interfere with CDC25 activity through an autoinhibitory mechanism. *trans*-acting inhibitors of CDC25 function that bind directly to SOS have not yet been identified. On the other hand, an autoinhibitory function of the Dbl domain on CDC25 activity has been described (84). X-ray crystallographic and biochemical studies indicate that activated Ras (Ras-GTP) can bind to the SOS REM domain and allosterically stimulate the Ras GEF activity of the CDC25 domain (31, 58). However, the SOS crystal structure indicates that accessibility of Ras-GTP to the allosteric site is restricted by the H2b helix of the Dbl domain (84) (Fig. 3A). Specific substitution mutations in the H2b helix at the interface with the REM domain can relieve some of this inhibition (84). A triple mutant of E268A/M269A/D271A has little effect on basal CDC25 activity but increases the sensitivity to Ras-GTP activation by 20-fold. We used a BLAST alignment between the human and *C. elegans* SOS proteins, along with SWISS-MODEL, to generate a three-dimensional model of *C. elegans* SOS-1 (Fig. 3B and C). In this model, it appears that the key structural determinants for autoinhibition by the Dbl domain and allosteric stimulation by Ras-GTP are conserved between the two proteins. Our *sy262* G322R mutation maps to the H3 helix of the Dbl domain, which lies near the H2b inhibitory helix. In the crystal structure of hSOS1 and our *C. elegans* SOS-1 model, multiple hydrophobic/bulky side chains in H2b face the surface of H3 (Fig. 3).

These side chains are effectively accommodated by G322 and C282 in the worm and human proteins, respectively. The G322R change may prevent H2b from acquiring the correct geometry necessary for blocking the allosteric Ras-GTP site in the REM domain. In fact, consistent with this model, we find that a C282R change in hSOS1 also generates an activated mutant with properties similar to those of the *C. elegans* SOS-1 G322R. hSOS1 C282R does not display an obvious increase in basal activity but can enhance EGF-dependent MAPK activation (Fig. 4). Thus, if our model is correct, the *sy262* mutation would provide strong support for the in vivo existence of the allosteric stimulatory/autoinhibitory functions of the REM and Dbl domains and would demonstrate their critical roles in regulating EGFR-Ras-MAPK signaling during development.

A central question, however, remains regarding the role of EGFR signaling in regulating SOS activity and Ras activation. Although the *sy262* G322R mutation weakly increases basal activity (Table 4), mutant SOS-1 is still largely dependent on EGFR signaling for pathway activity (Table 3). This dependence could reflect the requirement for phosphorylated receptors to translocate Grb2-SOS-1 complexes to Ras at the plasma membrane. However, it is also tempting to speculate that SOS-1 itself is modified by activated receptors and that this modification is necessary for its full activity. SOS is phosphorylated immediately following EGFR activation (76), and it has recently been reported that allosteric stimulation of SOS by Ras-GTP requires growth factor signaling, unless SOS is truncated at the N and C termini (12). One interpretation of these results is that receptor signaling is necessary to relieve autoinhibition by the Dbl domain and to allow positive feedback by Ras-GTP. Such feedback may ultimately be necessary to sustain sufficient levels of MAPK activity to drive specific cell fate changes, as seen during vulval development. Thus, the G322R change may bypass the requirement for receptor signaling to allow positive feedback by Ras-GTP but not bypass the requirement for activated receptors to translocate SOS to Ras at the plasma membrane. Alternatively, the G322R change may only partially increase the accessibility of the allosteric site to Ras-GTP. Thus, a subthreshold amount of EGFR signaling might still be required to cooperate with the G322R change to fully allow positive feedback regulation by Ras-GTP.

One unexpected result is that the *sos-1(sy262)* mutation can suppress one class of dominant-negative Ras mutation, but not another (Table 1). SOS-1 G322R can overcome inhibition conferred by a heterozygous Ras S89F mutation, but not a heterozygous Ras G10R or G15D mutation. SOS-1 G322R also can weakly improve signaling in Ras S89F homozygotes. Ras S89F homozygotes are normally inviable. However, we could recover hermaphrodites homozygous for both the Ras S89F and SOS-1 G322R mutations, and starting with 25 hermaphrodites, we could maintain this population for an additional 2 generations before they died. Thus, consistent with an overexpression analysis of the different classes of dominant-negative Ras mutants (42), we found that the S89F mutant retained some biologic activity and could be regulated by SOS-1.

All nine of the dominant-negative Ras mutations isolated in *C. elegans* affect residues conserved in human Ras proteins (42). The G10R and G15D changes occur in the phosphate-binding P loop. P-loop mutations, such as those affecting G15, severely impair nucleotide and effector binding while increasing the affinity for GEFs (18, 46, 63, 68). This class of dominant-negative mutant likely acts by sequestering a limiting amount of GEF into a nonproductive signaling complex. S89 is in helix 3 and does not appear to make contact with nucleotides or SOS (10, 66), although an S89F change may affect the positioning of the P loop (Fig. 5). S89F may be a weaker class of dominant-negative mutant due to a weaker perturbation in nucleotide binding and a weaker increased interaction with SOS. As tempting as this model is, it cannot be entirely complete or correct. *sur-5* reduction-of-function mutations were isolated as suppressors of a dominant-negative K16N P-loop mutation in Ras (35). *sur-5* mutations also suppress other P-loop mutations, but not an S89F mutation. If Ras S89F acted as a dominant negative through the same mechanism as the P-loop mutants, it should also be suppressible by loss of SUR-5, since it is a weaker mutant. These results have led to the proposal that P-loop mutants and the S89F mutant act through different mechanisms (35). One possibility is that there is a second Ras GEF that is selectively inhibited by SUR-5 and, under some conditions, may be able to feed into the Ras pathway (35) (Fig. 6). This notion is supported by evidence that an activated G13E Ras mutant still exhibits EGF-dependent activity in the complete absence of SOS-1 and that the *C. elegans* genome predicts the existence of at least five other Ras GEFs (15). In one model (Fig. 6, model 1), strong inactivation of SOS-1 by dominant-negative Ras P-loop mutants allows the second Ras GEF to be wired into the Ras pathway. Thus, this class of mutation would be suppressible by a *sur-5* mutation, but not by the *sos-1(sy262)* mutation. In contrast, an S89F Ras mutant may only partially inactivate SOS-1 and not allow the second Ras GEF to wire into the Ras pathway. Thus, this class of mutation would be suppressible by the *sos-1(sy262)* mutation, but not by a *sur-5* mutation. Alternatively (Fig. 6, model 2), the second Ras GEF may be con-

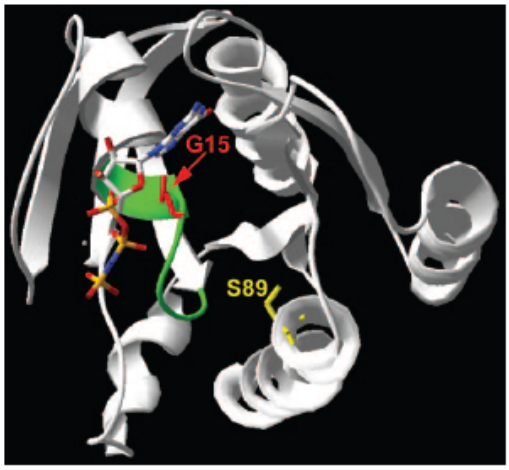

FIG. 5. Crystal structure of human H-Ras complexed with the GTP analogue GppNp (66). The phosphate-binding P loop is highlighted in green. The positions of residues that when mutated give rise to two classes of dominant-negative Ras proteins are indicated (G15, red; S89, yellow).

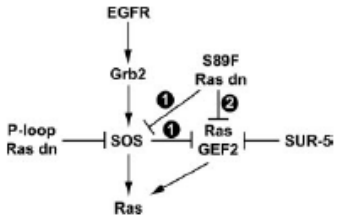

FIG. 6. Models for Ras GEF regulation by dominant-negative Ras mutants in *C. elegans* VPCs. A second Ras GEF (RasGEF2) functions in parallel to SOS. It may be constitutively wired into the Ras pathway, or it may feed in only when SOS is inactivated. RasGEF2 is selectively inhibited by SUR-5. P-loop dominant-negative Ras mutants, such as G15D, strongly inactivate SOS. In model 1, inactivation of SOS by P-loop mutants permits RasGEF2 to function in the Ras pathway. Further inactivation of SUR-5 allows RasGEF2 to promote even more Ras activation. S89F dominant-negative Ras mutants only partially inactivate SOS and fail to allow RasGEF2 to feed into the Ras pathway. Therefore, loss of SUR-5 in an S89F mutant background does not enhance Ras activation. In model 2, RasGEF2 is constitutively wired into the Ras pathway, and S89F dominant-negative Ras mutants selectively inactivate RasGEF2. Thus, in an S89F background, loss of SUR-5 still fails to promote Ras activation.

stitutively wired into the Ras pathway but selectively targeted by the S89F Ras mutant. In this case, the S89F mutation would still be suppressible by the *sos-1(sy262)* mutation, but not by a *sur-5* mutation. Selective effects of different dominant-negative Ras mutants on different GEFs may be a general property of Ras proteins. In *Saccharomyces cerevisiae*, a P-loop dominant-negative RAS2 mutant acts exclusively through a CDC25-dependent mechanism, while a D64Y (D57Y in human H-Ras) mutant can act independently of CDC25 (46).

Although the requirement for the SOS CDC25 domain in regulating RTK-mediated Ras signaling in vivo is well established (9, 15, 69, 75, 92), it is less clear to what extent and how the Dbl domain might regulate development. In fact, the first genetic role for the SOS Dbl domain has just recently been reported. In *Drosophila melanogaster*, Rac GEF activity from the Dbl domain, but not Ras GEF activity from the CDC25 domain, is necessary for ROBO-mediated axon guidance (32, 95). Our genetic data indicate that the SOS Dbl domain performs an additional critical function during development. It inhibits RTK-Ras-MAPK signaling. This form of inhibition is extremely significant. It is of the same magnitude as established *trans*-acting inhibitors, such as c-Cbl, RasGAP, and MAPK phosphatase (Table 5). Furthermore, although the worms appeared to be able to cope with the single loss of Dbl-conferred inhibition (through the *sy262* mutation), they were on the threshold of having abnormal development. In the further absence of RasGAP, which would also decrease Ras GTPase activity, vulval development was no longer normal, as 25% of the double-mutant animals displayed ectopic vulvae (Table 5). These results highlight the developmental importance of the Dbl domain in properly balancing Ras GEF and GAP activities in order to achieve proper signaling intensity.

The identification of a single missense mutation in the SOS-1 Dbl domain that can significantly alter development in sensitized backgrounds suggests that functionally similar mutations in hSOS1 may contribute to Ras-dependent malignancies. In fact, we found that a C282R mutation in hSOS1, which is analogous to the activating G322R change in *C. elegans* SOS1, also created a gain-of-function protein (Fig. 4). Moreover, while this work was in revision, it was reported that activating mutations in hSOS1 occur in patients with Noonan syndrome (73, 90). Approximately 50% of Noonan patients carry activating mutations in PTPN11, a positive regulator of Ras signaling (88), and a few other patients carry novel, weakly activating mutations in K-Ras (78). Aside from the developmental abnormalities associated with Noonan syndrome, patients are predisposed to develop juvenile leukemias and myeloproliferative disorders commonly associated with mutations in the Ras pathway (55). Noonan-associated SOS1 mutations occur throughout the gene, affecting the histone fold region, the Dbl domain, the PH domain, the REM domain, the CDC25 domain, and the helical linker between the PH and REM domains (73, 90). Our work agrees with the general conclusions of these studies, namely, that disruption of autoinhibition on the allosteric site promotes Ras activation in vivo. However, not all of the human mutations may act equivalently. Some mutations affecting the Dbl domain, the CDC25 domain, and the helical linker between the PH and REM domains enhance EGF-dependent Ras and MAPK activation, which is consistent with our genetic and biochemical studies with the G322R and C282R mutations (73). Interestingly, one of these mutations, M269R, lies in the H2b helix of the Dbl domain, which directly interacts with the Ras-GTP allosteric site (84). In vitro studies predicted that a mutation at M269 would disrupt this interaction and enhance Ras and MAPK activation in vivo (84). In contrast, a human W729L mutation in the REM domain, which directly affects a residue that mediates binding of Ras-GTP at the allosteric site, appears to act by increasing basal activity toward Ras while having little effect on MAPK activation (90). If the general model from all of these studies is correct, our data provide direct support for the causal link between the human mutations in SOS1 and the associated developmental syndrome. The contributions of activating mutations in the Ras pathway to human cancer have long been appreciated (11). However, the strong activated nature of the classic G12 mutations did not overtly predict the potential contributions of weaker mutations that more subtly alter Ras signaling intensity to cancer and developmental syndromes (6, 24, 26, 64, 74, 78, 89). Our work and the recent discoveries of novel classes of activating mutations in components of the Ras pathway in human disease highlight the complexity with which perturbations in a single signaling pathway can lead to diverse types of human disease.

ACKNOWLEDGMENTS

We thank Ben Neel for the hSOS1 cDNA clone and the hemagglutinin (HA)-ERK1 expression vector, Steve Lessnick for HEK 293 EBNA cells and polyethylenimine, and David Virshup for NIH 3T3 cells. We also thank Steve Lessnick, Don Ayer, Scott Kuwada, and members of the Moghal laboratory for critically reading the manuscript and Tommy Wong and Suzanne Elgort for help with figures. We also thank the reviewers for their insightful comments/criticisms about the manuscript. Some nematode strains used in this work were provided by the *Caenorhabditis* Genetics Center, which is funded by the NIH National Center for Research Resources (NCRR). We thank the *C. elegans* Reverse Genetics Core Facility at the University of British Columbia, which is part of the International *C. elegans* Gene Knockout Consortium, for providing the *rac-2(ok326)* deletion mutant.

This research was supported by Public Health Services grant R01 GM073184 from the National Institutes of Health to N.M. and the Howard Hughes Medical Institute, for which P.W.S. is an Investigator.

REFERENCES

1. Aghazadeh, B., W. E. Lowry, X. Y. Huang, and M. K. Rosen. 2000. Structural basis for relief of autoinhibition of the Dbl homology domain of proto-oncogene Vav by tyrosine phosphorylation. Cell 102:625–633.
2. Aroian, R., and P. Sternberg. 1991. Multiple functions of let-23, a *Caenorhabditis elegans* receptor tyrosine kinase gene required for vulval induction. Genetics 128:251–267.
3. Aronheim, A., D. Engelberg, N. Li, N. al-Alawi, J. Schlessinger, and M. Karin. 1994. Membrane targeting of the nucleotide exchange factor Sos is sufficient for activating the Ras signaling pathway. Cell 78:949–961.
4. Bargmann, C., and L. Avery. 1995. Laser killing of cells in *Caenorhabditis elegans*. Methods Cell Biol. 48:225–250.
5. Beitel, G., S. Clark, and H. Horvitz. 1990. *Caenorhabditis elegans ras* gene let-60 acts as a switch in the pathway of vulval induction. Nature 348:503–509.
6. Bentires-Alj, M., J. G. Paez, F. S. David, H. Keilhack, B. Halmos, K. Naoki, J. M. Maris, A. Richardson, A. Bardelli, D. J. Sugarbaker, W. G. Richards, J. Du, L. Girard, J. D. Minna, M. L. Loh, D. E. Fisher, V. E. Velculescu, B. Vogelstein, M. Meyerson, W. R. Sellers, and B. G. Neel. 2004. Activating mutations of the Noonan syndrome-associated SHP2/PTPN11 gene in human solid tumors and adult acute myelogenous leukemia. Cancer Res. 64:8816–8820.
7. Berset, T., E. F. Hoier, G. Battu, S. Canevascini, and A. Hajnal. 2001. Notch Inhibition of RAS signaling through MAP kinase phosphatase LIP-1 during *C. elegans* vulval development. Science 291:1055–1058.
8. Blume-Jensen, P., and T. Hunter. 2001. Oncogenic kinase signalling. Nature 411:355–365.
9. Bonfini, L., C. A. Karlovich, C. Dasgupta, and U. Banerjee. 1992. The Son of sevenless gene product: a putative activator of Ras. Science 255:603–606.
10. Boriack-Sjodin, P. A., S. M. Margarit, D. Bar-Sagi, and J. Kuriyan. 1998. The structural basis of the activation of Ras by Sos. Nature 394:337–343.
11. Bos, J. L. 1989. *ras* oncogenes in human cancer: a review. Cancer Res 49:4682–4689.
12. Boykevisch, S., C. Zhao, H. Sondermann, P. Philippidou, S. Halegoua, J. Kuriyan, and D. Bar-Sagi. 2006. Regulation of *ras* signaling dynamics by Sos-mediated positive feedback. Curr. Biol. 16:2173–2179.
13. Brenner, S. 1974. The genetics of *Caenorhabditis elegans*. Genetics 77:71–94.
14. Byrne, J. L., H. F. Paterson, and C. J. Marshall. 1996. p21Ras activation by the guanine nucleotide exchange factor Sos, requires the Sos/Grb2 interaction and a second ligand-dependent signal involving the Sos N-terminus. Oncogene 13:2055–2065.
15. Chang, C., N. Hopper, and P. Sternberg. 2000. *Caenorhabditis elegans* SOS-1 is necessary for multiple Ras-mediated developmental signals. EMBO J. 19:3283–3294.
16. Chardin, P., J. H. Camonis, N. W. Gale, L. van Aelst, J. Schlessinger, M. H. Wigler, and D. Bar-Sagi. 1993. Human Sos1: a guanine nucleotide exchange factor for Ras that binds to GRB2. Science 260:1338–1343.
17. Chen, N., and I. Greenwald. 2004. The lateral signal for LIN-12/Notch in *C. elegans* vulval development comprises redundant secreted and transmembrane DSL proteins. Dev. Cell 6:183–192.
18. Chen, S. Y., S. Y. Huff, C. C. Lai, C. J. Der, and S. Powers. 1994. Ras-15A protein shares highly similar dominant-negative biological properties with Ras-17N and forms a stable, guanine-nucleotide resistant complex with CDC25 exchange factor. Oncogene 9:2691–2698.
19. Clandinin, T., J. DeModena, and P. Sternberg. 1998. Inositol trisphospate mediates a Ras-independent response to LET-23 receptor tyrosine kinase activation in *C. elegans*. Cell 92:523–533.
20. Corbalan-Garcia, S., S. M. Margarit, D. Galron, S. S. Yang, and D. Bar-Sagi. 1998. Regulation of Sos activity by intramolecular interactions. Mol. Cell. Biol. 18:880–886.
21. Cox, G., J. Laufer, M. Kusch, and R. Edgar. 1980. Genetic and phenotypic characterization of roller mutants of *C. elegans*. Genetics 95:317–339.
22. Crespo, P., K. E. Schuebel, A. A. Ostrom, J. S. Gutkind, and X. R. Bustelo. 1997. Phosphotyrosine-dependent activation of Rac-1 GDP/GTP exchange by the *vav* proto-oncogene product. Nature 385:169–172.
23. Das, B., X. Shu, G. J. Day, J. Han, U. M. Krishna, J. R. Falck, and D. Broek. 2000. Control of intramolecular interactions between the pleckstrin homology and Dbl homology domains of Vav and Sos1 regulates Rac binding. J. Biol. Chem. 275:15074–15081.
24. Davies, H., G. R. Bignell, C. Cox, P. Stephens, S. Edkins, S. Clegg, J. Teague, H. Woffendin, M. J. Garnett, W. Bottomley, N. Davis, E. Dicks, R. Ewing, Y. Floyd, K. Gray, S. Hall, R. Hawes, J. Hughes, V. Kosmidou, A. Menzies, C. Mould, A. Parker, C. Stevens, S. Watt, S. Hooper, R. Wilson, H. Jayatilake, B. A. Gusterson, C. Cooper, J. Shipley, D. Hargrave, K. Pritchard-Jones, N. Maitland, G. Chenevix-Trench, G. J. Riggins, D. D. Bigner, G. Palmieri, A. Cossu, A. Flanagan, A. Nicholson, J. W. Ho, S. Y. Leung, S. T. Yuen, B. L. Weber, H. F. Seigler, T. L. Darrow, H. Paterson, R. Marais, C. J. Marshall, R. Wooster, M. R. Stratton, and P. A. Futreal. 2002. Mutations of the BRAF gene in human cancer. Nature 417:949–954.
25. Deckert, M., S. Tartare-Deckert, C. Couture, T. Mustelin, and A. Altman. 1996. Functional and physical interactions of Syk family kinases with the Vav proto-oncogene product. Immunity 5:591–604.
26. De Luca, A., I. Bottillo, A. Sarkozy, C. Carta, C. Neri, E. Bellacchio, A. Schirinzi, E. Conti, G. Zampino, A. Battaglia, S. Majore, M. M. Rinaldi, M. Carella, B. Marino, A. Pizzuti, M. C. Digilio, M. Tartaglia, and B. Dallapiccola. 2005. NF1 gene mutations represent the major molecular event underlying neurofibromatosis-Noonan syndrome. Am. J. Hum. Genet. 77:1092–1101.
27. Eblen, S. T., J. K. Slack, M. J. Weber, and A. D. Catling. 2002. Rac-PAK signaling stimulates extracellular signal-regulated kinase (ERK) activation by regulating formation of MEK1-ERK complexes. Mol. Cell. Biol. 22:6023–6033.
28. Egan, S. E., B. W. Giddings, M. W. Brooks, L. Buday, A. M. Sizeland, and R. A. Weinberg. 1993. Association of Sos Ras exchange protein with Grb2 is implicated in tyrosine kinase signal transduction and transformation. Nature 363:45–51.
29. Ellis, R., D. Jacobson, and H. Horvitz. 1991. Genes required for the engulfment of cell corpses during programmed cell death in *Caenorhabditis elegans*. Genetics 129:79–94.
30. Ferguson, E., and H. Horvitz. 1985. Identification and characterization of 22 genes that affect the vulval cell lineages of the nematode *C. elegans*. Genetics 110:17–72.
31. Freedman, T. S., H. Sondermann, G. D. Friedland, T. Kortemme, D. Bar-Sagi, S. Marqusee, and J. Kuriyan. 2006. A Ras-induced conformational switch in the Ras activator Son of sevenless. Proc. Natl. Acad. Sci. USA 103:16692–16697.
32. Fritz, J. L., and M. F. VanBerkum. 2002. Regulation of rho family GTPases is required to prevent axons from crossing the midline. Dev. Biol. 252:46–58.
33. Frost, J. A., H. Steen, P. Shapiro, T. Lewis, N. Ahn, P. E. Shaw, and M. H. Cobb. 1997. Cross-cascade activation of ERKs and ternary complex factors by Rho family proteins. EMBO J. 16:6426–6438.
34. Granato, M., H. Schnabel, and R. Schnabel. 1994. pha-1, a selectable marker for gene-transfer in *C. elegans*. Nucleic Acids Res. 22:1762–1763.
35. Gu, T., S. Orita, and M. Han. 1998. *Caenorhabditis elegans* SUR-5, a novel but conserved protein, negatively regulates LRT-60 *ras* activity during vulval induction. Mol. Cell. Biol. 18:4556–4564.
36. Guex, N., and M. C. Peitsch. 1997. SWISS-MODEL and the Swiss-Pdb-Viewer: an environment for comparative protein modeling. Electrophoresis 18:2714–2723.
37. Hajnal, A., C. Whitfield, and S. Kim. 1997. Inhibition of *Caenorhabditis elegans* vulval induction by gap-1 and by let-23 receptor tyrosine kinase. Genes Dev. 11:2715–2728.
38. Han, J., B. Das, W. Wei, L. Van Aelst, R. D. Mosteller, R. Khosravi-Far, J. K. Westwick, C. J. Der, and D. Broek. 1997. Lck regulates Vav activation of members of the Rho family of GTPases. Mol. Cell. Biol. 17:1346–1353.
39. Han, J., K. Luby-Phelps, B. Das, X. Shu, Y. Xia, R. D. Mosteller, U. M. Krishna, J. R. Falck, M. A. White, and D. Broek. 1998. Role of substrates and products of PI 3-kinase in regulating activation of Rac-related guanosine triphosphatases by Vav. Science 279:558–560.
40. Han, M., R. Aroian, and P. Sternberg. 1990. The let-60 locus controls the switch between vulval and nonvulval cell fates in *Caenorhabditis elegans*. Genetics 126:899–913.
41. Han, M., A. Golden, Y. Han, and P. Sternberg. 1993. *C. elegans* lin-45 *raf* gene participates in let-60 RAS-stimulated vulval differentiation. Nature 363:133–140.
42. Han, M., and P. Sternberg. 1991. Analysis of dominant negative mutations of the *Caenorhabditis elegans* let-60 *ras* gene. Genes Dev. 5:2188–2198.
43. Hosono, R., K. Hirahara, S. Kuno, and T. Kurihara. 1982. Mutants of *C. elegans* with Dumpy and Rounded head phenotype. J. Exp. Zool. 224:135–144.
44. Johnsen, R., and D. Baillie. 1991. Genetic analysis of a major segment [LGV(left)] of the genome of *Caenorhabditis elegans*. Genetics 129:735–752.
45. Jongeward, G., T. Clandinin, and P. Sternberg. 1995. sli-1, a negative regulator of let-23-mediated signaling in *C. elegans*. Genetics 139:1553–1566.
46. Jung, V., W. Wei, R. Ballester, J. Camonis, S. Mi, L. Van Aelst, M. Wigler, and D. Broek. 1994. Two types of RAS mutants that dominantly interfere with activators of RAS. Mol. Cell. Biol. 14:3707–3718.
47. Kaech, S., C. Whitfield, and S. Kim. 1998. The LIN-2/LIN-7/LIN-10 complex mediates basolateral membrane localization of the *C. elegans* EGF receptor LET-23 in vulval epithelial cells. Cell 94:761–771.
48. Kamath, R. S., A. G. Fraser, Y. Dong, G. Poulin, R. Durbin, M. Gotta, A. Kanapin, N. Le Bot, S. Moreno, M. Sohrmann, D. P. Welchman, P. Zipperlen, and J. Ahringer. 2003. Systematic functional analysis of the *Caenorhabditis elegans* genome using RNAi. Nature 421:231–237.
49. Karlovich, C. A., L. Bonfini, L. McCollam, R. D. Rogge, A. Daga, M. P. Czech, and U. Banerjee. 1995. In vivo functional analysis of the Ras exchange factor son of sevenless. Science 268:576–579.
50. Katz, W., G. Lesa, D. Yannoukakos, T. Clandinin, J. Schlessinger, and P. Sternberg. 1996. A point mutation in the extracellular domain activated

LET-23, the *Caenorhabditis elegans* epidermal growth factor receptor homolog. Mol. Cell. Biol. 16:529–537.
51. **Kim, J. H., M. Shirouzu, T. Kataoka, D. Bowtell, and S. Yokoyama.** 1998. Activation of Ras and its downstream extracellular signal-regulated protein kinases by the CDC25 homology domain of mouse Son-of-sevenless 1 (mSos1). Oncogene 16:2597–2607.
52. **King, A. J., H. Sun, B. Diaz, D. Barnard, W. Miao, S. Bagrodia, and M. S. Marshall.** 1998. The protein kinase Pak3 positively regulates Raf-1 activity through phosphorylation of serine 338. Nature 396:180–183.
53. **Kishore, R. S., and M. V. Sundaram.** 2002. ced-10 Rac and mig-2 function redundantly and act with unc-73 trio to control the orientation of vulval cell divisions and migrations in *Caenorhabditis elegans*. Dev. Biol. 241:339–348.
54. **Kornfeld, K., D. Hom, and H. Horvitz.** 1995. The ksr-1 gene encodes a novel protein kinase involved in Ras-mediated signaling in *C. elegans*. Cell 83:903–913.
55. **Lauchle, J. O., B. S. Braun, M. L. Loh, and K. Shannon.** 2006. Inherited predispositions and hyperactive Ras in myeloid leukemogenesis. Pediatr. Blood Cancer 46:579–585.
56. **Liu, J., P. Tzou, R. Hill, and P. Sternberg.** 1999. Structural requirements for the tissue-specific and tissue-general functions of the *Caenorhabditis elegans* epidermal growth factor LIN-3. Genetics 153:1257–1269.
57. **Lundquist, E. A., P. W. Reddien, E. Hartwieg, H. R. Horvitz, and C. I. Bargmann.** 2001. Three *C. elegans* Rac proteins and several alternative Rac regulators control axon guidance, cell migration and apoptotic cell phagocytosis. Development 128:4475–4488.
58. **Margarit, S. M., H. Sondermann, B. E. Hall, B. Nagar, A. Hoelz, M. Pirruccello, D. Bar-Sagi, and J. Kuriyan.** 2003. Structural evidence for feedback activation by Ras.GTP of the Ras-specific nucleotide exchange factor SOS. Cell 112:685–695.
59. **Moerman, D., and D. Baillie.** 1979. Genetic organization in *C. elegans*: fine-structure analysis of the unc-22 gene. Genetics 91:95–104.
60. **Moghal, N., L. R. Garcia, L. A. Khan, K. Iwasaki, and P. W. Sternberg.** 2003. Modulation of EGF receptor-mediated vulva development by the heterotrimeric G-protein Goαq and excitable cells in *C. elegans*. Development 130: 4553–4566.
61. **Moghal, N., and P. W. Sternberg.** 2003. The epidermal growth factor system in *Caenorhabditis elegans*. Exp. Cell Res. 284:150–159.
62. **Moghal, N., and P. W. Sternberg.** 2003. Extracellular domain determinants of LET-23 (EGF) receptor tyrosine kinase activity in *Caenorhabditis elegans*. Oncogene 22:5471–5480.
63. **Munder, T., and P. Furst.** 1992. The *Saccharomyces cerevisiae* CDC25 gene product binds specifically to catalytically inactive Ras proteins in vivo. Mol. Cell. Biol. 12:2091–2099.
64. **Niihori, T., Y. Aoki, Y. Narumi, G. Neri, H. Cave, A. Verloes, N. Okamoto, R. C. Hennekam, G. Gillessen-Kaesbach, D. Wieczorek, M. I. Kavamura, K. Kurosawa, H. Ohashi, L. Wilson, D. Heron, D. Bonneau, G. Corona, T. Kaname, K. Naritomi, C. Baumann, N. Matsumoto, K. Kato, S. Kure, and Y. Matsubara.** 2006. Germline KRAS and BRAF mutations in cardio-facio-cutaneous syndrome. Nat. Genet. 38:294–296.
65. **Nimnual, A. S., B. A. Yatsula, and D. Bar-Sagi.** 1998. Coupling of Ras and Rac guanosine triphosphatases through the Ras exchanger Sos. Science 279:560–563.
66. **Pai, E. F., U. Krengel, G. A. Petsko, R. S. Goody, W. Kabsch, and A. Wittinghofer.** 1990. Refined crystal structure of the triphosphate conformation of H-ras p21 at 1.35 Å resolution: implications for the mechanism of GTP hydrolysis. EMBO J. 9:2351–2359.
67. **Peitsch, M. C.** 1996. ProMod and Swiss-Model: Internet-based tools for automated comparative protein modelling. Biochem. Soc. Trans. 24:274–279.
68. **Powers, S., K. O'Neill, and M. Wigler.** 1989. Dominant yeast and mammalian RAS mutants that interfere with the CDC25-dependent activation of wild-type RAS in *Saccharomyces cerevisiae*. Mol. Cell. Biol. 9:390–395.
69. **Qian, X., L. Esteban, W. C. Vass, C. Upadhyaya, A. G. Papageorge, K. Yienger, J. M. Ward, D. R. Lowy, and E. Santos.** 2000. The Sos1 and Sos2 Ras-specific exchange factors: differences in placental expression and signaling properties. EMBO J. 19:642–654.
70. **Qian, X., W. C. Vass, A. G. Papageorge, P. H. Anborgh, and D. R. Lowy.** 1998. N terminus of Sos1 Ras exchange factor: critical roles for the Dbl and pleckstrin homology domains. Mol. Cell. Biol. 18:771–778.
71. **Reddien, P. W., and H. R. Horvitz.** 2000. CED-2/CrkII and CED-10/Rac control phagocytosis and cell migration in *Caenorhabditis elegans*. Nat. Cell Biol. 2:131–136.
72. **Riddle, D.** 1978. The genetics of development and behavior in I. J. Nematol. 10:1–16.
73. **Roberts, A. E., T. Araki, K. D. Swanson, K. T. Montgomery, T. A. Schiripo, V. A. Joshi, L. Li, Y. Yassin, A. M. Tamburino, B. G. Neel, and R. S. Kucherlapati.** 2007. Germline gain-of-function mutations in SOS1 cause Noonan syndrome. Nat. Genet. 39:70–74.
74. **Rodriguez-Viciana, P., O. Tetsu, W. E. Tidyman, A. L. Estep, B. A. Conger, M. S. Cruz, F. McCormick, and K. A. Rauen.** 2006. Germline mutations in genes within the MAPK pathway cause cardio-facio-cutaneous syndrome. Science 311:1287–1290.
75. **Rogge, R. D., C. A. Karlovich, and U. Banerjee.** 1991. Genetic dissection of a neurodevelopmental pathway: Son of sevenless functions downstream of the sevenless and EGF receptor tyrosine kinases. Cell 64:39–48.
76. **Rozakis-Adcock, M., R. Fernley, J. Wade, T. Pawson, and D. Bowtell.** 1993. The SH2 and SH3 domains of mammalian Grb2 couple the EGF receptor to the Ras activator mSos1. Nature 363:83–85.
77. **Rusanescu, G., T. Gotoh, X. Tian, and L. A. Feig.** 2001. Regulation of Ras signaling specificity by protein kinase C. Mol. Cell. Biol. 21:2650–2658.
78. **Schubbert, S., M. Zenker, S. L. Rowe, S. Boll, C. Klein, G. Bollag, I. van der Burgt, L. Musante, V. Kalscheuer, L. E. Wehner, H. Nguyen, B. West, K. Y. Zhang, E. Sistermans, A. Rauch, C. M. Niemeyer, K. Shannon, and C. P. Kratz.** 2006. Germline KRAS mutations cause Noonan syndrome. Nat. Genet. 38:331–336.
79. **Schwede, T., J. Kopp, N. Guex, and M. C. Peitsch.** 2003. SWISS-MODEL: an automated protein homology-modeling server. Nucleic Acids Res. 31:3381–3385.
80. **Scita, G., J. Nordstrom, R. Carbone, P. Tenca, G. Giardina, S. Gutkind, M. Bjarnegard, C. Betsholtz, and P. P. Di Fiore.** 1999. EPS8 and E3B1 transduce signals from Ras to Rac. Nature 401:290–293.
81. **Scita, G., P. Tenca, L. B. Areces, A. Tocchetti, E. Frittoli, G. Giardina, L. Ponzanelli, P. Sini, M. Innocenti, and P. P. Di Fiore.** 2001. An effector region in Eps8 is responsible for the activation of the Rac-specific GEF activity of Sos-1 and for the proper localization of the Rac-based actin-polymerizing machine. J. Cell Biol. 154:1031–1044.
82. **Sini, P., A. Cannas, A. J. Koleske, P. P. Di Fiore, and G. Scita.** 2004. Abl-dependent tyrosine phosphorylation of Sos-1 mediates growth-factor-induced Rac activation. Nat. Cell Biol. 6:268–274.
83. **Soisson, S. M., A. S. Nimnual, M. Uy, D. Bar-Sagi, and J. Kuriyan.** 1998. Crystal structure of the Dbl and pleckstrin homology domains from the human Son of sevenless protein. Cell 95:259–268.
84. **Sondermann, H., S. M. Soisson, S. Boykevisch, S. S. Yang, D. Bar-Sagi, and J. Kuriyan.** 2004. Structural analysis of autoinhibition in the Ras activator Son of sevenless. Cell 119:393–405.
85. **Spencer, A. G., S. Orita, C. J. Malone, and M. Han.** 2001. A RHO GTPase-mediated pathway is required during P cell migration in *Caenorhabditis elegans*. Proc. Natl. Acad. Sci. USA 98:13132–13137.
86. **Sternberg, P., and H. Horvitz.** 1986. Pattern formation during vulval development in *C. elegans*. Cell 44:761–772.
87. **Sundaram, M., and M. Han.** 1995. The *C. elegans* ksr-1 gene encodes a novel Raf-related kinase involved in Ras-mediated signal transduction. Cell 83: 889–901.
88. **Tartaglia, M., E. L. Mehler, R. Goldberg, G. Zampino, H. G. Brunner, H. Kremer, I. van der Burgt, A. H. Crosby, A. Ion, S. Jeffery, K. Kalidas, M. A. Patton, R. S. Kucherlapati, and B. D. Gelb.** 2001. Mutations in PTPN11, encoding the protein tyrosine phosphatase SHP-2, cause Noonan syndrome. Nat. Genet. 29:465–468.
89. **Tartaglia, M., C. M. Niemeyer, A. Fragale, X. Song, J. Buechner, A. Jung, K. Hahlen, H. Hasle, J. D. Licht, and B. D. Gelb.** 2003. Somatic mutations in PTPN11 in juvenile myelomonocytic leukemia, myelodysplastic syndromes and acute myeloid leukemia. Nat. Genet. 34:148–150.
90. **Tartaglia, M., L. A. Pennacchio, C. Zhao, K. K. Yadav, V. Fodale, A. Sarkozy, B. Pandit, K. Oishi, S. Martinelli, W. Schackwitz, A. Ustaszewska, J. Martin, J. Bristow, C. Carta, F. Lepri, C. Neri, I. Vasta, K. Gibson, C. J. Curry, J. P. Siguero, M. C. Digilio, G. Zampino, B. Dallapiccola, D. Bar-Sagi, and B. D. Gelb.** 2007. Gain-of-function SOS1 mutations cause a distinctive form of Noonan syndrome. Nat. Genet. 39:75–79.
91. **Tian, X., G. Rusanescu, W. Hou, B. Schaffhausen, and L. A. Feig.** 2002. PDK1 mediates growth factor-induced Ral-GEF activation by a kinase-independent mechanism. EMBO J. 21:1327–1338.
92. **Wang, D. Z., V. E. Hammond, H. E. Abud, I. Bertoncello, J. W. McAvoy, and D. D. Bowtell.** 1997. Mutation in Sos1 dominantly enhances a weak allele of the EGFR, demonstrating a requirement for Sos1 in EGFR signaling and development. Genes Dev. 11:309–320.
93. **Wang, W., E. M. Fisher, Q. Jia, J. M. Dunn, E. Porfiri, J. Downward, and S. E. Egan.** 1995. The Grb2 binding domain of mSos1 is not required for downstream signal transduction. Nat. Genet. 10:294–300.
94. **Wicks, S. R., R. T. Yeh, W. R. Gish, R. H. Waterston, and R. H. Plasterk.** 2001. Rapid gene mapping in *Caenorhabditis elegans* using a high density polymorphism map. Nat. Genet. 28:160–164.
95. **Yang, L., and G. J. Bashaw.** 2006. Son of sevenless directly links the Robo receptor to *rac* activation to control axon repulsion at the midline. Neuron 52:595–607.
96. **Yoon, C., J. Lee, G. Jongeward, and P. Sternberg.** 1995. Similarity of sli-1, a regulator of vulval development in *C. elegans*, to the mammalian proto-oncogene c-cbl. Science 269:1102–1105.
97. **Zang, M., C. Hayne, and Z. Luo.** 2002. Interaction between active Pak1 and Raf-1 is necessary for phosphorylation and activation of Raf-1. J. Biol. Chem. 277:4395–4405.
98. **Zipkin, I. D., R. M. Kindt, and C. J. Kenyon.** 1997. Role of a new Rho family member in cell migration and axon guidance in *C. elegans*. Cell 90:883–894.

APPENDIX B

COORDINATION OF GLUCOSE AND GLUTAMINE UTILIZATION BY AN EXPANDED MYC NETWORK

Appendix B is a perspective/mini review published in Transcription in August 2010 (Transcription 2010; 1:36-40). It is reprinted here with permission from the publisher and the authors. It primarily discusses subjects addressed in Chapter 1, but further expands the discourse on Myc regulation of glucose and glutamine metabolism in cancer. Marc G. Elgort contributed sections discussing Myc regulation of glycolytic targets and glutaminolysis.

Transcription 1:1, 36-40; July/August 2010; © 2010 Landes Bioscience

Coordination of glucose and glutamine utilization by an expanded Myc network

Mohan R. Kaadige, Marc G. Elgort and Donald E. Ayer*
Huntsman Cancer Institute; Department of Oncological Sciences; University of Utah; Salt Lake City, UT USA

Glucose and glutamine are the most abundant circulating nutrients and support the growth and proliferation of all cells, in particular rapidly growing and dividing cancer cells. Several recent studies implicate an expanded Myc network in how cells sense and utilize both glucose and glutamine. These studies reveal an unappreciated coordination between glycolysis and glutaminolysis, potentially providing new targets for therapeutic intervention in cancer.

Key words: glucose, glutamine, nutrient, mitochondria, MondoA, Myc, TXNIP

Submitted: 03/31/10

Accepted: 04/21/10

Previously published online: http://www.landesbioscience.com/journals/transcription/article/12142

*Correspondence to: Donald E. Ayer; Email: don.ayer@hci.utah.edu

An Expanded Myc Network

Classically, the Myc oncogene, a member of the basic helix-loop-helix leucine zipper (bHLHZip) family of transcription factors, contributes to human malignancy via a complex web of protein-protein and protein-DNA interactions. In the simplest version of this regulatory model, Myc forms heterodimers with Max, another bHLHZip factor, to bind CACGTG or related E-box sites in the promoters of pro-growth and division targets, activating their expression (Fig. 1A).[1] Activation of these Pol II targets is achieved via the recruitment of different chromatin modifying activities. Myc is a potent oncogene, yet with direct targets in the thousands, identifying which targets are absolutely required for its oncogenic function is a significant challenge. Myc's function in transcriptional repression at some targets,[1] its direct participation in Pol I- and Pol III-dependent transcription,[2] its role in global chromatin structure,[3] and potential Max-independent functions further complicate elucidation of Myc-dependent effector pathways.[4]

The pro-growth activity of Myc:Max complexes, is generally thought to be held in check by the related, but transcriptionally repressive Mxd (formerly Mad):Max or Mnt:Max complexes (Fig. 1A).[5] These repressive Max-containing complexes are thought, but not rigorously tested, to bind similar targets of Myc:Max complexes and repress their transcription by recruitment of histone deacetylase-containing corepressor complexes. Two additional bHLHZip proteins, MondoA and ChREBP,[6] provide the foundation of a parallel Myc network and present a new challenge to understanding the functional output of the network. In comparison to the wealth of information available for Myc, our understanding of MondoA and ChREBP and potential cooperative interactions with the Myc network is sparse. Recent papers suggest that one area of functional integration between Myc and MondoA/ChREBP is in sensing and adaptation to the growth-essential nutrients glucose and glutamine.

MondoA and ChREBP are both members of the bHLHZip family. Each is roughly 1,000 amino acids in length and about twice the size of Myc. Like Myc family members, the bHLHZip domain of MondoA and ChREBP is located close to their C-termini and their transcriptional activation domain (TAD) is located in the N-terminal half of each protein.[6] N-terminal to the TAD, each protein has five blocks of highly conserved sequence we have termed the Mondo Conserved Regions (MCRs) that play critical roles in controlling subcellular localization and transcriptional activity. MondoA and ChREBP both interact with a Max-like

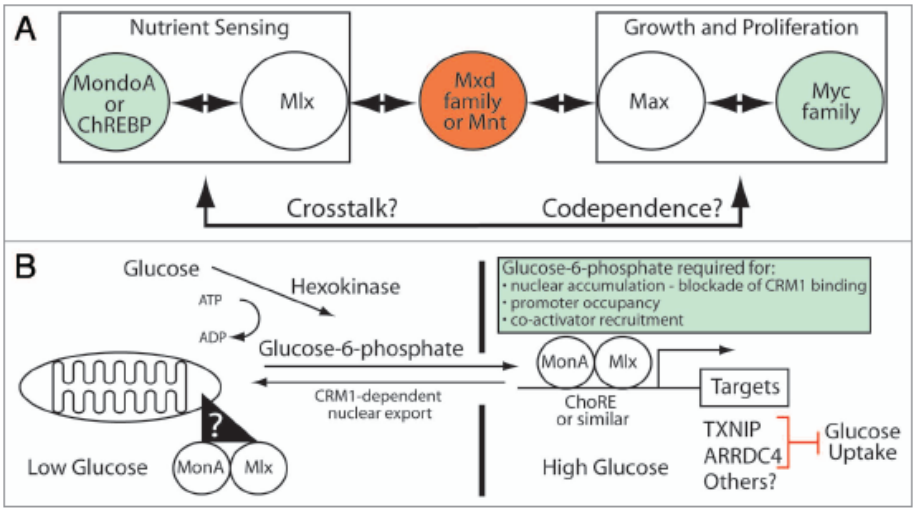

Figure 1. MondoA and ChREBP constitute a nutrient-sensing branch of an expanded Myc-network. (A) Our model of an extend Myc-network (see text for details). (B) MondoA functions as a sensor of intracellular glucose flux. Key aspects of our model include the mitochondrial-to-nuclear accumulation of MondoA:Mlx complexes in response to glucose-6-phosphate (G6P), the additional requirement of G6P for promoter occupancy and co-activator recruitment and MondoA:Mlx regulation of direct targets such as TXNIP and ARRDC4. The role of TXNIP and ARRDC4 as negative regulators of glucose uptake suggests that one key feature of MondoA:Mlx's ability to sense G6P is to restrict glucose uptake by a negative feedback loop.

bHLHZip protein called Mlx (Max-like protein x), to bind E-box-related sites in target genes (Fig. 1A). At present, our knowledge of direct targets for MondoA:Mlx and ChREBP:Mlx is limited and no genome-wide binding studies have been published. However, based on their similar binding to E-box elements, one can predict that Mlx-containing complexes will share some genomic binding sites with Max-containing complexes. Furthermore, Mlx interacts with both Mxd1 and Mxd4, suggesting potential cross talk between Max- and Mlx-centered networks (Fig. 1A).[6]

Whereas Myc, Max and Mad are constitutively nuclear, a distinguishing feature of MondoA and ChREBP is that they are held latently in the cytoplasm.[7,8] Both proteins accumulate in the nucleus following elevations in glucose metabolism. In the case of MondoA, the MondoA:Mlx complex enters the nucleus by sensing the glycolytic intermediate glucose-6-phosphate (G6P);[9] we have proposed that G6P regulates MondoA:Mlx localization allosterically (Fig. 1B).[10] In contrast, nuclear accumulation of ChREBP appears to be triggered by the pentose phosphate pathway intermediate, xylulose-5-phosphate (X5P); X5P is proposed to activate the phosphatase PP2A, which removes inhibitory phosphates in the nuclear localization sequence and adjacent to the DNA binding domain of ChREBP.[8] Nuclear accumulation is not sufficient for transcriptional activation by either MondoA or ChREBP;[10,11] thus, other mechanisms must be involved in promoter occupancy and/or co-activator recruitment. At present these mechanisms are poorly characterized, so further work is necessary in this area.

Consistent with their roles as glucose sensors, MondoA and ChREBP are most highly expressed in the skeletal muscle and liver,[6] respectively, which are central regulators of glucose homeostasis. Importantly, MondoA and ChREBP are likely responsible for the majority of glucose-dependent transcription in their respective target tissues.[9,12] While most highly expressed in post-mitotic tissues, MondoA and ChREBP are also expressed in a variety of cell lines and in a number of proliferative cell types, suggesting important roles in controlling glucose sensing and utilization during cell growth and proliferation.

Glucose and Glutamine Utilization in Cancer Cells

Rapid proliferation of cancer cells relies on growth factor signaling and the availability of the abundant nutrients glucose and glutamine.[13] Depending on cell context, Myc overexpression can drive addiction to either glucose or glutamine such that their removal from the culture medium triggers apoptosis.[14,15] Cancer cells shift glucose metabolism away from oxidative phosphorylation (OXPHOS) towards aerobic glycolysis, which is known as the Warburg effect. This metabolic transition is promoted by oncogenes such as Myc, hypoxia inducible factor (HIF), activated Ras and PI3K. Further, tumor suppressors such as p53 and PTEN can suppress this transition.[16] In aerobic glycolysis, the majority of the glucose-derived pyruvate is converted to lactate and secreted by the cell rather than entering the TCA cycle and OXPHOS for ATP production. OXPHOS is much more efficient at ATP production than aerobic glycolysis: 36 ATPs versus two ATPs from each molecule of glucose, respectively. However, flux through glycolysis is higher than through OXPHOS

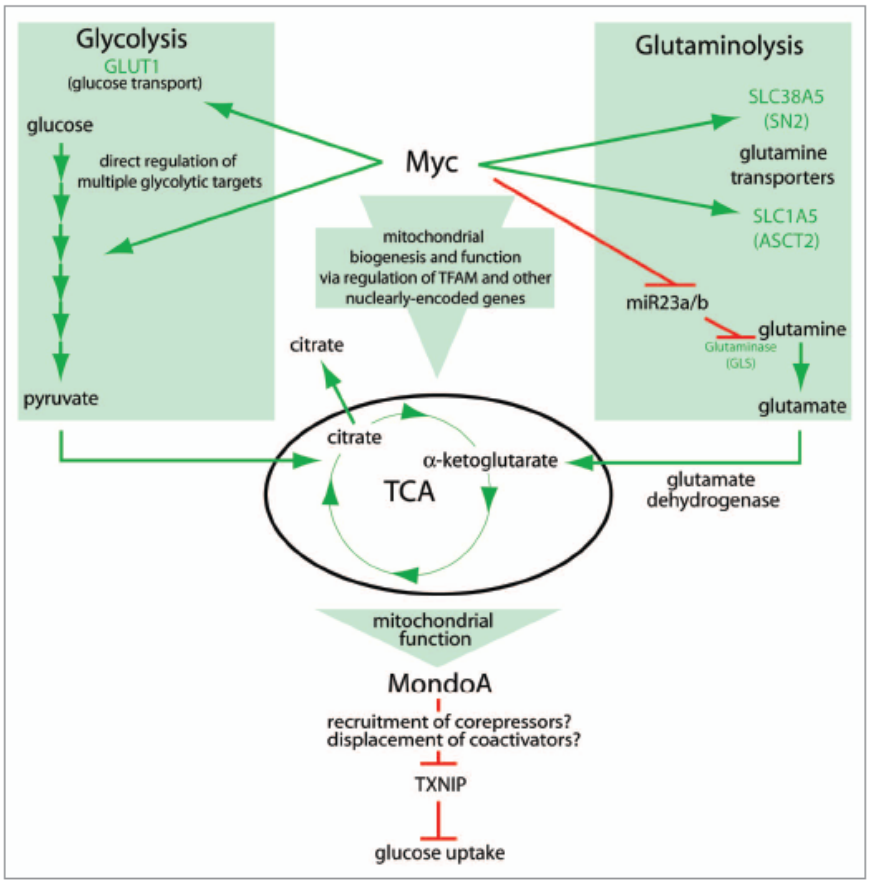

Figure 2. Myc and MondoA integrate cell growth signals. Myc can regulate glycolysis, glutaminolysis and mitochondrial activity, contributing to a functional TCA cycle. MondoA reads out TCA function, controlling glucose uptake through its regulation of TXNIP (see text for details).

and, as long as glucose is not limiting, glycolysis can produce sufficient ATP to support high proliferation rates.

The pyruvate that enters the TCA is used for the synthesis of other growth-supporting macromolecules, especially lipids required for membrane biosynthesis.[13] To support lipid synthesis, citrate, which is produced from pyruvate, is effluxed from mitochondria essentially short circuiting the TCA cycle (Fig. 2). Recent studies indicate this truncated TCA cycle can be refilled via glutaminolysis.[17] In glutaminolysis, glutamine enters cells through the transporters SLC38A5 and SLC1A5 and is metabolized to glutamate by glutaminase. Glutamate is metabolized to alpha-ketoglutarate (α-KG) by glutamate dehydrogenase, which localizes to the mitochondria. α-KG refills the TCA cycle in a process termed anapleurosis. Glutamine-derived carbons are primarily used to supply oxaloacetate, a precursor for fatty acid and lipid synthesis and NADPH; NADPH is used to support both lipid and nucleotide synthesis.[17] Thus, cancer cells must coordinate glycolytic and glutaminolytic fluxes to satisfy both bioenergetic and biosynthetic requirements. Below we discuss how Myc and Mondo families regulate metabolic gene expression and speculate on the outcome of cooperative regulation by these two families.

The Myc Network and Its Regulation of Aerobic Glycolysis

It has long been appreciated that the Myc oncogene plays a central role in the activation of aerobic glycolysis. Consistent with Myc's role in driving glucose consumption and lactate production, it directly activates transcription of virtually every glycolytic enzyme gene including the rate-limiting enzymes hexokinase II (HKII) and lactate dehydrogenase-A (LDH-A), and the glucose transporter GLUT-1 (Fig. 1B).[18] MondoA and ChREBP also regulate glycolytic targets;[19,20] yet their impact on aerobic glycolysis is not straightforward. For example, ChREBP loss slows proliferation

and reduces lactate levels and glucose uptake, suggesting that it can drive aerobic glycolysis.[21] By contrast, MondoA loss in some contexts stimulates growth and glucose uptake, likely via the loss of thioredoxin interacting protein (TXNIP) expression (see below),[9] whereas in other contexts MondoA loss reduces glycolysis.[19] Further complicating the regulation of aerobic glycolysis is the potential co-dependence of Myc and MondoA/ChREBP at some targets. For example, Myc and ChREBP are both required for the direct and glucose-dependent activation of liver-type pyruvate kinase (Pklr) transcription.[20] Thus, whereas it is well established that Myc can drive aerobic glycolysis, ChREBP and MondoA likely also play important roles in the partitioning of carbon flux necessary for cell growth and division, yet many of the mechanistic details are still missing.

Myc and Glutaminolysis

In transformed cells engaged in aerobic glycolysis, a dependence on mitochondrial function for biosynthetic reactions still exists. Myc has been shown to increase mitochondrial biogenesis and function via regulation of nuclearly encoded mitochondrial proteins and the mitochondrial transcription factor TFAM (Fig. 2).[22] These data support the hypothesis that Myc also drives proliferation by maintaining mitochondrial function. Myc has also recently been shown to increase both the transport and catabolism of glutamine in transformed cells via the direct transcriptional regulation of the glutamine transporters SLC38A5 and SCL1A5.[23] Myc can also increase the expression of glutaminase by two mechanisms. One study showed that Myc increases glutaminase mRNA,[23] while a second study showed that Myc transcriptional repression of miR-23a/b, derepressed glutaminase expression and subsequently elevated glutamine metabolism (Fig. 2).[24] Thus, in addition to its well-established role in driving aerobic glycolysis, Myc can also regulate mitochondrial function directly by regulating biogenesis and more indirectly by regulating glutaminolysis. While not formally tested, Myc-dependent glutaminolysis likely drives mitochondrial anapleurosis to support the biosynthetic reactions required to support high division rates.

MondoA Is a Glucose Sensor

One well-characterized direct and glucose-induced MondoA transcriptional target is TXNIP.[9] TXNIP appears to be a general sensor of cellular stress.[25] In cases of extreme stress, e.g., exposure of pancreatic β-cells to hyperglycemia, TXNIP triggers apoptosis.[26] Our studies indicate that MondoA is a critical regulator of hyperglycemia-induced TXNIP expression in a number of cell lines. In response to hyperglycemic growth conditions, MondoA:Mlx complexes accumulate in the nucleus, occupy the carbohydrate response elements (ChoREs) in the TXNIP promoter, and activate TXNIP expression (Fig. 1B).[9] How elevated G6P triggers the nuclear accumulation of MondoA:Mlx complexes remains to be elucidated; however, our data suggests an allosteric model where G6P binds MondoA directly to block nuclear export, promote promoter occupancy, and stimulate co-activator recruitment.[10] Hyperglycemic induction of TXNIP enforces a potent negative feedback circuit restricting glucose uptake and cell growth. Coupled with the finding that TXNIP loss is sufficient to induce aerobic glycolysis,[27] it is not surprising that many tumor tissues and tumor cells lines show reduced expression of TXNIP.[25] By contrast, high TXNIP expression seems to portend better outcome in gastric and breast cancers.[28,29] We propose that the MondoA-TXNIP regulatory axis is an important feature of how cells sense and respond to glucose, controlling cell growth by modulating levels of intracellular glucose available for ATP production and biosynthetic reactions.

MondoA Senses TCA Function

Our recent studies revealed a mechanism that coordinates glycolysis and glutaminolysis. In cells in medium with only glucose—cells do not divide under these conditions—MondoA is a potent activator of TXNIP expression, which restricts glucose uptake and cell growth.[30] As expected, addition of glutamine to glucose-only medium stimulates growth; but, surprisingly, glutamine represses MondoA-dependent TXNIP expression and stimulates glucose uptake. Thus, glutamine effectively represses glucose-induced and MondoA-dependent transcriptional activation of TXNIP. The mechanistic details of glutamine-dependent repression are not yet understood; however, it is clear that glutamine targets promoter-bound MondoA.[30] It is possible that glutamine triggers displacement or recruitment of co-activators and co-repressors (Fig. 2), respectively, or induces modifications to promoter-bound MondoA complexes.

Glutamine has several cellular fates, yet we observed that cell permeable analogs of α-KG completely phenocopy the glutamine-dependent repression of TXNIP.[30] Given that α-KG refills the TCA cycle, we proposed that MondoA functions as a transcriptional repressor of TXNIP downstream of a functional TCA cycle. How TCA-derived signals convert MondoA from a transcriptional activator to a transcriptional repressor is not known, but the localization of MondoA:Mlx complexes to the outer mitochondrial membrane places them at a privileged location to sense TCA cycle function.[19] The nature of the TCA-derived signal and how it is transmitted to the TXNIP promoter remains to be addressed experimentally.

Our study suggests a novel function for MondoA in coordinating glycolysis and glutaminolysis via its regulation of TXNIP. We propose that this coordination represents a metabolic growth checkpoint, restricting cell growth, via a TXNIP-dependent blockade of glucose uptake, when sub-threshold levels of glucose and glutamine are available. At higher glutamine concentrations, i.e., growth permissive conditions, TXNIP expression is repressed, glucose uptake is stimulated, and cellular metabolic programs are activated. A final implication of our study is that glutaminolysis, via TCA anapleurosis and MondoA-dependent repression of TXNIP, actually functions upstream of glucose uptake and glycolysis.

Do Myc and MondoA Coordinately Regulate Glucose Uptake in Transformed Cells?

Myc overexpression drives glutamine addiction via the regulation of glutamine transporters and glutaminase. While not yet formally tested, it seems likely that Myc-dependent glutaminolysis drives TCA anapleurosis, which we have shown converts MondoA to a transcriptional repressor at TXNIP. Reducing TXNIP levels is sufficient to stimulate glucose uptake and TXNIP deletion is sufficient to drive aerobic glycolysis.[27] Based on these observations, we propose that, in Myc-dependent tumor cells, high glutamine-derived TCA intermediates increase the relative transcriptional repression activity of MondoA at the TXNIP promoter, reducing TXNIP levels and elevating glucose uptake. Thus, in addition to its well-established role in direct regulation of target genes encoding glycolytic enzymes and glycolysis, we propose that Myc may also stimulate glucose uptake by this second glutaminolysis-dependent mechanism. Because Myc-overexpressing cells can be addicted to glutamine,[15] we wonder whether glutamine withdrawal in these cells may induce TXNIP, restrict glucose uptake, and drive cell death by this more indirect mechanism rather than by restriction of glutamine metabolism per se.

Summary

While Myc's role in driving aerobic glycolysis has been known for several years, only recently has its role in driving mitochondrial biogenesis and glutaminolysis been demonstrated. These findings place Myc as a central regulator of intermediary metabolism required to support the high energy and biosynthetic demands of rapidly dividing tumor cells. By contrast, the functions of MondoA in controlling intermediary metabolism are only now emerging. Its role as a potent negative regulator of glucose uptake via its regulation of TXNIP, suggests that in some contexts MondoA may antagonize Myc function by restricting nutrient availability. By contrast, MondoA can also function as a transcriptional repressor of TXNIP promoting glucose uptake downstream of glutaminolysis and a functional TCA cycle. Thus, in other contexts, MondoA may cooperate with Myc to coordinate glycolysis, glutaminolysis and cell growth. We suggest that determining the complex regulatory interactions between this extended Myc network will provide new insight into cancer cell metabolism and new opportunities for the development of cancer therapeutics.

References

1. Meyer N, Penn LZ. Reflecting on 25 years with MYC. Nat Rev Cancer 2008; 8:976-90.
2. White RJ. RNA polymerases I and III, non-coding RNAs and cancer. Trends Genet 2008; 24:622-9.
3. Knoepfler PS, Zhang XY, Cheng PF, Gafken PR, McMahon SB, et al. Myc influences global chromatin structure. EMBO J 2006; 25:2723-34.
4. Gallant P, Steiger D. Myc's secret life without Max. Cell Cycle 2009; 8:3848-53.
5. Hurlin PJ, Huang J. The MAX-interacting transcription factor network. Semin Cancer Biol 2006; 16:265-74.
6. Billin AN, Ayer DE. The Mlx network: evidence for a parallel Max-like transcriptional network that regulates energy metabolism. In: Eisenman RN, editor. The Myc/Max/Mad Transcription Factor Network. Heidelberg: Springer 2006; 255-78.
7. Billin AN, Eilers AL, Coulter KL, Logan JS, Ayer DE. MondoA, a novel basic helix-loop-helix-leucine zipper transcriptional activator that constitutes a positive branch of a max-like network. Mol Cell Biol 2000; 20:8845-54.
8. Uyeda K, Repa JJ. Carbohydrate response element binding protein, ChREBP, a transcription factor coupling hepatic glucose utilization and lipid synthesis. Cell Metab 2006; 4:107-10.
9. Stoltzman CA, Peterson CW, Breen KT, Muoio DM, Billin AN, et al. Glucose sensing by MondoA:Mlx complexes: a role for hexokinases and direct regulation of thioredoxin-interacting protein expression. Proc Natl Acad Sci USA 2008; 105:6912-7.
10. Peterson CW, Stoltzman CA, Sighinolfi MP, Han KS, Ayer DE. Glucose controls nuclear accumulation, promoter binding and transcriptional activity of the MondoA:Mlx heterodimer. Mol Cell Biol 2010; 30:2887-95.
11. Davies MN, O'Callaghan BL, Towle HC. Glucose activates ChREBP by increasing its rate of nuclear entry and relieving repression of its transcriptional activity. J Biol Chem 2008; 283:24029-38.
12. Ma L, Robinson LN, Towle HC. ChREBP*Mlx is the principal mediator of glucose-induced gene expression in the liver. J Biol Chem 2006; 281:28721-30.
13. Deberardinis RJ, Sayed N, Ditsworth D, Thompson CB. Brick by brick: metabolism and tumor cell growth. Curr Opin Genet Dev 2008; 18:54-61.
14. Shim H, Chun YS, Lewis BC, Dang CV. A unique glucose-dependent apoptotic pathway induced by c-Myc. Proc Natl Acad Sci USA 1998; 95:1511-6.
15. Yuneva M, Zamboni N, Oefner P, Sachidanandam R, Lazebnik Y. Deficiency in glutamine but not glucose induces MYC-dependent apoptosis in human cells. J Cell Biol 2007; 178:93-105.
16. Vander Heiden MG, Cantley LC, Thompson CB. Understanding the Warburg effect: the metabolic requirements of cell proliferation. Science 2009; 324:1029-33.
17. DeBerardinis RJ, Mancuso A, Daikhin E, Nissim I, Yudkoff M, et al. Beyond aerobic glycolysis: transformed cells can engage in glutamine metabolism that exceeds the requirement for protein and nucleotide synthesis. Proc Natl Acad Sci USA 2007; 104:19345-50.
18. Kim JW, Zeller KI, Wang Y, Jegga AG, Aronow BJ, et al. Evaluation of myc E-box phylogenetic footprints in glycolytic genes by chromatin immunoprecipitation assays. Mol Cell Biol 2004; 24:5923-36.
19. Sans CL, Satterwhite DJ, Stoltzman CA, Breen KT, Ayer DE. MondoA-Mlx heterodimers are candidate sensors of cellular energy status: mitochondrial localization and direct regulation of glycolysis. Mol Cell Biol 2006; 26:4863-71.
20. Zhang P, Metukuri MR, Bindom SM, Prochownik EV, O'Doherty RM, et al. c-Myc is required for the ChREBP-dependent activation of glucose-responsive genes. 2010; 24:1274-86.
21. Tong X, Zhao F, Mancuso A, Gruber JJ, Thompson CB. The glucose-responsive transcription factor ChREBP contributes to glucose-dependent anabolic synthesis and cell proliferation. Proc Natl Acad Sci USA 2009; 106:21660-5.
22. Li F, Wang Y, Zeller KI, Potter JJ, Wonsey DR, et al. Myc stimulates nuclearly encoded mitochondrial genes and mitochondrial biogenesis. Mol Cell Biol 2005; 25:6225-34.
23. Wise DR, DeBerardinis RJ, Mancuso A, Sayed N, Zhang XY, et al. Myc regulates a transcriptional program that stimulates mitochondrial glutaminolysis and leads to glutamine addiction. Proc Natl Acad Sci USA 2008; 105:18782-7.
24. Gao P, Tchernyshyov I, Chang TC, Lee YS, Kita K, et al. c-Myc suppression of miR-23a/b enhances mitochondrial glutaminase expression and glutamine metabolism. Nature 2009; 458:762-5.
25. Kim SY, Suh HW, Chung JW, Yoon SR, Choi I. Diverse functions of VDUP1 in cell proliferation, differentiation and diseases. Cell Mol Immunol 2007; 4:345-51.
26. Minn AH, Hafele C, Shalev A. Thioredoxin-interacting protein is stimulated by glucose through a carbohydrate response element and induces beta-cell apoptosis. Endocrinology 2005; 146:2397-405.
27. Hui ST, Andres AM, Miller AK, Spann NJ, Potter DW, et al. Txnip balances metabolic and growth signaling via PTEN disulfide reduction. Proc Natl Acad Sci USA 2008; 105:3921-6.
28. Chen JL, Merl D, Peterson CW, Wu J, Liu P, et al. Lactic acidosis triggers starvation response with paradoxical induction of TXNIP through MondoA. In review.
29. Shin D, Jeon JH, Jeong M, Suh HW, Kim S, et al. VDUP1 mediates nuclear export of HIF1alpha via CRM1-dependent pathway. Biochim Biophys Acta 2008; 1783:838-48.
30. Kaadige MR, Looper RE, Kamalannaadhan S, Ayer DE. Glutamine-dependent anapleurosis dictates glucose uptake and cell growth by regulating MondoA transcriptional activity. Proc Natl Acad Sci USA 2009; 106:14878-83.